Passage of Fibres Through Screen Apertures

by

Ashok Kumar
M.E., University of Roorkee, 1978
Dipl., Pulp & Paper Tech., University of Trondheim, 1983

A THESIS SUBMITTED IN PARTIAL FULFILLMENT OF
THE REQUIREMENTS FOR THE DEGREE OF
DOCTOR OF PHILOSOPHY

in

THE FACULTY OF GRADUATE STUDIES
Department of Chemical Engineering

We accept this thesis as conforming
to the required standard

THE UNIVERSITY OF BRITISH COLUMBIA
March, 1991

Department of Chemical Engineering
The University of British Columbia
2216 Main Mall
Vancouver, BC, Canada
V6T 1W5

Abstract

Passage of fibres suspended in water through apertures of dimensions greater than a fibre length and less than a fibre diameter has been examined at flow conditions approximating those in a pulp screen (large velocity parallel to the wall upstream of the aperture compared to the flow velocity within the aperture). Fibre behaviour was characterized in terms of three components: penetration of the leading tip into the aperture, rotation of the fibres on the downstream edge of the aperture, and fibre bending. Dimensionless numbers for each of these factors were derived from simple mass and force balances of fibres at an aperture entry. Experimental measurements of the magnitude of fibre passage were made on a single aperture located in a flow channel and in multiple apertures in a device simulating a commercial pulp screen in cross-section.

For stiff fibres, it was found that fibre passage changed greatly with the ratio of fibre length to aperture width (L/W). When L/W was less than 2, the relationship between fibre passage and aperture velocity was approximately an exponential curve. The passage data correlated well with the penetration parameter. On the other hand, when $L/W > 2$, up to measured values of $L/W = 6$, the relationship between fibre passage and aperture velocity corresponded to a cumulative probability distribution curve. This latter behaviour, and the absence of a correlation with penetration and rotation parameters, was ascribed to contact between the tip of the rotating fibre and the upstream wall of the aperture. This was confirmed by experimental observations. Flexible long ($L/W > 2$) fibres showed behaviour between the two cases described above.

The above observations were found to hold qualitatively for elevated concentrations up to a crowding factor of 4, multiple apertures, and the presence of pulses induced by a rotor of the type found in pulp screens. Accordingly, it appears that the findings are likely to hold in pulp pressure screens. An implication of this finding is that long stiff fibres may be best separated from short ones by choosing an aperture size such that $L/W > 2$ for the long fibre fraction and < 2 for the short fibre fraction.

Contents

List of Tables

List of Figures

xi

Acknowledgements

I dedicate this work to my parents, my wife, Sadhana, son, Abhinav, and daughter, Shipra for their love and encouragement.

Chapter 1

Introduction

Both woody and nonwoody plants are used as a source of papermaking fibre. The conversion of these raw materials into individual fibres is known as the science of "pulping" and the end-product so obtained is known as "pulp". Pulp is the fibrous raw material used for papermaking. Wood is the most abundant source of papermaking fibres and the pulp and paper industry is almost totally dependent on wood.

The fibres are elongated, tubular cells which are aligned parallel to one another in the wood and embedded in a matrix of non-fibrous material which is mostly lignin, but also contains some hemicelluloses, resins and gums. Fibres can be separated from the wood by chemical, mechanical or by a combination of both methods. In mechanical pulping, fibres are removed from the wood matrix by thermal softening of lignin and micro-abrasion. In chemical pulping, fibres are liberated because cooking liquor dissolves the lignin in the middle lamella between fibres.

A wide variety of undesirable material is either introduced or created when wood is reduced to pulp using any of the pulping processes. Both chemical and mechanical pulping processes produce a small quantity of "shives", which are bundles of fibres that have not been separated during cooking or refining action. Shives

reduce the strength and optical properties of paper and create problems on printing presses and in the production of coated papers. Shives must be removed from the pulp in order to produce high-quality paper.

Screening is the principal unit operation used to separate shives from the pulp in aqueous suspension. Wood fibres are 1–3 mm long and have high aspect ratios of about 50–100. Although the amount and dimensions of shives present in the pulp depend on the raw material and pulping process used, shives, in general, are a few fibres wide and have an aspect ratio similar to that of fibres. Pressure screens are widely used in the pulp and paper industry for shive removal. The size of the apertures employed in the screen plate to separate shives from fibres is larger than their diameters but smaller than their lengths. This means that most shives have at least one dimension (thickness) which is small enough to enable them to pass through the smallest aperture employed in the screen plate. Thus, the screen plate is not a physical barrier to all shives and, while shives generally do not pass through the apertures, most fibres do. The screening process, therefore, is a unique separation process which depends primarily on mechanisms rather than physical obstruction and is governed by other differences in properties, such as flexibility, and by the laws of probability screening.

In order to reduce the shive concentration of pulp from a typical value of about 1.0% to 0.5%, a pressure screen may reject about 10% of the feed pulp which then passes to the secondary and tertiary screening systems to reclaim the good fibre. The technical information on the working performance of the existing pressure screens and on the selection of screening systems for industrial applications are available in the literature. However, despite the widespread use of screens for shive removal, little has been published that gives insight into the fundamental understanding of how shives are separated from the pulp.

2

In fibre screening, the aim is to separate long fibres from short and/or stiff fibres from flexible ones. The general objective of this thesis is to understand the passage of highly asymmetric fibres through apertures larger than the minimum dimensions of fibres and to identify the relative importance of the key factors which affect the passage.

The relevant screening literature is reviewed in this dissertation in Chapter 2. Although a large number of technical articles has been published on pulp screening, most of the work has focussed on hardware development and the selection of best screening systems for industrial applications so that rejects can be discarded with a minimum loss of good fibre or treated with the least amount of equipment and energy. The aim here was not to review all this screening literature in detail but to concentrate upon those studies which added scientific insight to the process. However, some aspects related to equipment used in the industry and performance characteristics of screening systems are briefly reviewed. The summary of the Literature Review section focusses on the subject of this dissertation and concludes with a statement of objectives for this research work.

Chapter 3 presents an approximate analysis of fibre passage through a screen aperture under conditions which are likely to exist in a pressure screen.

Chapter 4 presents an experimental program for carrying out the research work. Nylon and rayon fibres were used as model fibres. The length distribution of these fibres is narrow. The fibres were selected to have lengths corresponding to the lengths of wood-pulp fibres and also flexibilities matching to those of pulp fibres and shives. The experimental work is divided into two parts:

1. To determine how various fibre, flow and screen plate variables affect the separation of long fibres from short fibres and/or stiff fibres from flexible ones in dilute concentrations in a steady flow past a single slot.

3

2. To test the robustness of the findings in 1. with conditions approaching those of commercial pulp screens, *i.e.* increased concentration, change in entry geometry, multiple slots and pulsed purging.

The experimental results are reported and discussed in Chapter 5. Chapter 6 summarizes the major findings of this work. The conclusions drawn from the research are given in Chapter 7. The recommendations for future research work are given in Chapter 8. The appendices are introduced to record information and subsidiary findings which are important in clarifying the main text.

Chapter 2

Literature Review

2.1   Fibre Screening

The separation of one type of solid particles from another is often accomplished by solid-solid screening. The general principles of screening are described in a number of texts (B1,B2,M1,P1,R1). In this separation process, desired particles are separated from undesirable ones by selective passage of desirable particles through apertures. Selective passage through an aperture may be caused by barrier screening, probability screening or a combination of the two. For convenience, we will refer to the undesirable particles as contaminants.

In barrier screening, the size of the contaminants is such that they can not fit through the apertures on any dimension. Particles larger than the size of apertures are retained and those that are smaller pass through.

In probability screening, both the accept and reject material can pass through the aperture because the minimum dimension of all particles is less than the aperture size. However, the maximum dimension of the particles is larger than the apertures. Particle passage is therefore governed by the factors such as particle orientation and interaction with other particles (B2,K1). In pulp, contaminants may span a considerable size range. Thus, industrial pulp screens perform both

barrier and probability screening. The present study, however, is focussed on the separation of shives from good fibres or, in general, long fibres from short and/or stiff from flexible ones. Specifically, the study is aimed at separation of highly asymmetric fibres by apertures larger than the minimum dimension of the particles. Thus, the focus of this work is on probability screening.

2.2 Physical Properties of Fibres and Shives

The properties of wood fibres are described in numerous publications (I1,M2,P2,R2,S1). The most important fibre properties affecting pulp screening are length, width and flexibility (H1,S2,Y1). There is a wide range of values for fibre properties given in these publications due to the wood variability that exists naturally from tree to tree, species to species, and within a tree. Based on these publications, the average fibre length of commercially important softwoods varies from 2–5 mm and their width from 30–45 μm. Hardwood fibres are 1–2 mm long with a fibre width of about 20 μm.

A shive is a small bundle of fibres that have not been separated from each other during the pulping process. There is no general agreement in the industry on the precise geometric dimensions of shives. Clark (C1) defined a chemical pulp shive as a fibre bundle that is unable to pass through a slot 0.15 mm wide and at least 3 mm long. He suggested a mechanical pulp shive be defined as a particle at least 3 mm long and 0.08 mm wide. The classification of shives based on the anlysis by an optical shive analyzer differs in approach as it gives a count of all particles having a width greater than 0.75 mm and length greater than 0.3 mm.

It gives separate counts for 16 different groupings of length and width (H1). Shives have also been defined based on the problems caused by their size such as web breaks and linting for mechanical pulps (B3,C2,C3,H2,L1,M3,S3). Studies

6

(A1,A2,A3) have shown the importance of the origin and size of shives in un-bleached pulp to optimize and influence the particle elimination during bleaching. It was found that the amount of bleaching should be determined by the cleanliness requirement *i.e.* the absence of particles such as shives in the bleached pulp. It was observed that semibleached pulp quality tends to be more sensitive to the shives present in unbleached pulp than those in fully bleached pulp. This occurs because the rate of shive removal in pulp bleaching is slower than the rate of brightness development (A3,F1).

Stiffness is also an important property that influences the screening process. Schniewind *et al.* (S4) and Samuelson (S5) measured deflection of pulp fibres by clamping them in water and, using such beam type tests, they reported the rigidity of chemical pulp fibres. Tam Doo and Kerekes (T1) measured wet fibre flexibility using fibre bending in a cross flow of water to avoid fibre clamping. Soszynski (S6) used load-elongation procedure to measure the stiffness of nylon monomer in the elastic regime and then reported the values of the elastic modulus. Claudio-da-Silva Jr. (C4) reported stiffness values using morphological and ultrastructural data.

There are no published measurements of the stiffness of shives. Gooding (G1) estimated shive stiffness by assuming them to be simple beam-like composites. All wood fibres in a bundle were considerd to be identical and intimately bonded to each other to simplify the analysis. The stiffness values for pulp fibres and the model fibres used in this study are given in Table A.6 (see Appendix A).

Wood pulp fibres are hydrophillic and retain the imbibed water in the fibre wall, lumen and microfibrills. Thus, fibres have an apparent mass and volume. The density of the fibre wall is about 1500 kg/m^3 (S7) and that of water at 20°C is about 998 kg/m^3 (C5). The apparent density of pulp fibres varies with the

7

amount of imbibed water and is 1123 kg/m^3 for a typical water retention ratio at knee, WRRk, of 2.0 kg/kg (see Section A.3 of Appendix A). This means that the apparent density of pulp fibres and shives in aqueous suspension is only slightly greater than that of water and therefore these fibres can be considered nearly neutrally buoyant.

2.3 Equipment Used for Pulp Screening

Pulp screens are used for a variety of purposes such as shive screening, fibre fractionation and equipment protection. The equipment used for shive removal can be categorized as: vibrating flat screens, centrifugal, and rotary type atmospheric screens and pressure screens. The design, operating principle and dynamics of these screens differ considerably (C6,L2,L3,S8). In the early days, flat screens were used to remove contaminants in fine pulp screening. These are barrier screens having screen plate apertures smaller than the smallest shive diameter. Flat screens have low capacity, require high maintenance and now find limited use in the modern pulp and paper industry. In both rotary atmospheric and centrifugal screens, the plate apertures are much larger than the average shive diameter, but shives normally do not pass through the apertures. These are probability screens and it is believed that a mat of fibres forms adjacent the screen plate and the interstices in the mat rather than the size of apertures control the removal efficiency (B4,C2,L4).

Pressure screens came into existence in the 1960's and have since been in widespread use in the industry. These are probability screens and were developed to provide higher throughput and better shive removal efficiency. Figure 2.1 shows the principal features of a typical pressure screen used commercially for pulp screening. The pulp enters tangentially at the top of the screen and passes downward through a narrow annular zone between the screen plate and a cylindrical

rotor. The accept pulp passes radially outward through the screen while reject pulp continues down the annular screening zone to the reject outlet. The screen plate is stationary and its configuration is very critical to screen performance. The size and type (holes or slots) of the screen plate apertures are selected based on the application. Rotor designs vary among manufacturers depending on the application. A drum type rotor having hemispherical bumps on a cylindrical shape is shown in Figure 2.1. The thickness of the annular zone between screen plate and rotor also varies from one screen type to another. In spite of the differences in shape, all rotors serve the same function. They accelerate the pulp suspension to a high tangential velocity and along with the axial flow, establish the necessary flow field adjacent to the screen plate. Also, the lugs or vanes on the rotor produce pulses and turbulence that prevent apertures from plugging.

2.4 Performance Characterization of a Pressure Screen

Because probability screening is affected by flow conditions, it is necessary to define efficiency in terms of the three flows entering or leaving a screen: the feed flow, accept flow and reject flow. Efficiency (E_R) is defined as the mass of shives in the reject flow as a percentage of shives in the feed flow. Reject rate (R) is the overall portion of the feed pulp that passes to the reject stream and is normally based on pulp mass fractions. The relationship between various parameters and basic equations for screen efficiency are given in Tappi Information Sheets (T2). A typical E-R curve which describes screen performance is shown in Figure 2.2. Efficiency increases as the reject rate is increased. The aim is to achieve high shive removal efficiency with minimum loss of good fibres, *i.e.* high efficiency at low reject rates. In industry, an E-R curve is determined experimentally by measuring efficiency at
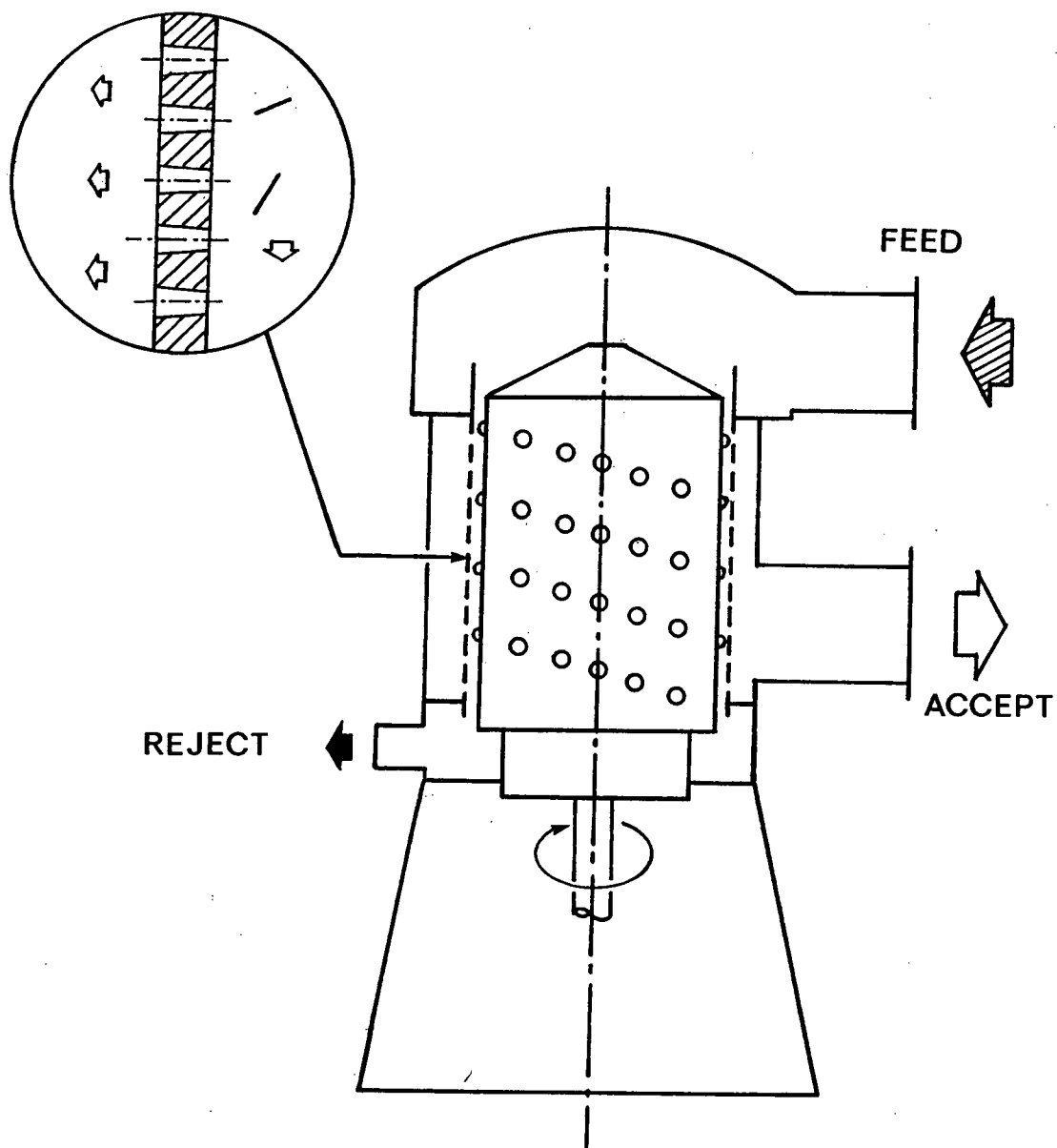
Figure 2.1: A typical pressure screen used in the industry for pulp screening.
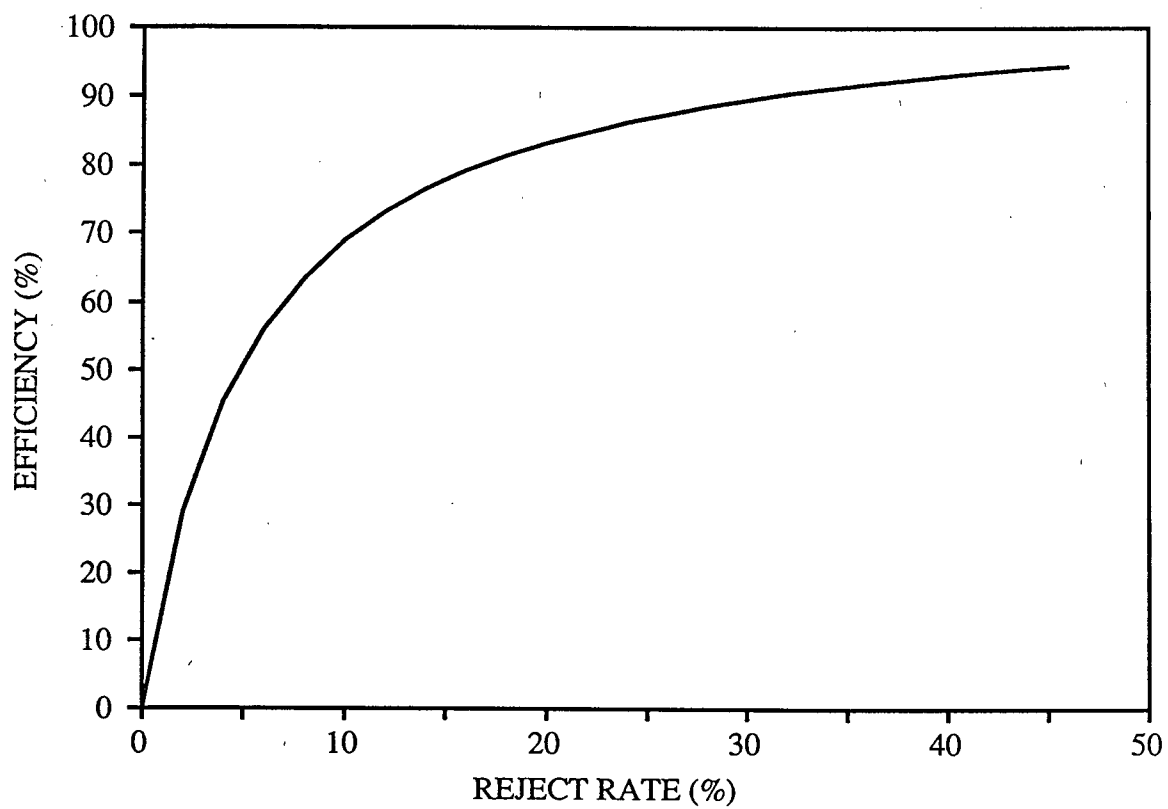
Figure 2.2: Performance curve of a pressure screen.

various reject rates. The challenge is to develop a curve from a small number of scattered data points. To assist in this, theoretical models have been proposed to link and extrapolate experimental data. Nelson (N1) presented the following equation which has found widespread use in pulp screening:

$$E_R = \frac{R}{1 - \alpha + \alpha R} \tag{2.1}$$

Equation 2.1 is not based on any mathematical proof. The variable α is referred to as the screening quotient, a characteristic of the screen hardware. If $\alpha = 0$, $E_R = R$, the concentration of contaminants in the feed stream equals that in the reject stream; the screen merely splits the feed stream into two streams of equal contaminant concentration and thus no screening takes place. Higher values of α denote better screen performance. At $\alpha = 1$, $E_R = 1$ for all R. The usefulness of Equation 2.1 is based on the fact that α, which defines screen performance, is independent of the reject rate. In reality, it has some limitations since a reliable value of α is difficult to obtain in practice. Also, α does vary to some extent with process parameters such as reject rate and shive level in the feed.

Another E-R equation for probability screening may be obtained by extending the work of Kubat and Steenberg (K1). They modelled a screen plate as a row of apertures acting in series. If their variables are expressed in terms of efficiency and reject rate, the following equation is obtained:

$$E_R = R^\beta \tag{2.2}$$

The power β may also be used as a screening index like α in Equation 2.1. At $\beta = 1$, $E_R = R$; no screening takes place, and at $\beta = 0$, $E_R = 1$ for all R. Thus, decreasing values of β represent better screening.

In a more recent publication, Gooding and Kerekes (G2) derived the above two equations for solid-solid screens. They showed that Equation 2.1 represented the case of perfect mixing adjacent the screen plate and gave the following equation:

$$E_R = \frac{R}{R + \frac{P_c}{P_p} - \frac{P_c}{P_p}R} \tag{2.3}$$

P_c and P_p are the "Passage Ratios" (defined later) of contaminants and pulp fibres. Equation 2.3 is similar to Equation 2.1 in which $\alpha = 1 - (P_c/P_p)$.

The second equation was shown to be the case of plug flow model assuming no axial mixing in the annular screening zone. However, perfect radial mixing was assumed. The equation is:

$$E_R = R^{\left(\frac{P_c}{P_p}\right)} \tag{2.4}$$

This equation is similar to Equation 2.2 where $\beta = P_c/P_p$.

Equations 2.3 and 2.4 derived by Gooding and Kerekes represent the two limiting cases of mixing inside a screen and therefore define the bounds in which real screens work. They also extended these two equations to include barrier screening in addition to probability screening. Most important, they related α and β to the "Passage Ratio" for fibres at a slot. Thus, their work directly links performance equations to passage ratio measurements at a single slot.

2.5   Design of Screening System for Industrial Applications

The performance of an individual screen depends on the properties of fibres and contaminants to be removed, type of screen plate used, operating consistency, reject rate and a number of other factors (H2,L1,L2,N2,T3). To maintain high efficiencies,

high reject rates must be used, and this reject stream must therefore be further treated. Thus, a system configuration involving several screens is used in order to produce the desired pulp quality. Steenberg (S9) has proposed some general guidelines for designing a screening system. Hooper (H3) has recommended some general principles and their use in designing the flow sheet for specific grades of pulp. A number of case studies (C7,C8,F2,H4) has been done on modern screens and screening systems with the aim of optimizing the system for a specific application.

The removal of shives from mechanical pulps and its influence on pulp properties have been studied by a number of researchers (B5,F3,G3,P3). However, due to the problems in defining and measuring particles such as shives (B6,H5,K2,T4,T5), it has been very difficult to repeat the results of shive removal efficiency and thus the problem of comparing the results still remain.

In a screening system, screens can be used as fractionating units to separate mechanically certain types of fibres from a mixture to produce at least two fractions containing fibres with different properties. Generally the aim is to separate long fibres from short ones. Screens have been used as fractionators mainly in board mills (B7,C9), and to a lesser extent in mills using virgin fibre (A4).

Optimizing the performance of a screening system is a key to obtain desired product quality. Studies have been carried out to develop models for optimizing the performance of a screening system and these models have been examined by using industrial data (D1,H6,N3). General purpose computer-based modelling systems have also been used for evaluating and optimizing the design of screening systems (D2).

2.6 Flow of Fibre Suspensions Through Apertures in Screening Situations

2.6.1 Flow of Fluid Through Apertures

Despite the large number of factors affecting screening, in essence, the process is one of determining whether particles in suspension pass or do not pass through a given aperture. This aspect of screening is therefore crucial.

In pulp screens, fluid from a flow parallel to the screen plate is drawn into a series of apertures. Flows of this type have been examined in various hydrodynamics for specific purposes. For example, McNowen (M4) studied bifurcating flows in manifolds by considering a single tube branch from a circular conduit. Loss coefficients for the tubes were obtained.

Investigations have also taken place to determine the effect of slot flow on the boundary layer of the main flow that turns to enter into the slot. For example, Thomas and Cornelius (T6) examined the flow into a slot from a laminar boundary layer. They observed the expected boundary layer separation and recirculating zone shown in Figure 2.3. They determined conditions at which separated flow would reattach to the slot wall by measuring a/w and b/w for various slot Reynolds number and mean flow velocity gradients. They gave empirical relationships to determine a/w and b/w for various flow conditions.

In summary, the hydrodynamics literature contains useful information on energy loss characteristics of slots and flow patterns from well-defined main flows, but the complex cases of flow into slots from unsteady-state turbulence and pulsatile flow found in pulp screens remain to be investigated.
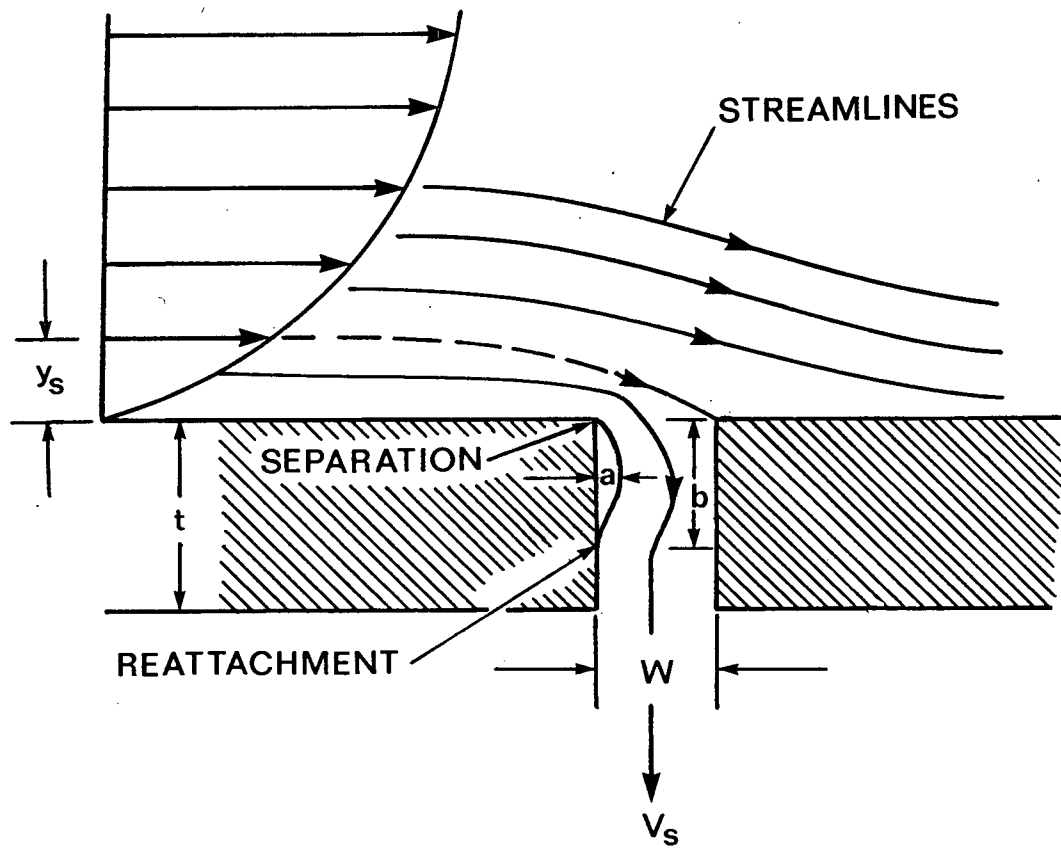
Figure 2.3: Flow bifurcation at a slotted plate (T7).

2.6.2   Two Phase Flow Through T-Junctions

The principal interest in screening is to separate a solid phase from a liquid and therefore studies of two-phase flow in geometries which cause flow splitting are of interest. A number of papers have been published on two-phase flows in T-junctions and manifolds encountered in many industrial applications. Although studies have considered gas-liquid, gas-solid and liquid-solid systems, the work done with the solid-liquid system is meagre. Bugliarello and Hsiao (B8) studied the phase separation of neutrally buoyant particles in a laminar flow and found that the degree of separation, expressed as the ratio of the concentration of the dispersed phase in the branch to that in the upstream flow, increased as the size of branch was reduced. Most of the other experimental studies (M5,N4,T7) have been concerned with the sampling through small branches in a vertical downward flow. In these studies, the effects of branch velocity, branch size, particle size and upstream flow conditions on the separation ratio were determined. In a more recent work, Nasr-El-Din *et al.* (N5,N6) studied particle segregation in slurry flow through T-junctions of vertical, horizontal and side orientations. The effects of particle size, upstream solids concentration, upstream velocity, ratio of branch to upstream velocity on the separation ratio were studied. These studies are useful in predicting the distribution of solid particles in branches due to flow bifurcation, but they are of limited use when applied to fibre screening due to following fundamental differences between these systems and fibre suspensions:

1. In most of the studies of two-phase slurry flow through T-junctions, the branch size is larger than the dimensions of particles to be segregated.

2. In most of the studies with slurry flow, the particles were considered symmetric and rigid (*e.g.*, sphericle particles of length to diameter ratio=1). On the

other hand, fibres have a very high aspect ratio of 50–100 and are flexible.

3. In many of the two-phase slurry flow studies, there was a significant difference in the density of particles and suspending medium. Thus, inertia was often a major factor in the separation of particles. In pulp screening, fibres are nearly neutrally buoyant and thus inertia can be expected to play a relatively small role.

2.6.3 Flow of Fibre Suspensions Through Apertures

The literature contains a number of studies on fibres of the type of interest in this work. Most of these studies have been limited to flow behaviour in pipes. Norman *et al.* (N7) critically reviewed the major fundamental investigations in relation to the flow of pulp suspensions in pipes within the framework of basic flow mechanisms (plug, mixed and turbulent flow) and three basic study levels (empirical, network and fibre). They concluded that the flow behaviour of fibre suspensions is controlled by the volumetric concentration, aspect ratio and modulus of elasticity of the fibres. Mason (M6) considered the orientation of rigid fibres in simple shear flow and predicted that fibres tend to align in the direction of flow. However, in the case of turbulent flows, the eddies will tend to destroy the preferred orientation. In these and many other studies of fibre suspensions, there is little published on the motion of fibres through apertures smaller than the length of a fibre as is the case in screening. What follows is a brief review of scientific work related specifically to this problem.

Kubat and Steenberg (K1) treated the screening process from a statistical point of view. The passage of particles through the interstices of a screening element was considered as an independent elementary process describable in terms of average passage probabilities. They suggested that the average passage probability of a

certain particle type is influenced by factors such as the relative geometrical dimensions of particles and the screen openings, the hydrodynamic field around the screen openings and the interaction between particles passing the screening element. Their quantitative analysis did not establish the relative importance of these parameters.

Andersson and Bartok (A5) investigated the passage of fibres in a dilute suspension through a mesh by considering a flow which had a substantial component parallel to the screening surface. They defined a term "permeability" as the relative concentration of fibres on the accept side and feed side of a mesh. They observed that permeability increased with decreased fibre length and fibre stiffness. They did not attempt a theoretical explanation of their findings and thus their results remain strictly empirical and of limited use.

Estridge (E1) and Abrams (A6) studied the retention of stiff nylon fibres in a dilute fibre suspension flowing normal to the screens (open rectangular wire mesh) having very high open area (> 82%). The retention was obtained by making periodic measurements of the concentration downstream of screens as the upstream concentration was known. The effect of only two variables — fibre length and screen mesh-size was studied. They assumed random fibre orientation and position upstream, due to fluid turbulence, and the fluid flow was practically unaffected by the presence of the highly open screen. They concluded that the fluid pattern upstream of the screens did not influence fibre retention. This is not the case in pulp screens as will be discussed later.

Riese et al. (R3) used the basic approach of Estridge and Abrams but utilised more realistic screens by having circularly perforated plates with open areas in the range of 8 to 41%. A dilute suspension (< 3 mg/l) of stiff nylon fibres was caused to flow normal to the perforated screen plates. It was observed that fluid

19

forces aligned a fibre parallel to the direction of flow, and the velocity of a fibre was roughly equal to the velocity of fluid along its length. This alignment and the probability of fibre passage through the plate increased as the flow through the plate increased. They argued that a fibre approaching an aperture from a flow normal to the screen plate could be expected to rotate to some degree as it passes over an aperture. Fluid flow patterns, which played no role in the work of Estridge and Abrams, were found to be the most influential variable in their study. They also made a quantitative analysis of the process, and based on the concept of inviscid flow, developed a theory by which retentions could be predicted.

In a more recent work, Gooding (G1) studied the motion of fibres near a screen slot using very dilute fibre concentrations (< 0.05 g/l) in a laboratory flow loop having a single slot channel. The average bulk velocities that may exist near an aperture in an industrial pressure screen were estimated and then used as a guideline in the single slot tests. Gooding and Kerekes (G2) defined a term "Passage Ratio": the concentration of pulp fibres or contaminants in the aperture flow divided by the corresponding concentration upstream of the aperture. The effect of fibre properties and flow variables on passage ratio was studied (G1).

Gooding and Kerekes (G4) also filmed the trajectories of individual nylon fibres in the entry zone of an aperture using high speed photography. The fibre trajectories were classified into five different types of motion based on whether fibres contact the slot wall or not, and whether on contact with the slot wall, fibres pass into the slot or back into the main flow.

Table 2.1 summarizes their findings for 3 mm nylon fibres and a 0.5 mm wide slot. The data of Table 2.1 show when V_s/V_u was inceased from 0.39 to 1, yielding an increase in the passage ratio from 0.09 to 0.86, the fibres contacting the slot out of the total fibres observed increased from 24% to 35%. Moreover, a sizeable

percentage of the fibres contacting the slot were immobilized there, meaning they were close to entering or not entering. The total incidence of motion types D and E was equal to the passage ratio. Although these data are few, they show that fibre interaction with the downstream wall of the slot is an important factor in determining fibre passage through the apertures.

Based on the analysis of trajectories of individual fibres, Gooding and Kerekes proposed that screening took place by two mechanisms — (1) a "wall effect" and (2) a "turning effect". The wall effect occurs because all fibres passing through the slot came from a thin "exit layer" adjacent to the upstream wall. The thickness of this layer was less than the fibre length and increased with the slot velocity. Fibre concentration in this zone was lower than in the mainstream flow. The exit layer therefore was one of diminished concentration of fibres. Furthermore, the concentration of shive-like fibres in this layer was less than pulp-like fibres. Thus, a screening effect can be obtained by simply removing the exit layer from the mainstream flow. Fibres in this layer were oriented parallel to the wall and thus had to turn to enter into the slot. The turning effect caused more flexible pulp-like fibres to bend and follow the streamlines into the slot while stiff shive-like fibres tended to rotate and were swept away by the mainstream flow over the slot.

The studies of Gooding and Kerekes and many others on the mechanism of screening have been carried out at dilute concentrations, in fact, at less than the critical concentration which was defined by Mason (M6) as the concentration above which fibre-fibre interaction becomes important (see Appendix B). This is typically 0.015 to 0.06% on volumetric basis for fibres having aspect ratios in the range of 50–100. A fibre suspension can be termed as dilute, semi-concentrated or concentrated depending on the level of interfibre contact. This can be estimated by calculating the "crowding factor", N, (K3,K4). N represents the number of fibres

Table 2.1: Types of fibre motion observed by Gooding and Kerekes (G4) using high speed photography for 3 mm nylon fibres and a 0.5 mm wide slot.

Motion Type	Description	Test 1	Test 2
	Velocity Ratio, V_s/V_u Exit Layer Thickness, (mm) Passage Ratio	0.39 0.2 0.09	1 0.53 0.86
B, C & D	Fibres contacting the wall (% of the total number of fibres observed in a 1.5 mm thick layer from the wall)	24	35
B	Fibres going into the mainstream flow after contacting the wall (%)	15	9
C	Fibres immobilized on the downstream wall of the slot after contacting the slot (%)	8	20
D	Fibres passing through the slot after contacting the slot wall (%)	1	6
A	Fibres move downward without contacting the slot (% of the total fibres observed)	76	56
E	Fibres passing through the slot without contacting the slot (% of the total fibres observed)	0	9

in the volume swept out by the length of a single fibre. This indicates the level of restraint of rotational motion. N can be calculated from the volumetric concentration of fibres, C_v, fibre length, L, and fibre diameter, d, using the following equation

$$N = \frac{2}{3}C_v \left(\frac{L}{d}\right)^2 \qquad (2.5)$$

In industry, pulp is screened at consistencies of 1–4% where substantial interaction between fibres occur. Fibres also interact with the apertures when trying to pass through them. Fibre interaction with apertures may cause the fibres to accumulate at the entry of the aperture resulting in "stapling". Stapling is likely to be governed by factors such as fibre length, distance between the centres of two neighbouring apertures, pulp consistency, velocities in the screening zone and through apertures, level of turbulence and rotor speed. The effect of these parameters on fibre accumulation or on the passage of fibres through apertures has not been systematically investigated. It has been speculated in some studies that, at higher consistencies, fibre interaction with apertures should merely result in a new screen geometry. This may be true in case of atmospheric screens but seems to be highly unlikely in pressure screens where substantial turbulence is created by the rotor used to prevent aperture plugging. Thus, fibre to fibre interaction in suspension (K5) and fibre interaction with the apertures affect the passage of fibres through apertures. This effect at elevated concentrations has not been studied.

2.7 Bulk Velocities Inside a Pressure Screen

The importance of the hydrodynamic flow field in the screening zone and its influence was discussed in the previous section. The velocities in a pressure screen produce forces which determine the degree of separation of one fibre type from another. There are three main velocities inside a pressure screen — the radial,
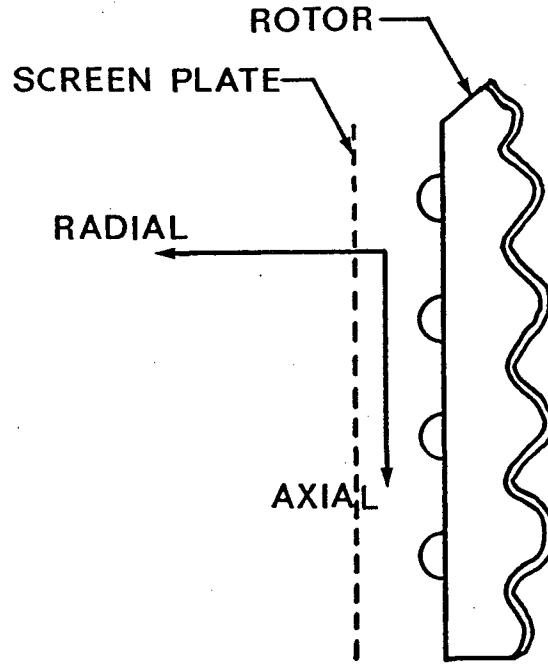
Figure 2.4: Velocities inside a pressure screen.

axial, and tangential as shown in Figure 2.4.

The velocity through the screen plate apertures is the radial velocity. In order to pass through the apertures, flow from the feed side has to turn, converge and accelerate. Passage of the rotor past an aperture creates pressure pulses which superimpose a time-varying component of velocity on the mean aperture velocity. The velocity is thought to reverse direction resulting in momentary backflushing. These factors complicate the determination of the radial velocity through screen apertures.

As a first approximation, we may consider the bulk velocity through an aperture, V_s, as a representative value of aperture velocity. V_s is defined as follows:

$$V_s = \frac{Q_s}{A_s} = \frac{\text{volumetric flow rate through the slots}}{\text{open area of the screen plate}}$$

The axial velocity is in the direction of the axis of rotation, parallel to the screen

plate. This velocity depends on the flow rate in the annular zone and the distance between the screen plate and rotor.

The tangential velocity is parallel to the surface of the screen plate and at right angles to the radial and axial velocities. This velocity depends on the design of the rotor and varies from one screen to another. The resultant mean velocity of pulp flow in the plane of the screen plate in the annular zone is the vector sum of axial and tangential velocities.

In spite of its importance, the flow field within the screening zone has not been studied in detail and the average velocities in the annular zone and within the apertures have not been measured. Koffinke (K6) suggested that in case of secondary fibre screening, the radial velocity should not exceed 1.2–1.8 m/s. Another source (H3) refers to a maximum pressure drop of 70–100 kPa across the screen plate as a criterion to achieve maximum efficiency or to avoid plugging of the screen plate. Gooding (G1) estimated the average bulk velocities near an aperture by using typical feed and accept flow rates for screening conditions in a pressure screen operation. A representative bulk velocity parallel to the feed side of the screen plate was estimated to be about 6 m/s and the bulk velocity through the apertures as about 1 m/s (G1). Although this simple analysis is approximate, it provides a useful basis for conducting fundamental screening studies.

2.8 Recent Developments

In the last decade, there have been some significant developments in the design of pressure screens with the aim of improving throughput and handling higher consistencies. Traditionally, pulp has been screened using screen plates with smooth surfaces and specifications have been limited to the size of holes or slots and open area of the screen plate. During the early 1980's, "contour" screen plates

were developed in which the surface of the screen plate facing the feed flow was milled to provide various configurations of ridges and grooves. Some examples are shown in Figure 2.5. Various patterns are used for contoured plates by various manufacturers. The selection is based on factors such as fibre type, type of furnish, desired operating consistency and end product requirement. Improvements in shive removal efficiency at constant capacity or increase in capacity and reduction in reject thickening have been reported for a number of commercial installations (F3,H7,J1,M7,M8,P4). The development of contour screen plates has also enabled the pressure screens to operate as barrier screens (B9).

The success of contoured screen plates has led to the development of various new rotor concepts in recent years. This is due to the fact that the rotor and screen plate work in combination and therefore need to be optimized together. Rotors that produce high pressure pulsations have been designed (L5,M8) for screens to operate in the consistency range of 4–5%. A medium consistency "MC" screen has been developed by Kamyr for screening pulp at consistencies over 10% (G5).

In spite of the widespread use of contoured screen plates, the exact difference between how contoured and smooth plates work is not known. In a recent study, Halonen et $al.$ (H9) investigated the flow field above smooth and Profile™ slots. The flows were simplified and the average upstream and slot velocities were maintained in a flow loop consisting of smooth and Profile™ slots. It was reported that the velocity measurements were made by using Laser Doppler Anemometry. The following differences in the flow field between two plate types were found:

1. The shape of the profile caused the flow parallel to the plate surface to turn more smoothly towards a slot than in case of a slot in smooth plate.

2. In case of profile plate, the boundary layer on the feed side of the plate was

Smooth Plates

Drilled or Punched
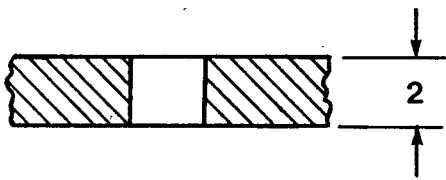
Conically Drilled
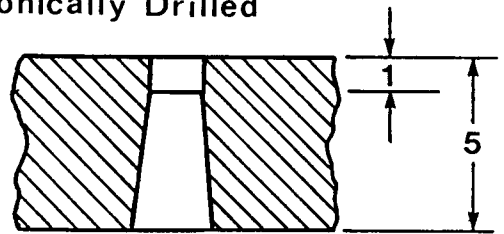
Contoured Plates

Profile Conical
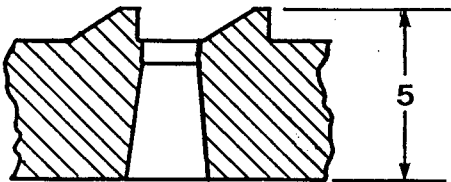
(Nima) Wave
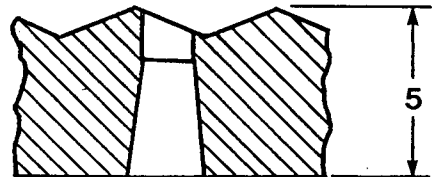
All dimensions are in mm.

Figure 2.5: Smooth and contoured screen plates used for pulp screening.

about three times thicker than in case of smooth plate.

3. The kinetic energy of turbulence was much larger for a profile plate.

The above study was carried out using water without the presence of any fibres. To date, no work has been reported on the fundamental differences in the flow fields between smooth and contoured slots using fibre suspensions under flow conditions that exist in a pressure screen.

2.9 Summary of Literature Review

From this review of the literature, it can be concluded that little is known about fibre screening from a fundamental standpoint, *i.e.* the passage of fibres at a single aperture. Moreover, there is little systematic scientific information or data available from which an attempt can be made to obtain a fundamental understanding of screening. Based on this state of knowledge, useful next steps in research are to obtain good data that clearly show the effects of major screening variables and simple quantitative parameters that characterize screening behaviour.

2.10 Objectives of This Research

The objectives of this thesis are:

1. To identify the relative importance of the key variables which affect the passage of fibres through a single screen aperture.

2. To make an approximate theoretical analysis of fibre behaviour at a screen aperture under conditions likely to exist in a pressure screen.

3. Test the validity of the above theoretical and experimental findings at conditions approaching that of commercial pulp screens, *i.e.* higher concentrations, multiple apertures, contoured surfaces and pulsed purging.

Chapter 3

An Approximate Analysis of Fibre Passage into Apertures

3.1 Introduction

A full, rigorous theoretical analysis of fibre passage into slots would be the most desirable basis for predicting fibre passage, and for obtaining the key dimensionless numbers that govern passage. However, such an analysis is a formidable problem given our current knowledge of screening. Indeed, it is a formidable problem in even simpler single phase or two-phase systems.

Starting upstream of the slot, there is a boundary layer at the wall surface. This boundary layer is affected by the main flow and the flow into slots. Also, there is a concentration gradient of fibres near the wall, and most fibres, but not all, are oriented in the flow direction with some rotational motion (G1).

Once a fibre reaches the entry zone of the slot, the entry flow field imposes hydrodynamic drag upon the fibre, causing translational and rotational acceleration into the slot. The degree of acceleration is determined by the hydrodynamic drag on the fibre caused by the relative flow and by the inertia of the fibre both in translation and rotation. At the same time, the fibre may bend as a result of forces imposed on it. The fibre may also come in contact with the upstream edge of the

30

slot. All these factors may determine the degree of fibre penetration into the slot.

Because a fibre continues to move at a high speed across the opening of the aperture, penetration may not be complete before the fibre comes in contact with the downstream edge of the slot wall. Momentarily, translational motion in the direction of main flow or slot flow may cease altogether. The hydrodynamic drag forces imposed by these flows create opposing moments on the fibre which bend and rotate the fibre over the edge of the slot. Fibre bending causes the moment acting on the fibre to diminish. If bending is large, the frictional resistance between the fibres and the wall may come into play as an additional force resisting translational motion.

A preliminary attempt was made to model the above problem by some simplified equations of motion but the problem was too complex. For example, modelling a combination of rotation and bending induced by hydrodynamic drag in a flow field which in itself is not well defined was too uncertain for practical use. This short-coming would be even more severe in flow fields affected by the periodic passing of rotating foils.

In light of the complexity of this problem, consideration was given to obtaining the dimensionless numbers that determine the fibre passage through apertures using simple dimensional analysis, for example using the Buckingham Pi method. However, this approach did not take advantage of the available physical knowledge of the problem described above. An intermediate approach based on some physical understanding of the problem was deemed most appropriate. Accordingly, the approach adopted in this study was to divide the problem into some key conceptual components and derive approximate parameters for each from simple material and force balances.
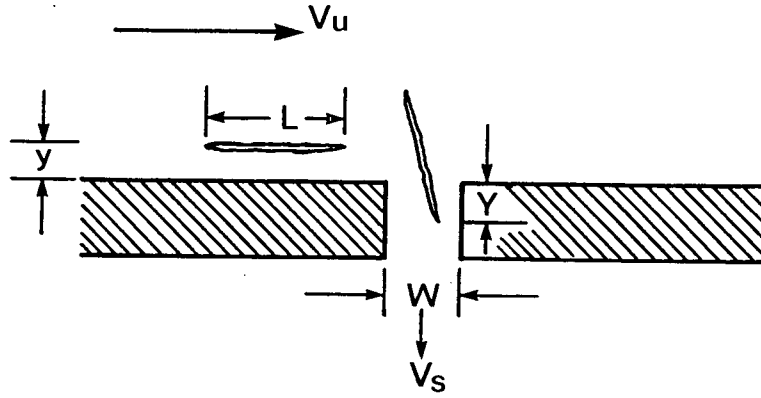
Figure 3.1: Fibre in the exit layer turning to enter into the slot.

3.2 Analysis

3.2.1 Factors Affecting Fibre Passage Through the Slot

To begin with, probability screening discussed earlier on the passage of a fibre of length, L, diameter, d, through an aperture of size, W, where $d < W < L$ will be described. The relevant dimensions are shown in Figure 3.1.

Gooding and Kerekes (G4) found that fibre passage into a slot was determined by two factors: a "wall effect" and a "turning effect". The former is due to the fact that there is a diminished concentration of fibres near the upstream wall in a zone, y, less than a fibre length, L, *i.e.* $y < L$. This is probably due to the migration of fibres away from the wall as a result of fibre rotation, and is therefore dependent on fibre stiffness as well as fibre length. A key result of this wall layer is that it alone leads to a screening effect when this part of the feed flow, having less fibres, or fibres of differing size, is diverted into the aperture.

Gooding and Kerekes also observed a "turning effect" in which fibres from within this layer rotated or bent on passage over the slot. As shown earlier in Table 2.1, this often resulted in fibre interaction with the downstream edge of the slot, which itself appeared to affect fibre passage. In many cases, however, there was no contact with the downstream wall, but this condition was largely confined to fibres which did not pass into the slot (see Table 2.1). This probably occured because fibres were not sufficiently influenced by the aperture flow to cause penetration owing to fibre orientation perpendicular to the wall or fibre distance from it.

From the above observations, it would appear that the problem of fibre passage can be considered in three aspects — (a) penetration of fibre into the aperture; (b) rotation upon entry; (c) the effect of bending on these two factors.

3.2.2 Penetration

A key factor in passage is the degree to which the leading tip of a fibre can be drawn into the slot. As described in the previous section, Gooding and Kerekes showed that fibres which passed into the slot under conditions found in typical pulp screens came from a layer very near the wall. The distance y (see Figure 3.1) was much less than a fibre length. Because $d < y < L$, most fibres must therefore be oriented parallel to the wall. The fibres would also tend to have preferred orientations in the flow direction. Thus, once the leading tip of the fibre reaches the slot, the fibre may turn if it is stiff, or turn and bend if it is flexible.

Fibre turning is illustrated in Figure 3.1. Here, V_u is the upstream bulk velocity parallel to the feed side of screen plate and is typically about 6 m/s. (Note: This is a bulk velocity which ignores the boundary layer at the walls. It will be used in this analysis as a characteristic velocity on the feed side of the screen.) V_s is the

bulk slot velocity which is typically about 1–1.5 m/s (see Section 2.7). If the forces and time over the slot are sufficient, the fibre will penetrate a distance Y into the slot. For the condition of $y \ll L$ and $L > W$, where W is the slot width, we can estimate Y approximately from the time spent by the fibre over the slot, W/V_u. Assuming that the fibre vertical velocity (y direction) is proportional to V_s, we can postulate a simple approximate relationship as

$$Y = k_1 \cdot \frac{W}{V_u} \cdot V_s \tag{3.1}$$

where k_1 is a constant. We should note that the above assumption is most likely to be true when y is small and L is small. If not, a more detailed analysis is required, for example taking into account that the y direction flow above the aperture diminishes from V_s with y.

- When $Y \gg L$, it is appparent that passage is very easy, yielding a passage ratio, $P = 1$. (Passage ratio is defined in Section 4.2.2).

- When $Y \ll L$, passage is not likely to occur at all, thus $P = 0$.

- When $Y \simeq O(L)$, passage may or may not occur. In this case, if we assume a specific linear relationship between Y and L, *i.e.*

$$Y = k_2 L \tag{3.2}$$

where k_2 is a constant, Equation (3.1) then becomes

$$k_2 L = \frac{k_1 W V_s}{V_u} \tag{3.3}$$

$$\frac{k_2}{k_1} = \frac{W}{L} \cdot \frac{V_s}{V_u} \tag{3.4}$$

34

The ratio k_2/k_1 reflects the degree of penetration relative to fibre length. Since we do not know values for k_1 and k_2 in Equation (3.4), we at this point may simply consider $\frac{WV_s}{LV_u}$ to be a useful dimensionless parameter in describing passage from kinematic considerations. For convenience, we call it the Penetration Parameter, P_e. Thus

$$P_e = \frac{WV_s}{LV_u} \qquad (3.5)$$

The penetration parmeter can be derived in another manner using a simple mass balance of fluid entering the slot. If the flow rate through the slot (V_sW) is related to the fraction of the upstream layer drawn into the slot, expressed as size k_3L, we obtain the material balance $V_sW = k_3V_uL$. Rearrangement of the terms in this equation also yields $P_e = k_3$, where k_3 is defined above.

In summary, the penetration parameter can be viewed as an approximate physical representation of the degree of fibre penetration into a slot or the size of the main flow relative to fibre length drawn into the slot. This analysis does not take into account the fact that a gradient of fibre concentration exists near the upstream wall, and that fibres have differing orientations in the plane of the wall as well as perpendicular to it. Thus, the penetration parameter at this state of knowledge is only linked in a general way to fibre passage. Nevertheless, it is clear that it is a potentially important grouping of variables with physical meaning.

3.2.3   Rotation

Although the above analysis is based purely on kinematic considerations, fibre behaviour is created by forces. As the leading tip of a fibre enters the entry zone of an aperture, the forces created by V_s cause turning. This turning is a combination of displacement, rotation, and bending towards the aperture entry. The strength of

these forces depend on y, V_s and W. As in the analysis of penetration, it is beyond the scope of this work to analyze rotation in detail: However, it is reasonable to assume that the penetration parameter on its own reflects the level of fibre rotation into the aperture for stiff fibres, that is, where displacement is small (as assumed by $y << L$) and where bending is insignificant.

Once the leading tip of a fibre penetrates into an aperture, the leading tip is likely to come into contact with the downstream wall of the aperture because the fibre continues moving over the entry at an upstream velocity determined by V_u. On contact with the downstream edge of the slot, V_s and V_u impose moments on the fibre with the downstream edge of the aperture as a fulcrum. As stated earlier, this behavior occurs when $Y \simeq 0(L)$. In this case, we may assume that the penetration distance, Y, can be expressed as a fraction of the fibre length that penetrates the slot. Under these conditions, there may be two distinct types of behaviour.

(a) $Y < W$

In this case, the moment on the fibre is entirely due to the hydrodynamic forces. Increases in V_u or V_s can be expected to promote rotation of the fibre into the main flow or into the slot respectively.

(b) $Y > W$

In this case, rotation of the fibre out of the aperture causes the leading tip to come into contact with the upstream wall. This introduces a wall force, F_w. This force becomes part of the moment balance. Its consequences will be discussed later.

Case (a): $Y < W$ (Figure 3.2)

If we take as an average value $k_2 = 0.5$ (see Equation (3.2) for the definition of

k_2), the above case occurs at

$$0.5L \simeq W$$

$$L/W \leq 2 \tag{3.6}$$

To determine the approximate degree of rotation, we can calculate the moments acting on the fibre by the forces which are due to V_u and V_s. Then

$$\text{Moment} = \text{Force} \times \text{distance} \tag{3.7}$$

Since fibre may momentarily cease translational motion on impact with the downstream edge of the slot, the relative velocity between the fibre and fluid may be as high as V_u or V_s. For typical values of V_u, V_s, and fibre diameter, the Reynolds number based on the fibre diameter is in the range of 40–300. This falls in the transition range between shear drag and form drag. Assuming the latter to be the case, and taking an average drag coefficient to be $C_D = 1.0$, the relative drag force is given by velocity squared. Assuming further that the angles θ_1 and θ_2 between the fibre and plate surfaces are equal, a simple relative moment balance yields

$$Y^2 V_s^2 = (L - Y)^2 V_u^2$$

on rearranging terms, we obtain

$$V_s = V_u \left(\frac{L}{Y} - 1 \right) \tag{3.8}$$

substituting $Y = \frac{k_1 W V_s}{V_u}$ from Equation (3.1) into (3.8) yields

$$V_s = V_u \left[\frac{L}{(k_1 W V_s / V_u)} - 1 \right]$$

$$V_s = V_u \left[\frac{1}{k_1 P_e} - 1 \right] \tag{3.9}$$

37

Dividing the L.H.S. of Equation (3.9) by the R.H.S. yields a measure of the relative moment causing fibre to enter the slot to that causing it to rotate out of the slot. We can call this the Rotation Parameter, R_o, where

$$R_o = \frac{V_s}{V_u} \left(\frac{k_1 P_e}{1 - k_1 P_e} \right) \qquad (3.10)$$

The dependence of R_o on P_e and V_s/V_u shown in Equation (3.10) would differ only slightly if Stokesian drag were assumed in place of form drag and angles θ_1 and θ_2 were not assumed equal. Thus, the key observation is that the kinetic parameter R_o contains the penetration parameter and V_s/V_u. Thus, the Penetration Parameter has two effects. First it plays a role in determining the penetration of a fibre into a slot. Second, it plays a role in the moment balance on a fibre coming into contact with the downstream edge of a slot, thus determining for a given level of penetration whether a fibre will rotate in or out of a slot. Given this strong influence, and the fact that P_e already contains V_s/V_u, it is reasonable to expect that the Penetration Parameter alone may suffice in many cases to characterize rotation as well as penetration.

Case (b): $Y > W$ (Figure 3.2)

The important difference here is that, upon rotation, the fibre contacts the upstream slot wall. This exerts a force F_w which contributes to the moment balance as shown in Figure 3.2. F_w can become very large. The principal impact of this added force is that an increase in V_u does not rotate the fibre out of the slot, nor does an increase in V_s necessarily rotate fibre into the slot. Rather, in the latter case, an increase in V_s may merely diminish F_w. Only when $F_w = 0$, can V_s cause rotation into the slot. More precisely, rotation into the slot occurs when counterclockwise moment (due to V_s) exceeds clockwise moment (due to V_u). Thus

Case (a): $Y < W$ Case (b): $Y > W$
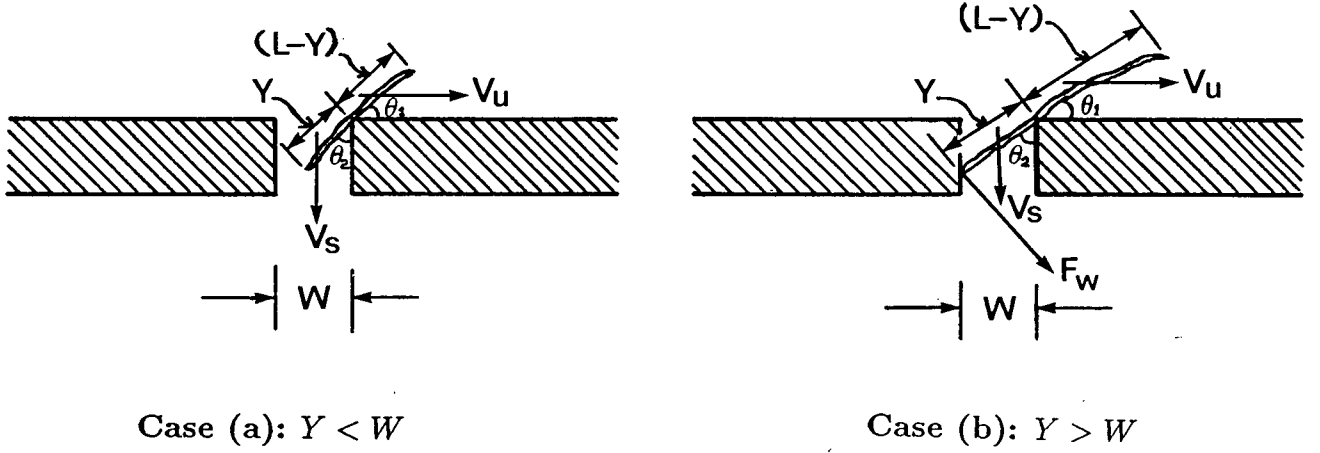
Figure 3.2: Fibre immobilized at the downstream wall of the slot. $Y > W$.

as V_s increases, no increase in passage ratio is expected until some threshold level is reached. The approximate condition at which case (b) can be expected to occur is when $Y > W$.

If $k_2 \simeq 0.5$, this occurs when $L/W > 2$.

These considerations suggest that for stiff fibres at $L/W > 2$, the Penetration Parameter is insufficient to describe fibre passage and, moreover, a threshold level of V_s/V_u may be required to cause fibre passage. It may further be noted that a large L/W and a small V_s/V_u tend to create a small value of the Penetration Parameter at which this condition will occur.

3.2.4 Bending

Up to now, the stiff fibres were considered, that is, ones that do not bend significantly over the aperture. Increasing flexibility of fibres introduces new factors into this analysis.

First, the leading tip of a fibre will bend on passing over the aperture. Su-

perimposed on rotation and translation, this will tend to increase penetration and therefore increase the likelihood of passage.

Second, on coming into contact with the downstream wall, the fibre will tend to bend as well as rotate about the downstream edge. Bending will tend to diminish the effect of rotation in causing the fibre to pass into or out of the aperture. First, when the fibre bends, the moment created by hydrodynamic forces is diminished. Second, the bending of fibres around the edge of the apertures increases normal forces between fibres and the wall in the feed flow or slot flow directions restraining fibre movement in the direction of the two principal flows. Hence there will be increased resistance to translational movement in the direction of the feed flow or the aperture flow which must occur if the fibre is to move one way or the other.

An attempt was made to derive a bending parameter to account for the above effects, but the complexity of the analysis proved to be beyond what was justifiable in this work. We can, however, derive a parameter to reflect the relative degree of bending, B_e, expressed as deflection, δ, divided by the fibre length, L. A relationship between this ratio and the hydrodynamic force causing bending $(\rho\,d\,L\,V^2)$ of a fibre of stiffness EI can be obtained from a typical expression for elastic bending of beams. Thus, B_e behaves as follows:

$$B_e = \frac{\delta}{L} \propto \frac{\rho L^3 V^2 d}{EI} \tag{3.11}$$

The parameter B_e illustrates how various factors affect bending. For example, it shows, in an approximate way, that the angle of bending (δ/L) over the downstream edge of an aperture depends strongly on fibre length, L, fibre diameter, d, fluid velocity, V, and fibre stiffness, EI. Thus fibre length and flow velocity affect all three parameters considered here: penetration, rotation and bending.

3.3 Summary

1. A simplified, approximate kinematic analysis of fibre behaviour near an aperture has yielded a Penetration Parameter that reflects the effect of key variables on fibre penetration into aperture.

2. A simple kinetic analysis of moments about downstream edge of the aperture imposed by hydrodynamic forces indicates that the Penetration Parameter modified by a velocity ratio reflects the effect of fibre rotation, and that threshold levels of V_s/V_u may be important.

3. Fibre bending appears to increase passage because of increased penetration and to decrease passage because of stapling on the downstream edge of the slot. The effect of bending depends on fibre stiffness, flow velocity, and fibre length.

4. Fibre rotation and bending involve fibre interaction with the downstream wall. It is reasonable to conclude that the parameters discussed here will also play a role in determining how fibres staple and therefore obstruct passage through a slot.

Chapter 4

Experimental Program

4.1   Fibre Properties

Wood fibres are elongated, tubular objects having irregular geometry and surface features due to differences in morphological characteristics and the pulping process used to liberate the fibres from the wood.   There are differences due to wood variability that exists naturally from tree to tree, species to species and within a tree.   For this reason, model nylon and rayon fibres were used in the experimental work of this thesis.   These fibres were available in the Department of Chemical Engineering at UBC, and were originally obtained from E.I. du Pont de Nemours & Co. and cut into lengths by Fibertex Ltd.   The fibres from this source had been used in previous investigations by Horie (H8), Gooding (G1), Soszynski (S6) and Bennington (B10).

A comparison of the properties of pulp fibres with nylon and rayon fibres is given in Appendix A. The important physical properties are summarized in Table 4.1. The nylon and rayon fibres selected for this study represent the typical length range of pulp fibres (1–3 mm).   Nylon fibres are thicker than pulp fibres and the rayon fibres have a thickness close to hardwood pulp fibres.   The nylon fibres are much stiffer than pulp fibres while the stiffness of rayon fibres is similar to that of pulp

fibres. The apparent density of nylon and rayon fibres is quite close to that of pulp fibres (see Table A.7). Thus, from a hydrodynamic point of view, synthetic fibres are reasonable approximations of pulp fibres.

4.2 Flow Loop With a Single Slot Channel

4.2.1 Description of the Experimental Set Up

The schematic of the flow loop showing the principal components of this apparatus is given in Figure 4.1. A is the reservoir in which fibre suspensions were prepared for the trial runs. The operating volume in the reservoir was about 180 litres in most of the tests. The reservoir also served as a supply tank for the pump during a trial run. Fibres were stored in water in the reservoir 24 hours in advance of any trial to ensure that no change in physical properties occured during the trial because of water absorption. Storing fibres in water for 24 hours also ensured that the suspension was at about 18–20°C in most cases. A variable speed mixer, B, was used to mix the fibre suspension uniformly and to avoid fibre settling in the tank when higher concentrations were used.

A centrifugal pump, C, driven by a 15 hp motor was connected to a variable speed drive to allow a desired flow rate to be pumped through the flow loop. D is the by-pass line which was shut off most of the time. A magnetic flow meter, E, was used to measure the flow rate. Most of the piping in the flow loop was 38 mm PVC.

The key element in this flow loop is the plexiglas test section, G, which is shown in Figure 4.2. The detailed dimensions are given in Figure 4.3. It contains a 350 mm long channel of 20 mm × 20 mm square cross section. The channel height of 20 mm corresponds to the radial distance between the rotor drum and screen

Table 4.1: Properties of the Fibres Used in the Present Study.

Fibre Identification	Fibre length (mm)			Fibre diameter dry (mm)	Stiffness $(N \cdot m^2 \times 10^{12})$
	L_n	S.Dev.	L_w		
Nylon 1 mm 15 Denier	0.993	0.017	1.046	0.043^a	329
Nylon 1.5 mm 15 Denier	1.46	0.02	1.55	0.043^a	329
Nylon 3 mm 15 Denier	3.17	0.035	3.44	0.043^a	329
Rayon 1 mm 4.5 Denier	1.018	0.005	1.113	0.02^a	3.2 (dry)
W R Cedar kraft (R12)	3.17	0.08	3.62	0.03^b	3.5^c

Denier is the weight in g of 9000 m long filaments

L_n — Arithmetic average fibre length
L_w — Weighted average fibre length by length
a — Calculated from denier and fibre density
b — Average fibre width = 0.035 mm (I1), 15% reduction during pulping
c — Average value taken for softwoods.
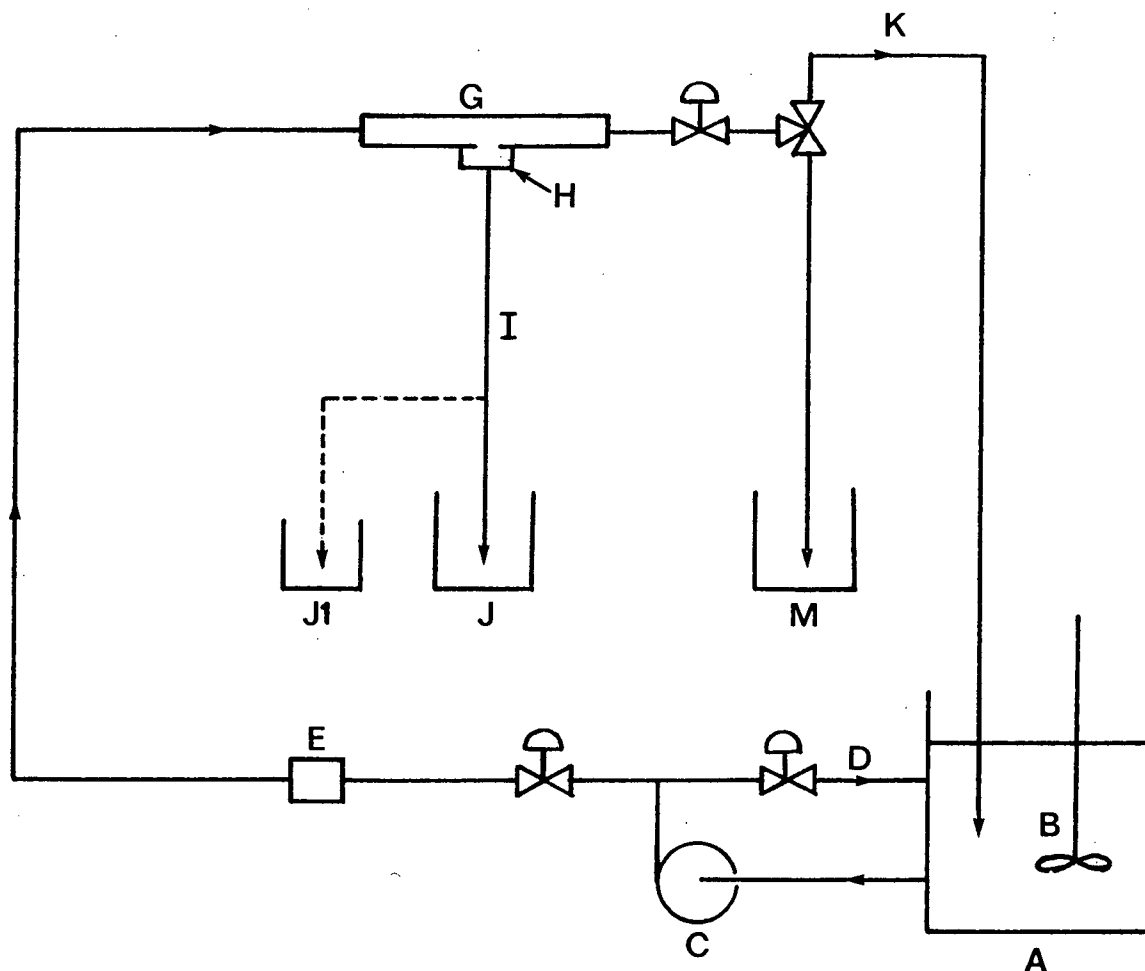
A.	Reservoir	H.	Plenum
B.	Mixer	I.	Accept Line
C.	Pump	J.	Accept Flow Container
D.	Bypass Line	J1.	Accept Sampling Receptacle
E.	Magnetic Flow Meter	K.	Reject Line
G.	Plexiglas Test Section	M.	Reject Sample Receptacle

Figure 4.1: Schematic of flow loop having single slot channel.

plate of an industrial screen with a lobed shape rotor. There is a single slot in the bottom wall of the channel perpendicular to the channel axis. This slot simulates an aperture of a pressure screen. The slot dimensions are given in Figure 4.4. Slot widths of 0.25, 0.5, 1 and 1.5 mm were used to study the effect of the ratio of fibre length to slot width (L/W) on passage ratio. In all other runs, a 0.5 mm wide slot was used. The slot was flared to a larger dimension on the discharge side as is normal with the commercial screen plates to reduce pressure losses. The velocity in this plexiglas test section could be varied from 1 m/s to 12 m/s and is similar to the velocity parallel to the screen plate of an industrial screen. It is called here the upstream velocity, V_u, which was kept constant at 6.5 m/s in most tests, except in those tests where effect of upstream velocity as a parameter was considered.

The entry to the channel was an abrupt contraction from a circular pipe of 38 mm diameter. The developing flow downstream created a flow field which, though not measured, could be estimated from similar flows reported in the literature. Lissenburg *et al.* (L6) investigated the effect of a constriction on turbulent pipe flow and measured the turbulence intensity. They found that the ratio of the turbulence velocity component to the local mean velocity in a pipe 10 diameters beyond a constriction was about 0.09 at the centre of the pipe and 0.30 very close to the wall. In our channel, the slot was located at 9.6 equivalent diameter from the channel entry. The Reynolds number in the channel based on the equivalent diameter of the channel was about 130,000 in most tests.

The flow through the slot passes into a small chamber, **H**, and then flows to a container, **J**, through a 8 mm i.d. Tygon R-3603 flexible tubing, **I**. The flexible tubing was squeezed to purge air from the test section before a trial or to clear the slot of any fibre accumulation during the trial.

The flow through the slot, and thus the pressure drop across the slot, was
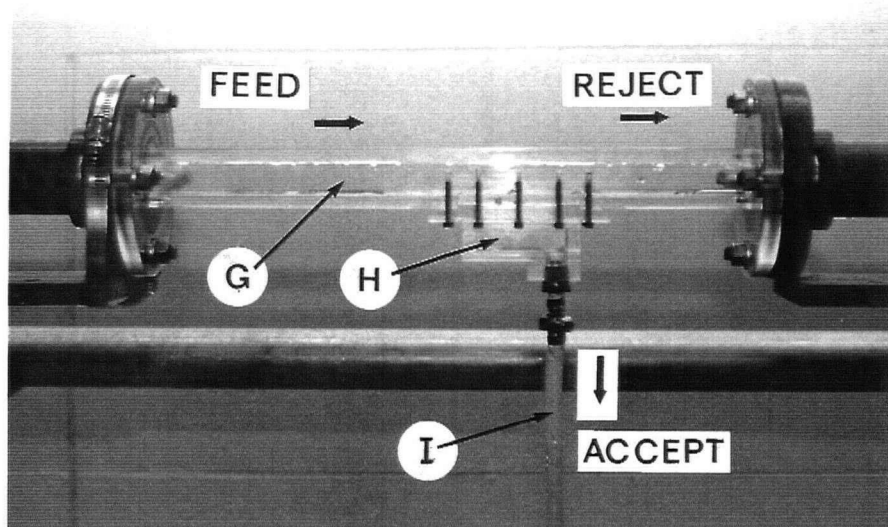
(a) Plexiglas Test Section. See Figure 4.1 for nomenclature.
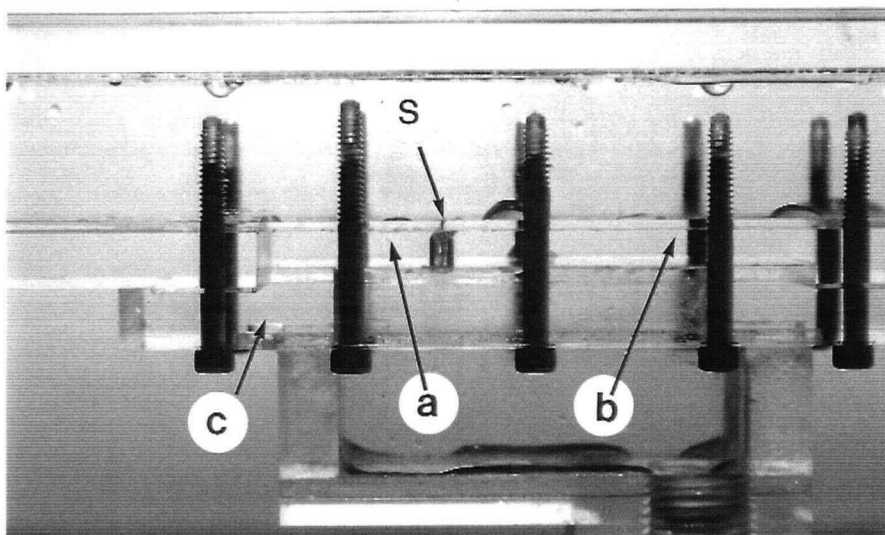
(b) Pieces a and b are to be changed to change the slot dimensions or geometry.

Figure 4.2: Single slot plexiglas channel showing details of interchangeable section.
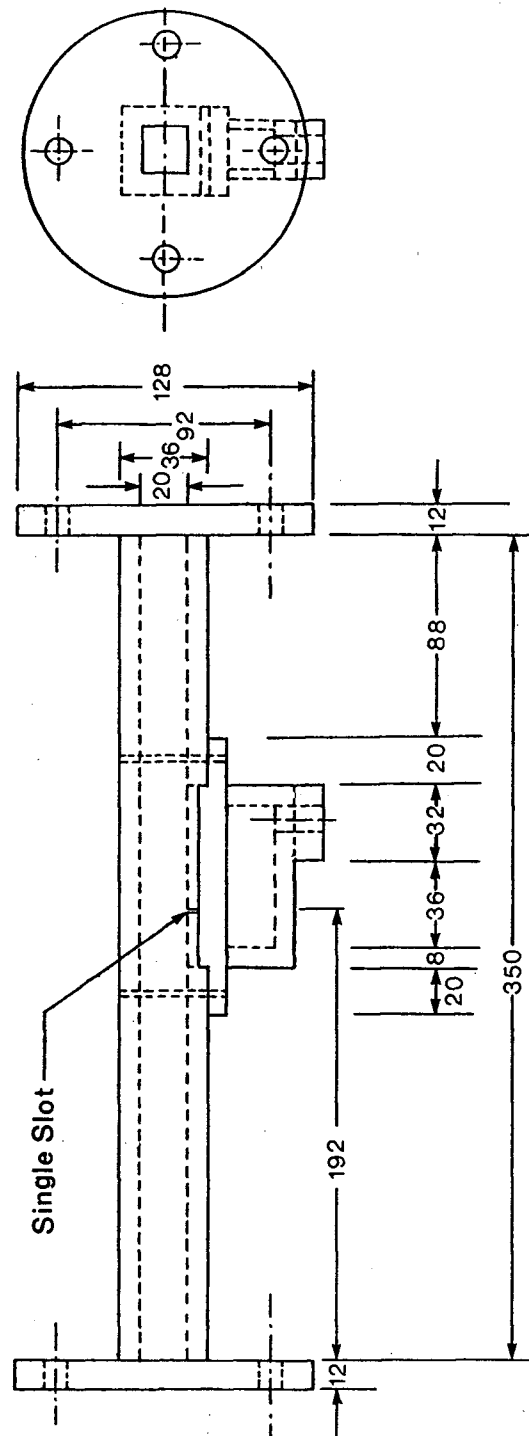
All dimensions are in mm.

Figure 4.3: Details of single slot test channel.

Smooth Slot
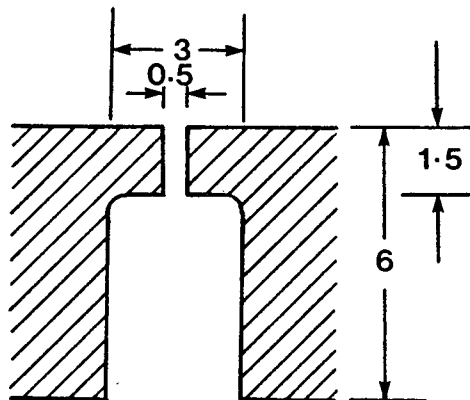
Contoured Slots

C1 Slot
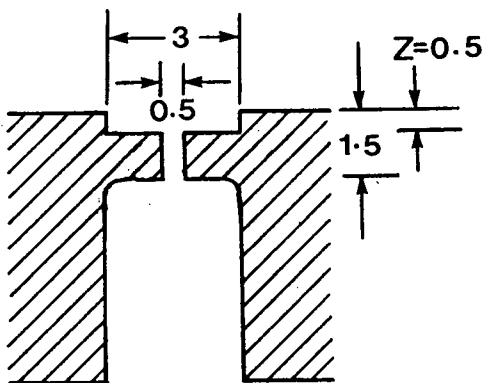
C2 Slot
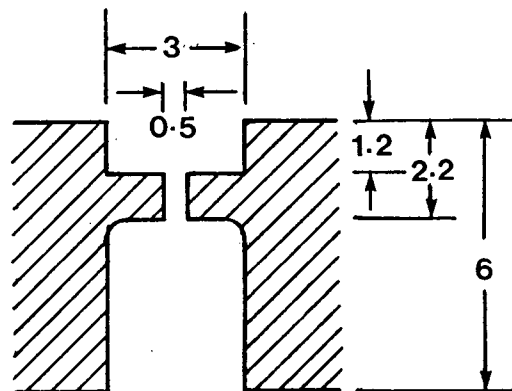
All dimensions are in mm.

Figure 4.4: Slot geometry and dimensions of smooth and contoured slots.

49

controlled by using tapered plastic inserts of different sizes in the tubing outlet. The velocity through the slot referred to throughput in these tests is the bulk velocity obtained by dividing flow rate by the slot area. For convenience, it is simply referred to as V_s, the "slot velocity". It could be varied from 0–10 m/s through a 0.5 mm wide slot.

When the desired experimental conditions were established, the samples were taken for flow rate and concentration measurements simply by moving the flexible tubing to a sample receptacle, **J1**. One trial run took about 15 minutes during which the accept sample was collected for less than 1 minute. The accept flow through the flexible tube was very small compared to the suspension operating volume in the reservoir which was about 180 litres. Due to this reason, the accept flow was not sent directly to the reservoir. However, container **J** was emptied into the reservoir as soon as about 3–4 litres of accept flow were collected.

Most of the flow from the plexiglas test section returns to the reservoir through reject line, **K**. A three-way valve in the reject line was used to sample the reject flow into the reject sample receptacle, **M**. Since this volume was large, sub-samples were taken for fibre concentration measurements.

4.2.2 Procedure For Single Slot Tests

To start with, tests were carried out at very dilute concentrations which were chosen on the basis of: (1) no fibre-fibre interaction and (2) keeping the slot unobstructed. It was found that the concentration needed for an unobstructed slot was much smaller than the upper limit of dilute concentration which can be estimated by the crowding factor, N. Such low concentrations were expressed as number of fibres/l. The relationships between the different fibre concentrations, *e.g.* number of fibres/l, volumetric concentration, mass concentration and the crowding factor,
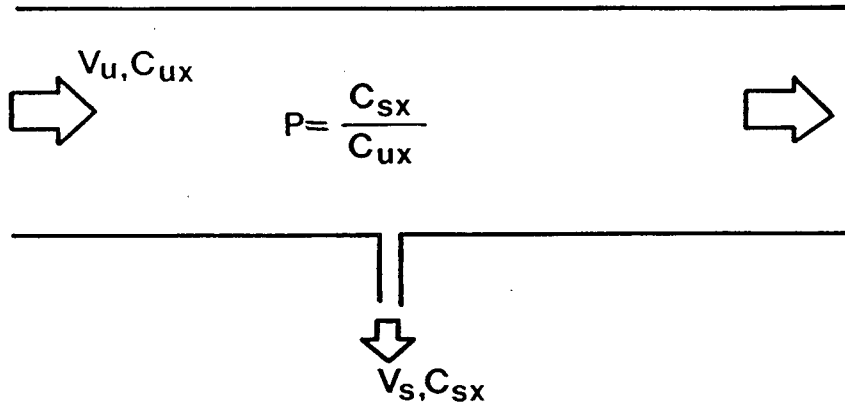
Figure 4.5: Flow adjacent to a screen plate in a pressure screen. Passage ratio (P) was defined by Gooding and Kerekes (G2).

are given in Appendix B.

The effect of key variables such as fibre length, slot width, slot velocity, upstream velocity and fibre flexibility was established by measuring passage ratios through a single slot. "Passage Ratio" is defined as the concentration of particles in the flow through an aperture divided by the corresponding concentration of particles upstream of the aperture (G2) as shown in Figure 4.5. The ratio of the former concentration to the latter describes the likelihood of a particle passing through an aperture.

The accept and feed samples were collected and the concentrations were measured either by counting the fibres manually or by using a Kajaani FS-100 Fibre Length Analyzer depending on the level of concentration. The techniques used for measuring fibre concentration are discussed in Appendix C. The experimental data for single slot tests at dilute concentrations are given in Appendix D.

The studies at dilute concentrations were then extended to higher concentra-
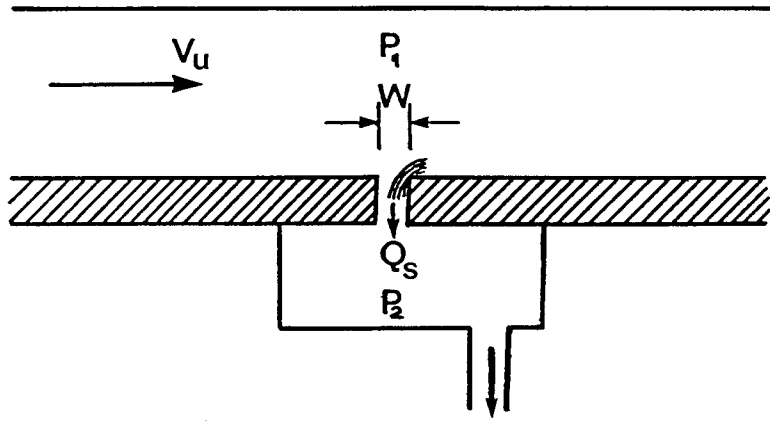
Figure 4.6: Fibre build-up at the slot entry at higher concentrations.

tions. For these tests, V_u was kept constant at 6.5 m/s and the pressure on the feed side of the slot, P_1, was maintained equal to that used at dilute concentrations (see Figure 4.6). The pressure on the accept side, P_2, therefore depended on the flow rate through the slot which was set by using a given plastic insert in the outlet of the flexible tubing. In other words the pressure drop across the slot (P_1-P_2) was set to achieve the required flow rate, Q_s, for an unobstructed slot.

With an increase in feed concentration, fibres start accumulating in the slot. This fibre accumulation results in increased flow resistance and thus reduces the flow through the slot. Since the flow through the slot was less than 5% of the main flow, this additional resistance did not affect P_1 and, hence, the feed flow acted as an "infinite reservoir". With increased feed concentration, accept flow through the slot was measured while upstream conditions, $i.e$ V_u and P_1, were kept constant. Passage ratios were measured by weighing the accept and feed samples instead of counting the fibres. As this flow loop with a single slot has no means for purging the slot, the latter eventually gets plugged at higher concentrations. The concentration at which the slot gets completely plugged was experimentally found

as well as the factors which affected this concentration. The experimental data for single slot tests at higher concentrations are given in Appendix D.

In the above studies, the plane of entry to the slot was in the same plane as the supporting plate and both were parallel to the upstream flow. For convenience, this is called "a smooth slot" and is shown in Figure 4.4. In the recent past, contoured screen plates have been used in the industry. These can be of two generic types: one in which the plane of the slot is flush with the wall but the plate is a series of ridges; another in which the plate is parallel to the flow but the entry plane to the slot is recessed from this plane with an opening of larger size between the slot entry plane and the plate surface (see Figure 2.5). The robustness of the findings for a smooth slot were tested on 2 slots of the latter type (also shown in Figure 4.4) at dilute concentrations, i.e in an unobstructed slot as well as at higher concentrations. Passage ratios of contoured slots were compared with those of a smooth slot to see whether the findings for the smooth slot hold with this change in entry geometry.

4.2.3 Photography

To characterize fibre stapling qualitatively, fibre accumulation at the slot entry was photographed using an Olympus OM–2, 35 mm camera, with back illumination from 300 watt quartz bulbs shining through a light diffuser. KODAK black & white film of ASA 400, TMAX type was used.

The movement of fibre flocs was observed by high speed photography using a Kodak Ektapro 1000 Motion Analyzer high speed video camera manufactured by the Eastman Kodak company. It records at 30, 60, 125, 500 and 1000 frames per second, and 1 to 6 pictures per frame. The system can record up to 30 seconds at 1000 frames per second. The system can play back tape in slow motion or one

frame at a time. All images can be viewed live or replayed on the system's monitor. The diffused light from back illumination by a 12 V halogen bulb, gooseneck 700 series, was used.

4.3   Flow Loop With a Sectional Screen

4.3.1   Description of the Experimental Set Up

Tests were also carried out in an apparatus more closely simulating a commercial pressure screen, which for convenience is called the "Sectional Screen" (SS). Figure 4.7 shows a photograph of the sectional screen and its flow loop. The fibre suspension for the tests was prepared in a reservoir, **A**, having a capacity of 130 litres. A variable speed mixer, **B**, was used to mix the fibre suspension properly and avoid fibre settling in the tank when higher concentrations were used. **C** is an open-impeller centrifugal pump used to pump the fibre suspension through feed piping, **F**, to the sectional screen. The by-pass line, **D**, was shut off most of the time. The feed flow rate was measured by a magnetic flowmeter, **E**.

The sectional screen itself, **G**, is in essence a plexiglas cross-section of a commercial screen with inside diameter of 381 mm and axial length of 46 mm. Its screen plate, **H**, is also of plexiglas and has an outside diameter of 305 mm and a thickness of 6 mm. The screen plate has ten slots of 0.5 mm width. Its rotor, **I**, has two blades with foil type tips similar to the one used in a commercial pressure screen. The rotor is driven by a 2 hp D.C. motor, **J**, having the provision for speed control, **K**. A variety of rotors and screen plates can be accomodated in the SS. The photographs in Figure 4.8 give a closer view of the SS showing the rotor and slots of the screen plate. The detailed dimensions are given in Figure 4.9. The flow field inside the SS is mainly determined by the tangential velocity created by the rotor as it is the case in commercial screens. For this reason, feed inlet and reject

54

A. Reservoir

B. Mixer

C. Pump

D. Bypass Line

E. Magnetic Flow Meter
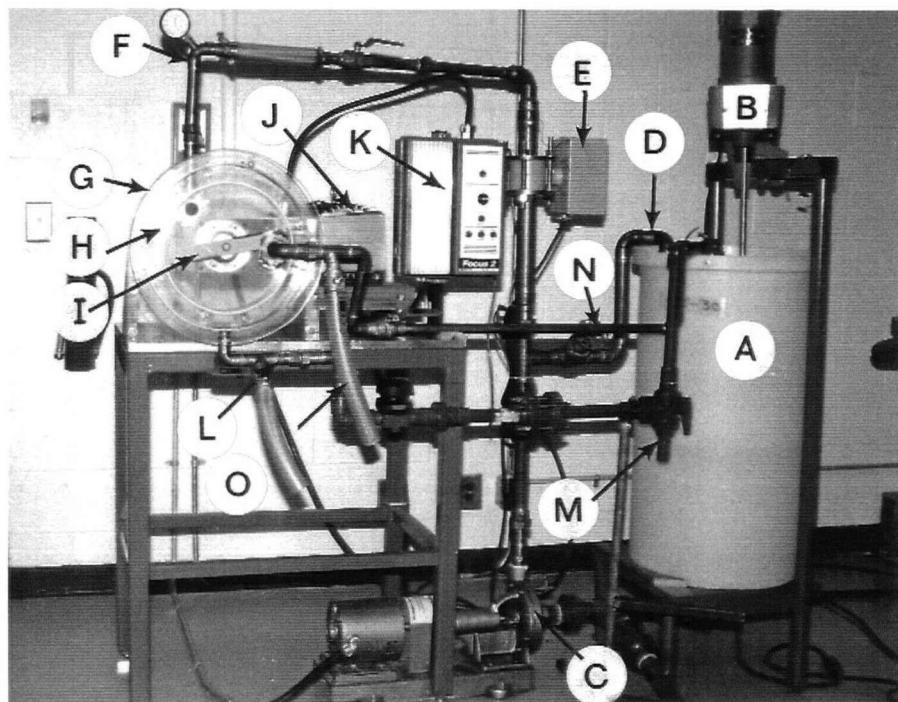
F. Feed Line

G. Sectional Screen

H. Screen Plate

I. Rotor

J., K. Variable Speed D.C. Drive

L. Accept Line

M. Accept Sampling Line

N. Reject Line

O. Reject Sampling Line

Figure 4.7: Sectional screen flow loop.
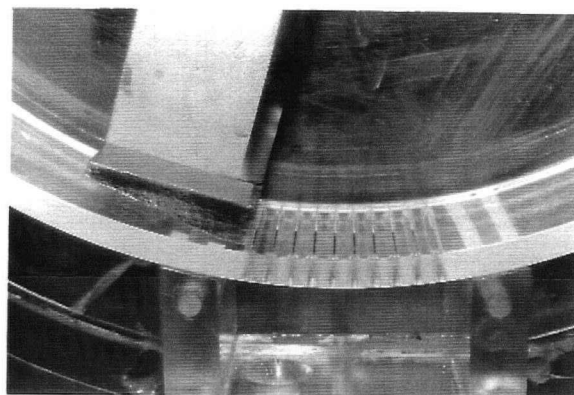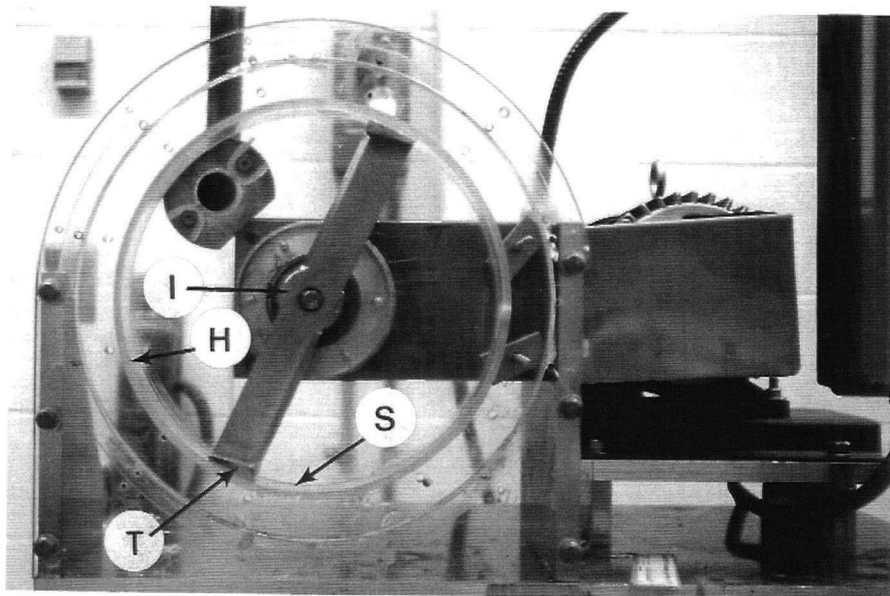
H – Screen Plate   S – 0.5 mm wide slots
I – Rotor   T – Tip of the rotor

Figure 4.8: Sectional screen with the top cover removed. Rotor tip and the slots are clearly shown.
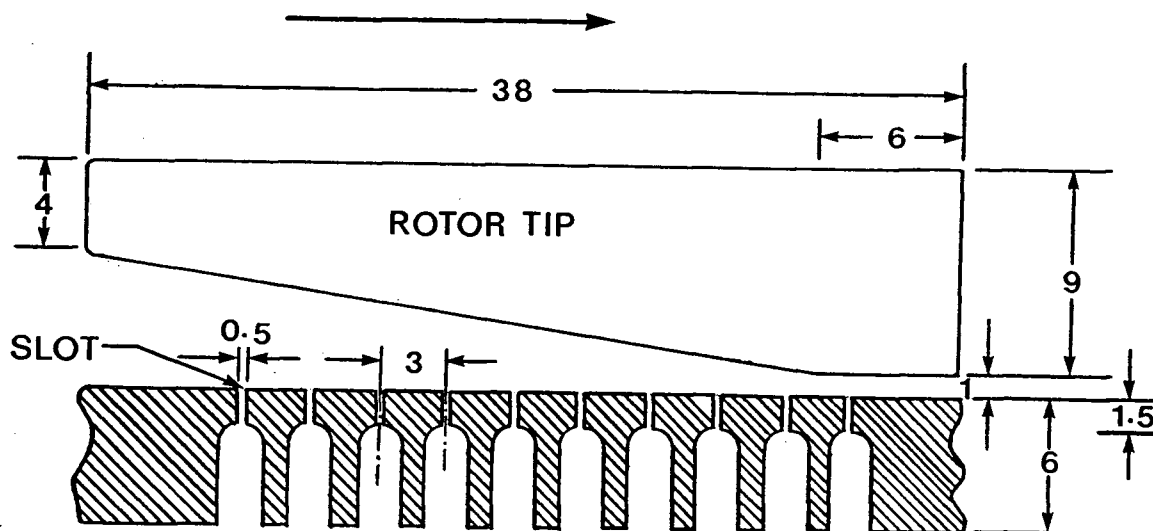
Figure 4.9: Details of rotor tip and slots in the screen plate.

outlet ports were so located as not to have any influence on the flow that reached the slots. The operating rotor tip speed was 3–15 m/s.

The accept flow through the slots passes into a small chamber and then flows to the reservoir via accept line, **L**. The accept flow was controlled by a diaphragm valve in the accept line. The nominal velocity through the slots could be varied in the range of 0–3.5 m/s. A three-way valve in the accept line was used to collect the accept sample for flow and concentration measurements. The reject flow from the screen passes to the reservoir through reject line, **N**. The reject sample was collected by opening the valve in the reject sampling line, **O**, while fully closing the valve in the reject line.

4.3.2 Procedure

The objective was to test the robustness of the findings for a single slot channel under conditions more representative of real pulp screens. To accomplish this, passage ratios were also measured through a 0.5 mm wide single slot in the screen plate of the SS at dilute concentrations. The accept flow piping of Figure 4.7 was modified to accomodate the 8 mm flexible tubing in the accept port attached to the chamber which receives the accept flow through the slot. To control the accept velocity through the slot, plastic inserts of varying sizes were used in the tubing outlet in the same way as was done in case of the single slot channel tests. The bulk velocity through the slot could be varied in the range of 0–4 m/s. A rotor speed giving a tip speed of about 6.5 m/s, equal to V_u in case of single slot channel, was used for comparing results.

Passage ratios were also measured through multiple slots in the sectional screen at dilute concentrations. A screen plate having ten slots in series was used. The width of the slots was 0.5 mm and the distance between the centres of two adjacent slots (slot spacing) was 3 mm. Passage ratios were then compared with the results obtained in the single slot channel and in the SS with a single slot. The effects of slot velocity, rotor tip speed and fibre type on passage ratio were examined next. Passage ratios were measured at higher suspension concentrations. The plugging concentrations for nylon and rayon fibres were determined, and also the effect of higher rotor tip speeds in keeping the slots purged at a higher concentration. The experimental data for the SS tests are given in Appendix E.

58

Chapter 5

Results and Discussion

5.1 Studies in a Single Slot Channel at Dilute Concentrations

5.1.1 Effect of Fibre Properties and Flow Variables

The influence of fibre length, fibre flexibility, slot width, slot velocity and upstream velocity was investigated in a flow loop having a single slot plexiglas test section, which has been described in Section 4.2. Passage ratios through an unobstructed slot were determined by measuring the accept and feed concentrations using either a Kajaani FS–100 fibre length analyser or counting the fibres manually (see Appendix C) depending upon the feed concentration used.

Effect of Slot Velocity and Fibre Length

Figure 5.1 shows the effect of slot velocity, V_s, on the passage ratio at an upstream velocity (V_u) of 6.5 m/s with fibre length as a parameter. The range of slot velocities was extended far beyond that expected in an industrial pressure screen (1–1.5 m/s). This was done in order to exaggerate and clarify the effect of increased slot velocity on the passage ratio. It can be seen that the passage ratio generally increased with increase in slot velocity.
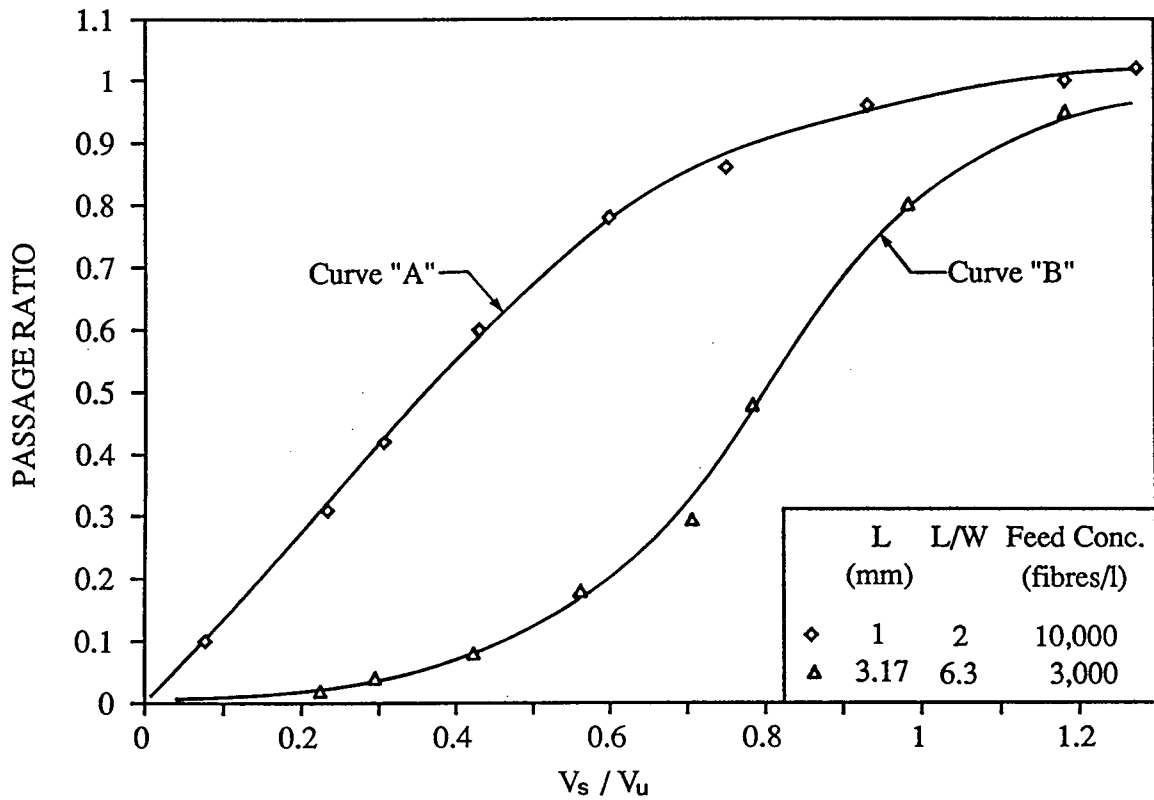
Figure 5.1: Effect of slot velocity and fibre length on passage ratio of nylon fibres. The error bars are shown in Figure C.1 (see section C.2 of Appendix C).

Nature of Passage Ratio Curves for Short and Long Fibres

Figure 5.1 also shows a significant difference in the relationship between the passage ratio and the slot velocity for short 1 mm nylon fibres and long 3 mm nylon fibres for a 0.5 mm wide slot. At a given slot velocity, the longer fibres have lower passage ratios. More importantly, there is a distinct difference in the shape of the passage ratio curves for short and long stiff fibres. For short fibres, the shape appears to be an exponential relationship between the passage ratio and the slot velocity. For convenience, we shall call this shape "A". In contrast, for longer fibres, an S-shaped curve, similar to a cumulative probability distribution curve is obtained. For convenience, we shall call this curve shape "B". The existence of these two distinct shapes of curve was suggested by the data of Gooding (G1), but the present data show these trends conclusively.

The above findings of an "A" curve and a "B" curve are of considerable industrial importance because the separation of two sizes of fibres is often the key objective in screening. Therefore conditions which lead to the maximum difference in passage ratio between two types of fibres is a key design target in probability screens. It is obvious that having accept material follow curve "A" and reject material curve "B" is likely to lead to larger separation efficiencies than if both accept and reject material follow the same shape of curve.

Postulated Explanation for the Differences in the Nature of Curve A and Curve B Based on Theoretical Analysis

The difference in the two curves of Figure 5.1 may have several explanations. The longer fibre may have fewer fibres near the wall. A threshold V_s may be therefore required to get any significant penetration. Once penetration occurs, there may

also be substantial differences in fibre behaviour with regard to fibre immobilization on the downstream edge of the slot. As postulated in Section 3.2.2, fibre contact with the slot and its subsequent rotation on the downstream wall of the slot is also an important factor in determining passage and in stapling. As described in Appendix F, V_s/V_u is a key factor in deciding the mode of stapling. In the ranges of V_s/V_u studied here, fibres were observed as vertical staples on the downstream edge of the slot even though fibres continued to pass through the aperture. At $V_u = 6.5$ m/s and V_s in the range of 0.5–6 m/s, fibres contact the downstream edge of the slot as a fulcrum as shown in photographs of Figure 5.2 which also show the difference in the way 1 and 3 mm nylon fibres contact the slot.

For case (a), $L = 1$ mm giving $L/W = 2$ since $W = 0.5$. Thus, as described in Section 3.2.2, fibres do not physically contact the upstream wall of the slot when rotating over the downstream edge. Although the trajectories of fibres were not filmed, this behaviour is illustrated by the nature of stapling in Figure 5.2(a). For this case, it was postulated that passage ratio will be strongly affected by V_s/V_u. Indeed, this is shown from the shape of curve "A" for which the passage ratio increases with V_s from zero in the form of a power law relationship.

For case (b), $L = 3$ mm giving $L/W = 6$ since $W = 0.5$ mm. Also, because $Y > W$, fibres in this case can physically contact the upstream slot wall when rotating over the downstream edge. This is indicated by the nature of stapling shown in Figure 5.2(b). For such conditions, a threshold V_s/V_u would be required to induce increased passage. The existence of such a threshold is evident from the shape of curve B in Figure 5.1. There is no appreciable increase in passage ratio until V_s/V_u attains a value of about 0.45. Thereafter, the passage ratio increases with increased V_s/V_u at a much faster rate, and at $V_s/V_u > 1$, the passage ratios of the 1 and 3 mm nylon fibres are almost the same. This difference is also evident
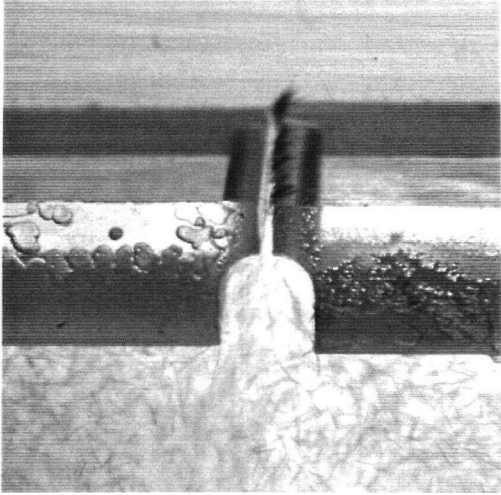
(a) 1 mm nylon fibres.
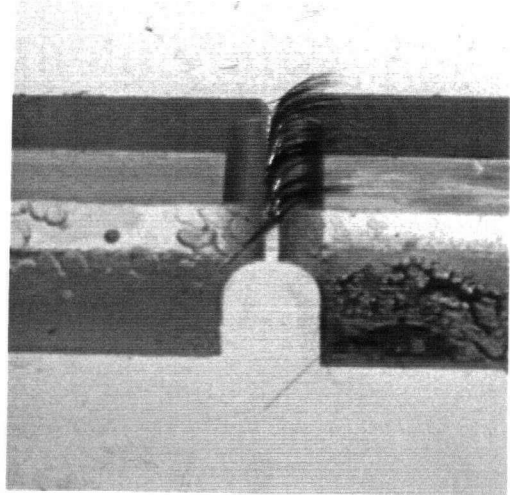
(b) 3 mm nylon fibres.
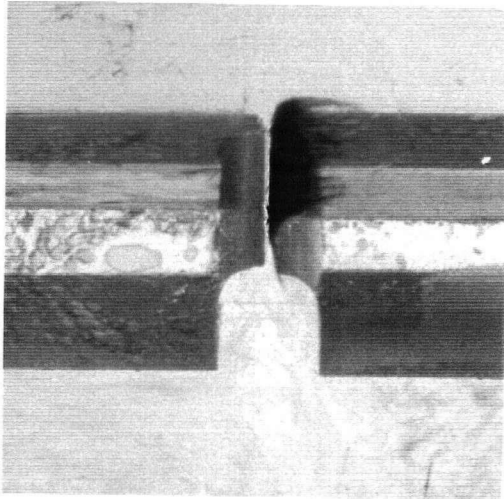
(c) 1 mm rayon fibres.
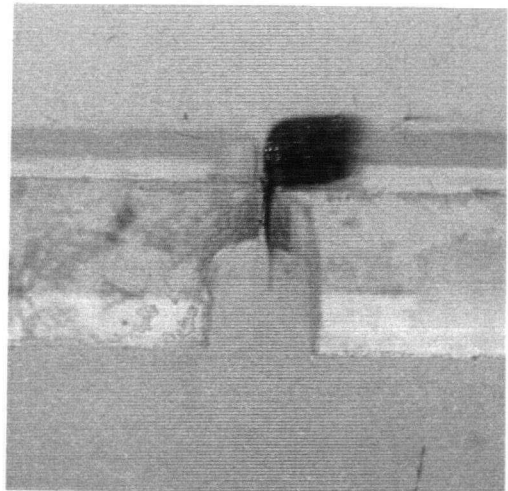
(d) Kraft (R12) W R Cedar.

Figure 5.2: Vertical staples on the downstream edge of a 0.5 mm wide slot. $V_s/V_u \simeq$ 0.4.
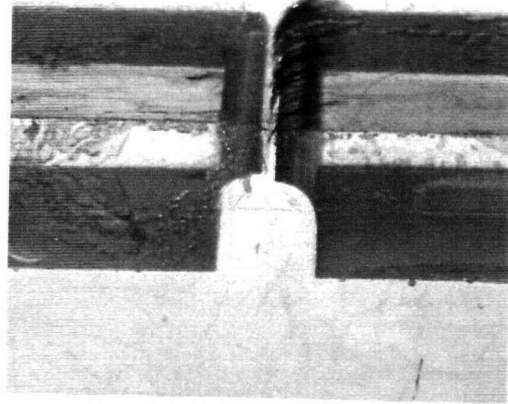
Figure 5.3: 3 mm nylon fibres on the downstream edge of a 0.5 mm smooth slot. $V_s/V_u = 0.8$.

by comparing the photographs of Figure 5.2(b) with that of Figure 5.3. In the latter case, fibres now do not physically contact the upstream edge of the slot due to higher V_s, and thus $F_w = 0$.

The above postulated explanation of curves A and B based on the "slot wall effect" does not constitute a proof that this is the factor responsible for the difference in the natures of curve A and curve B. The complex effect of upstream factors that affect penetration must also be considered. However, the logic of the analysis, the nature of the passage ratio data, and observations of stapled fibres strongly suggest that the "slot wall effect" is an important factor in determining curve A or curve B behaviour.
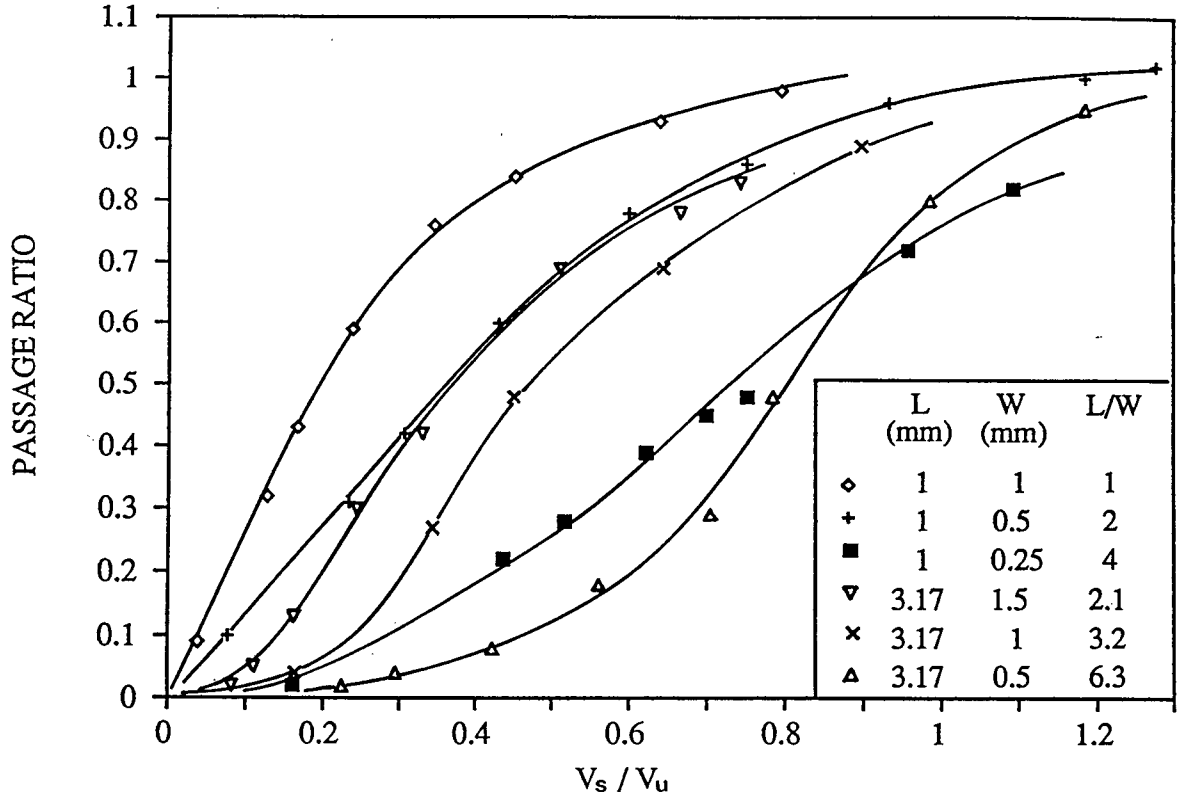
Figure 5.4: Passage ratio of nylon fibres against V_s/V_u showing the effect of L/W on the shape of passage ratio curves.

Ratio of Fibre Length to Slot Width (L/W)

The dependence on L/W of curve A and B behaviour was further examined by using slot sizes of 0.25, 0.5 and 1 mm for 1 mm nylon fibres, and 0.5, 1 and 1.5 mm for 3 mm nylon fibres. The results are shown in Figure 5.4. Passage ratios are plotted as a function of L/W against V_s/V_u, although V_u was 6.5 m/s in all the cases.

It is evident from Figure 5.4 that for a given fibre length, passage ratio at a given V_s/V_u decreased as the slot size decreased. Also, at a given V_s/V_u, passage ratio increased with decreasing L/W. Most important, the shape of passage ratio curve changed from a "B" type to "A" type over this range of L/W, specifically

around $L/W = 2$–3. This was the range suggested earlier at which the "slot wall effect" was expected to become important. This value of L/W therefore appears to be the useful criterion to determine whether a stiff fibre follows curve A or curve B behaviour, *i.e.* curve A at $L/W \leq 2$ and curve B at $L/W > 2$. The data of Figure 5.4 also suggest two other important findings: (1) the largest difference between curves occurs at $V_s/V_u \simeq 0.5$ and (2) at $V_s/V_u \geq 0.9$, the passage ratio approaches 1 for both types of curve behaviour.

In examining Figure 5.4, it may be noted that for a 0.25 mm slot, the S shape is distinctly less pronounced than that for 1 mm slot, despite the fact that the former has a higher L/W. This is probably due to the growing importance of factors such as slot entry radius, smoothness of slot edges, and machining factors owing to the very small dimensions of the slot width.

Role of Upstream Velocity

The effect of varying upstream velocity is shown in Figure 5.5 for 1 mm nylon fibres. It is apparent that the curves shifted in magnitude but their nature remained of type A. In general, passage ratios at a given slot velocity were higher for lower V_u. There was no significant difference in the change in passage ratios with the change in slot velocity in the range of upstream velocity considered here.

Earlier in our analysis, it was postulated that P_e would be a good dimensionless number to correlate passage ratios. This is evident from Figure 5.6 which shows that all the passage ratio data for curve A ($L/W \leq 2$) correlate very well with P_e. Indeed, we can obtain the following empirical relationship for the passage ratio:

$$P = 1 - 1.33e^{-5.7P_e} \qquad R^2 = 0.90 \qquad (5.1)$$

The data do not correlate better with the rotation parameter, which includes
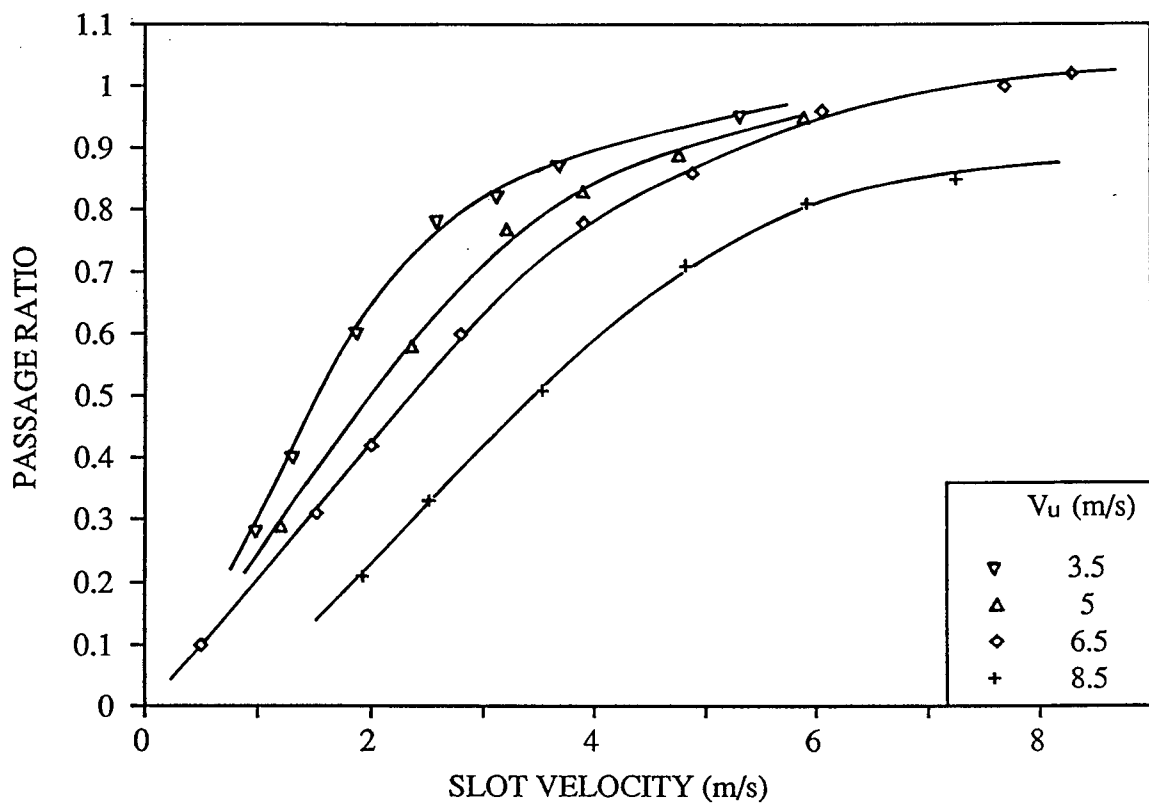
Figure 5.5: Passage ratio of 1 mm nylon fibres against V_s showing the effect of upstream velocity (V_u). Feed concentration = 12,500 fibres/l. (N = 0.006).
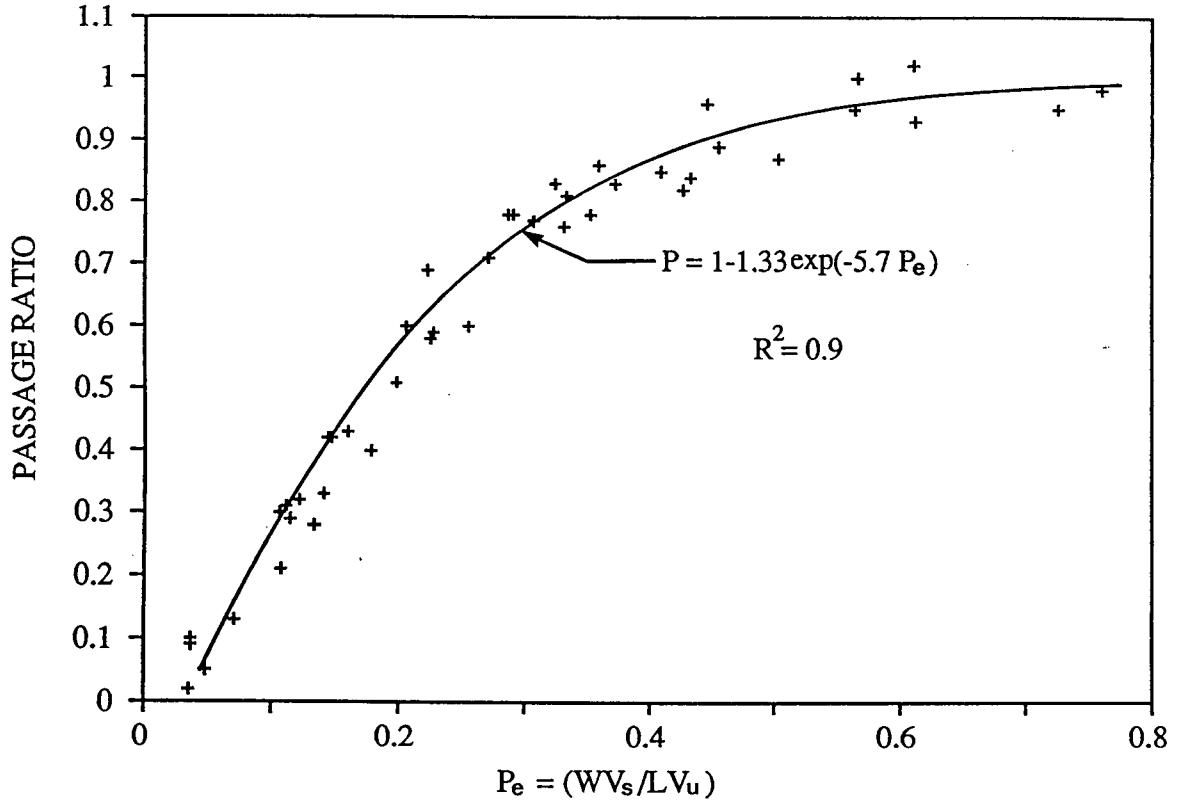
Figure 5.6: Passage ratio data for type "A" curves versus penetration parameter $(\frac{W}{L} \frac{V_s}{V_u})$.

V_s/V_u, a term resulting from kinetics. Also, the inclusion of a bending parameter does not improve the correlation. For example, if we consider the effect of B_e as a power law relationship or a linear additive term with P_e, the following empirical correlations are obtained:

$$P = 0.175 + 1.42P_e + 0.0038B_e \qquad R^2 = 0.84 \tag{5.2}$$

and

$$P = 2.2(P_e)^{1.02}(B_e)^{-0.018} \qquad R^2 = 0.85 \tag{5.3}$$

The good R^2 in Equation (5.1) compared to (5.2) and (5.3) shows that the data of curve A are well explained by kinematic considerations or simple flow splitting.

This suggests that passage in this range is strongly governed by the upstream conditions.

For 3 mm nylon fibres, the effect of varying V_u on passage ratio is shown in Figure 5.7. Here too, the passage ratio curves shifted in magnitude but the shape of curves remained essentially of type B. Moreover, in addition to a shift in magnitude, the S-shape of the curve became a more pronounced, tending more towards a step function increase at low upstream velocities. On the other hand, at high upstream velocity, the same absolute change in slot velocity had a smaller effect in increasing the passage ratio. There was a spread in data when passage ratios were plotted against P_e as shown in Figure 5.8. The following correlation is obtained when passage ratio data is fitted to the flow splitting model:

$$P = 1 - 1.45e^{-8.68P_e} \qquad R^2 = 0.62 \qquad (5.4)$$

A poor R^2 shows that unlike the case for Equation (5.1), P_e alone is not sufficient to explain the data of curve B. The correlation was not improved by using V_s/V_u as an additional parameter in the correlation. However, inclusion of B_e in the same form as in Equations (5.2) and (5.3), gave the following empirical correlations:

$$P = -0.141 + 3.31P_e + 0.00346B_e \qquad R^2 = 0.94 \qquad (5.5)$$

$$P = 91.2(P_e)^{3.97}(B_e)^{0.37} \qquad R^2 = 0.90 \qquad (5.6)$$

Comparison of Equations (5.5) and (5.6) with Equations (5.2) and (5.3) shows that unlike the earlier case, addition of B_e term to P_e improves the correlation significantly for the passage ratio data of curve B behaviour.

Effect of Fibre Flexibility

All data described thus far are for nylon fibres having the same stiffness ($EI = 329 \times 10^{-12}$ Nm^2). Thus, B_e was changed as a result of changes in fibre length

69
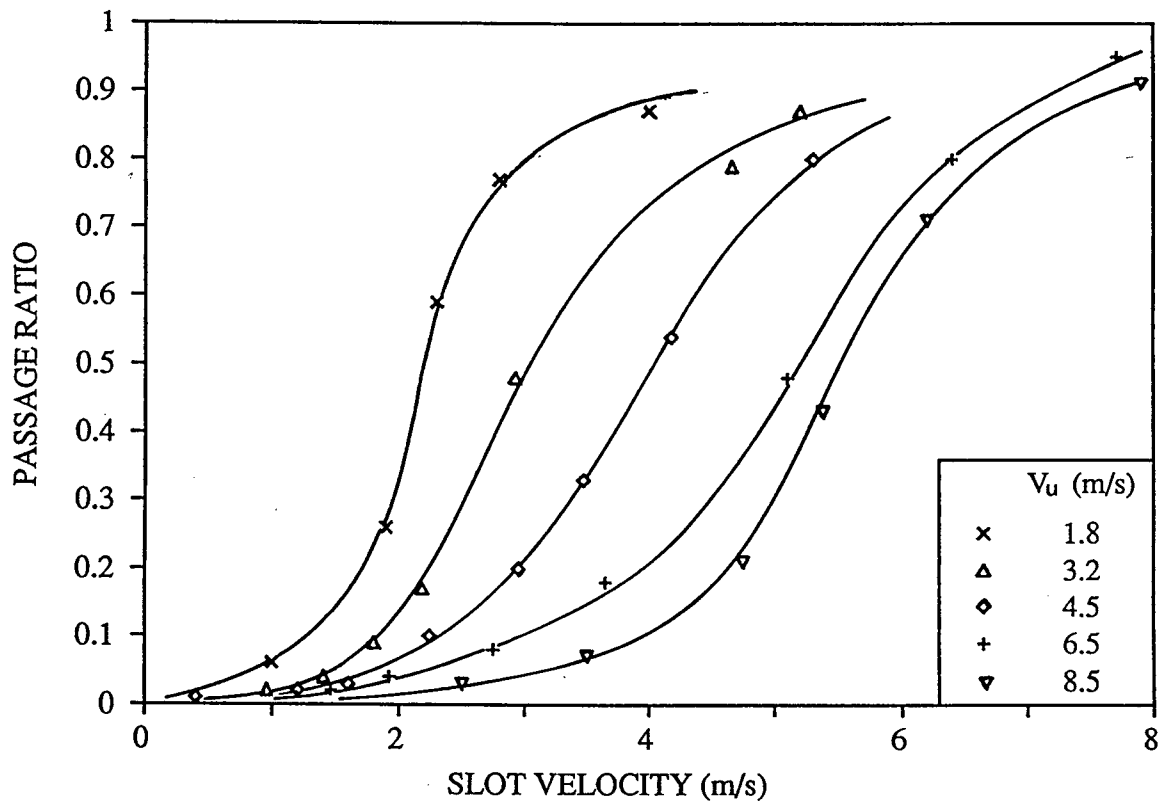
Figure 5.7: Passage ratio of 3 mm nylon fibres against V_s showing the effect of upstream velocity (V_u). Feed concentration = 3,000 fibres/l ($N = 0.06$).
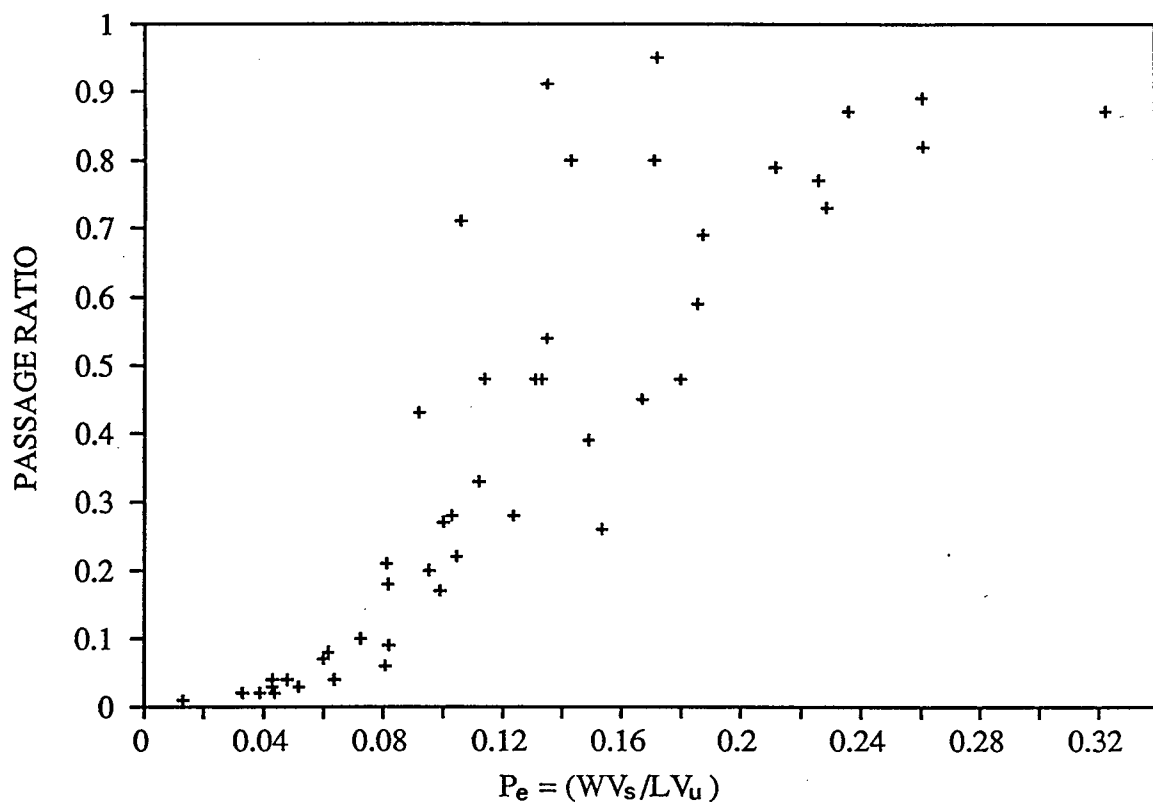
Figure 5.8: Passage ratio data of type "B" curve against Penetration Parameter $(\frac{W}{L} \frac{V_s}{V_u})$.

and velocity only. To explore the effect of stiffness and diameter, rayon and pulp fibres which are about 100 times more flexible than the nylon fibres, *i.e.* $EI = 3.2 \times 10^{-12}$ Nm^2 and $EI = 3.5 \times 10^{-12}$ Nm^2 respectively (see Table A.6) were tested.

Figure 5.9 shows that the short flexible rayon fibres having $L/W < 2$ also gave a type A curve, with a slightly higher passage ratio than the stiffer nylon fibres. Thus, even for flexible fibres, $L/W \simeq 2$ yields type "A" behaviour. The similarity to the nylon fibres suggests that the penetration parameter and the correlation of Equation (5.1) would hold in this case as well.

The only long ($L/W > 2$) flexible fibres tested were the pulp fibres having a weighted average length of 3.6 mm. These fibres yielded a significantly higher passage ratios than the stiffer 3.2 mm long nylon fibres. Moreover, it showed a distinct shift towards type "A" behaviour, with only a slight trace of "B" behaviour as shown in Figure 5.9. From this very limited data, it would appear that stiffness as well as L/W determines the existence of type "A" or type "B" behaviour. The bending parameter may be used to ascertain if this is the case. Table 5.1 gives the values of the bending parameter calculated by using a representative value of velocity as 6 m/s. For long flexible fibres, $B_e = 1.2 \times 10^4$, whereas it is 3.2×10^2 for 1 mm rayon fibres. In contrast, the corresponding value of B_e for 1 mm and 3 mm nylon fibres is 5.4 and 2×10^2 respectively. These data indicate that the "B" type behaviour occurs when both $L/W > 2$ and B_e is less than some critical level. All that can be said here is that when $B_e \leq 2 \times 10^2$, "B" behaviour occurs and that, when $B_e \geq 1.2 \times 10^4$, it appears not to occur. Thus, the correlations of Equation (5.5) and (5.6) for stiff fibres are valid only over a low range of B_e, which at a minimum is $B_e < 2 \times 10^2$.

Physical explanations for the effect of flexibility may be postulated. Bending

Table 5.1: Bending Parameter (B_e) at a Velocity of 6 m/s.

Fibre Type	B_e
1 mm nylon	5.4
3.2 mm nylon	2×10^2
1 mm rayon	3.2×10^2
3.6 mm kraft pulp fibres (R12)	1.2×10^4

affects the passage ratio in several ways. The photographs of Figure 5.2(a) and (c) show that 1 mm flexible rayon fibres bend more than 1 mm stiff nylon fibres under identical velocity conditions. Due to more bending, 1 mm rayon fibres probably follow the fluid streamlines and penetrate the aperture with greater ease and result in higher passage ratio. Stapling causing slot plugging is not of any importance here as a very dilute fibre concentration ($N = 0.02$) was used.

The passage ratio of 3.6 mm flexible kraft fibres increased with V_s/V_u from 0 while 3.2 mm nylon fibres required a threshold V_s/V_u before an appreciable increase in passage ratio was achieved. A possible explanation for a threshold V_s/V_u for 3.2 mm stiff nylon fibres was given in Section 5.1.1. As suggested in our analysis, more bending will cause the 3.6 mm flexible kraft fibres to penetrate more into a slot. Because of bending, fibres do not contact the upstream wall of the slot. This is evident from the photograph of Figure 5.2(d). This means that no force is exerted by the wall on long flexible fibres. The passage ratio thus increases with an increase in V_s/V_u with no threshold conditions due to more bending of flexible
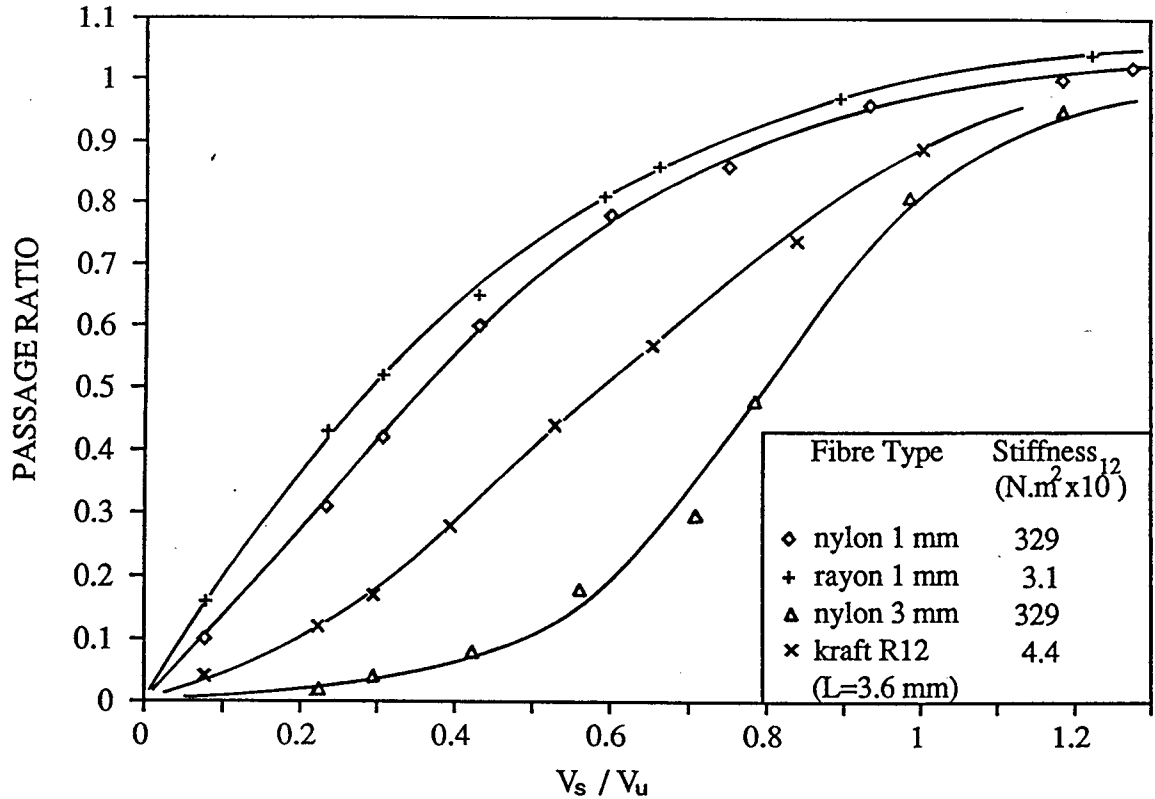
Figure 5.9: Passage ratio versus V_s/V_u showing the effect of fibre flexibility for stiff (nylon) and flexible (rayon and kraft pulp) fibres of similar average fibre lengths. $V_u = 6.5$ m/s and $W = 0.5$ mm.

fibres which follow the fluid streamlines. Here too, stapling may not affect the passage of fibres as a dilute fibre concentration ($N = 0.08$) was used.

5.1.2 Comparison With Other Studies

The only known data to which these results may be directly compared are those of Gooding (G1). These data are compared in Figure 5.10. As is evident, the agreement is good. The trend of these results is also consistent with other laboratory studies and industrial pulp screening data (F4,S2,Y1) in which, for fibres of equal length, more flexible fibres yield a higher passage ratio. For fibres of equal flexibility, shorter fibres yield higher passage ratios.
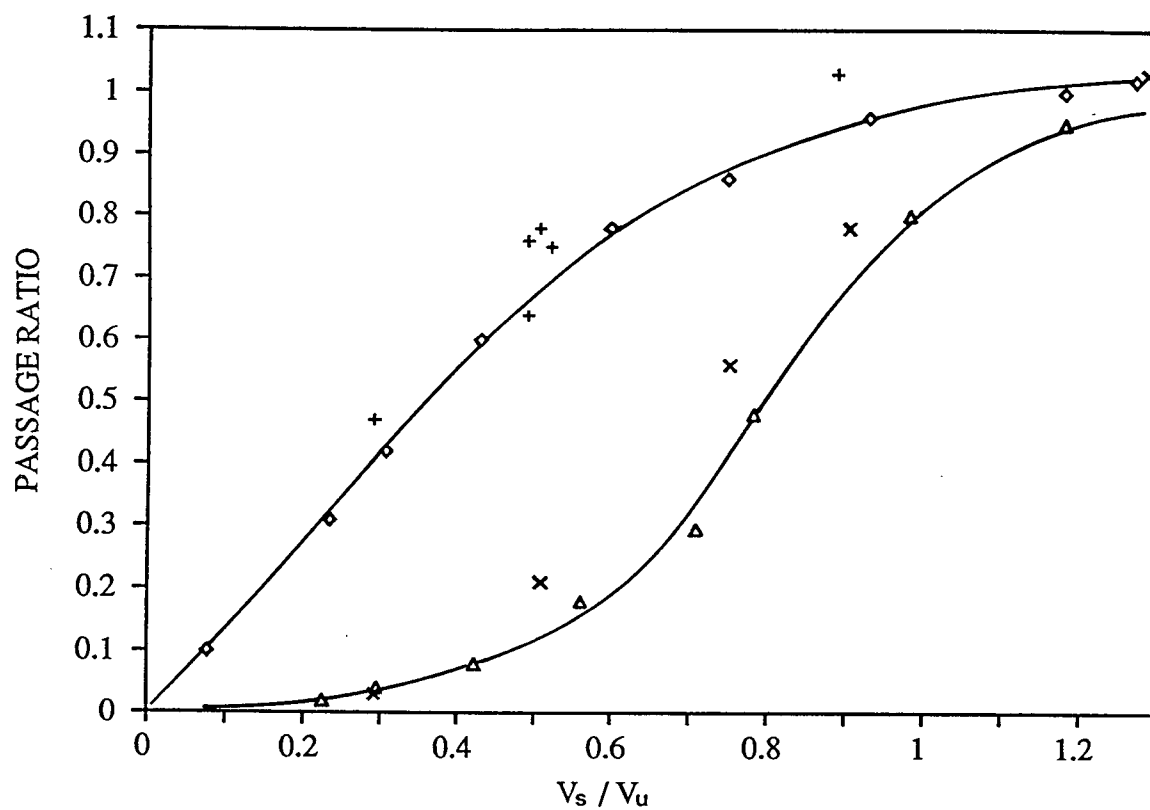
Figure 5.10: Comparison of the present study with Gooding's (G1) data. The lines are drawn through the data obtained in the present study. Gooding's data are shown by symbol (+) for 1 mm nylon and by symbol (×) for 3 mm nylon fibres.

In spite of the significant differences (described in Section 2.6.3) between this study and the work of Nasr-El-Din *et al.* (N5) for particle segregation in slurry flow through tees, the general observations of the effect of experimental variables on passage ratio are similar. They observed that the separation ratio increased with increase in velocity ratio V_s/V_u and decreased with decrease in branch size at a given velocity ratio. Also, at a given velocity ratio, the separation ratio decreased with increase in particle size. As expected, their separation curves had shapes similar to our A type curve. However, the results cannot be compared in absolute terms.

5.1.3 Summary

1. For stiff fibres, two distinct types of passage ratio curves were observed depending primarily on the ratio of fibre length to slot width (L/W). For $L/W < 2$, the passage ratio curve A is given by a power law relationship between passage ratio and slot velocity. For $L/W > 2$, the shape of curve B is akin to a cumulative probability distribution curve. This finding is of considerable industrial importance in the separation of long fibres from short fibres for it suggests conditions at which a large difference in passage ratios can be obtained.

2. A plausible explanation for the differing shapes of curve A and B is that penetration of the longer fibre may lead to a force from the upstream aperture wall acting on the fibre to cause rotation into the slot for the conditions at which curve B was found. On the other hand, data of curve A appear to be well explained by simple flow splitting and is thus mainly governed by upstream conditions.

3. In general, experimental results are consistent with other laboratory studies

and, in particular, are in good agreement with results of Gooding (G1).

5.2   Elevated Concentrations — Single Slot

Industrial screening is carried out at high concentrations (1–3%) using screen plates with multiple apertures and a rotor to keep the fibre suspension in tangential motion and prevent the screen plate apertures from plugging. In this section, the aim was to report the findings of the effect of feed concentration on the passage of fibres through the slot and to show the degree to which the findings of previous section are applicable at higher feed concentrations with no pulsed purging.

5.2.1   Effect of Feed Concentration on Passage Ratio

To study the effect of feed concentration on passage ratio, the upstream conditions: upstream velocity, V_u, and pressure on the feed side of the slot, P_1, (see Figure 5.11) were maintained equal to that of the no stapling condition. In the beginning of a trial, conditions were established to achieve a given accept flow rate through the slot. This means that P_2 was also set corresponding to the given accept flow rate for the no stapling condition. After this, feed concentration was increased while all other conditions were left constant. Since the area of the slot was partially obstructed in these tests, the true V_s is unknown. Therefore, in subsequent tests, the measured accept flow rate through the slot, Q_s, is reported.

With increase in feed concentration, fibres start accumulating in the slot, thereby decreasing Q_s. The effect of increasing feed concentration on Q_s is shown in Figure 5.12. As is evident, Q_s decreased with increased feed concentration. Passage ratios against feed concentration are plotted in Figure 5.13. The passage ratio data followed a trend similar to those of the accept flow versus feed concentration of Figure 5.12. With increase in feed concentration, the number of fibres accumu-
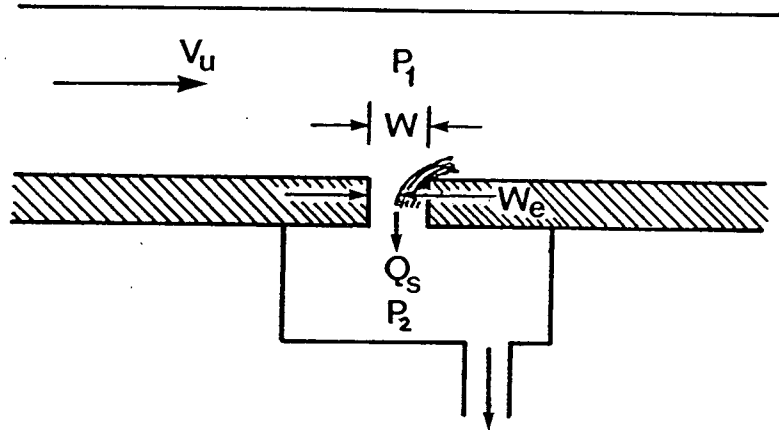
Figure 5.11: Fibre build-up at the slot entry in a single slot channel.

lating at the slot entry increases. The obvious effect of this fibre build-up over the slot is the reduced slot size ($W_e < W$ as shown in Figure 5.11) and the reduced flow through the slot. The combined effect of these two factors is the decrease in passage ratio with increased feed concentration.

Figure 5.13 shows an important difference in the passage ratio behaviour between 1 and 3 mm nylon fibres at an increased feed concentration. For $L/W < 2$, 1 mm nylon fibres, which follow curve A, resulted in an equilibrium passage ratio at feed concentration up to 13.5 g/l ($N = 4.4$). The slot was only partially plugged. On the other hand, 3 mm nylon fibres ($L/W = 6$), which follow B type curve at dilute concentrations, plugged the slot completely at a feed concentration of 0.33 g/l ($N = 1.2$). This plugging behaviour can be attributed to the differences in the way these fibres behave on contact with the downstream edge of the slot as postulated in our analysis (see Section 3.2.2).

As described in Appendix F, V_s/V_u affects the mode of stapling, and the effect
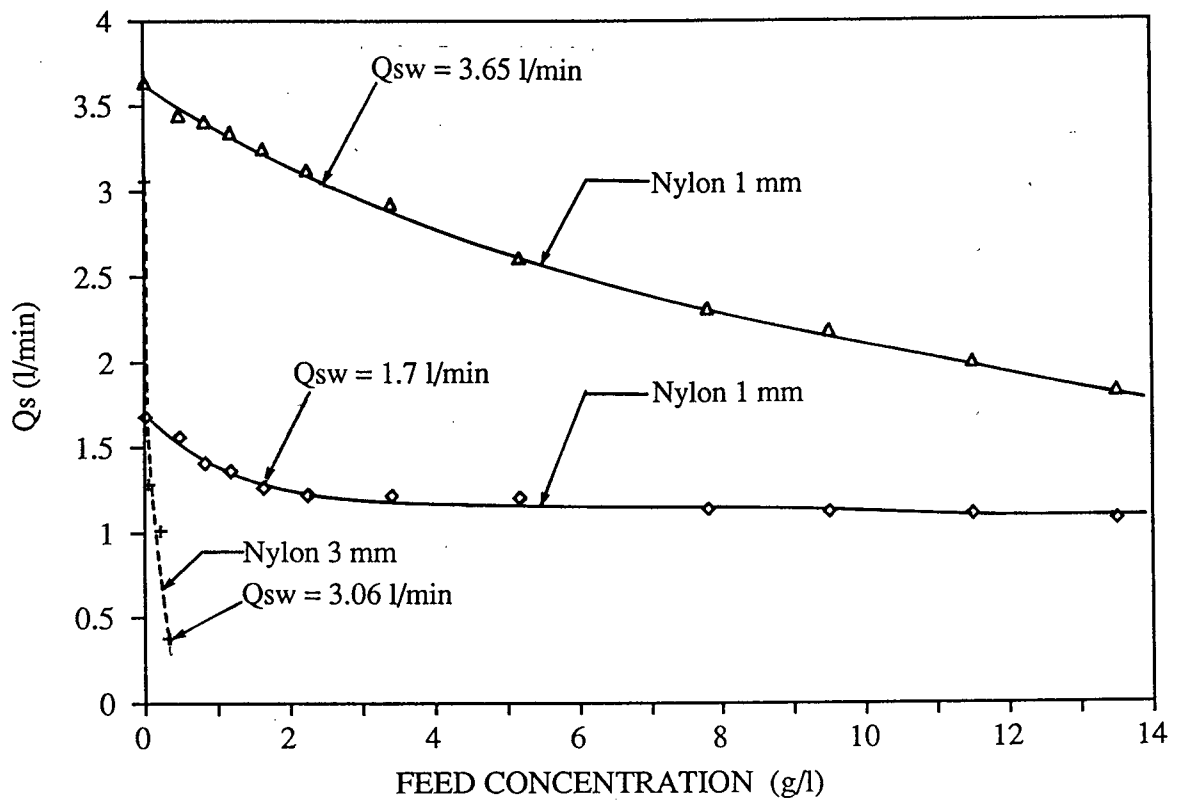
Figure 5.12: Effect of feed concentration on flow through the slot (Q_s) for 1 and 3 mm nylon fibres.
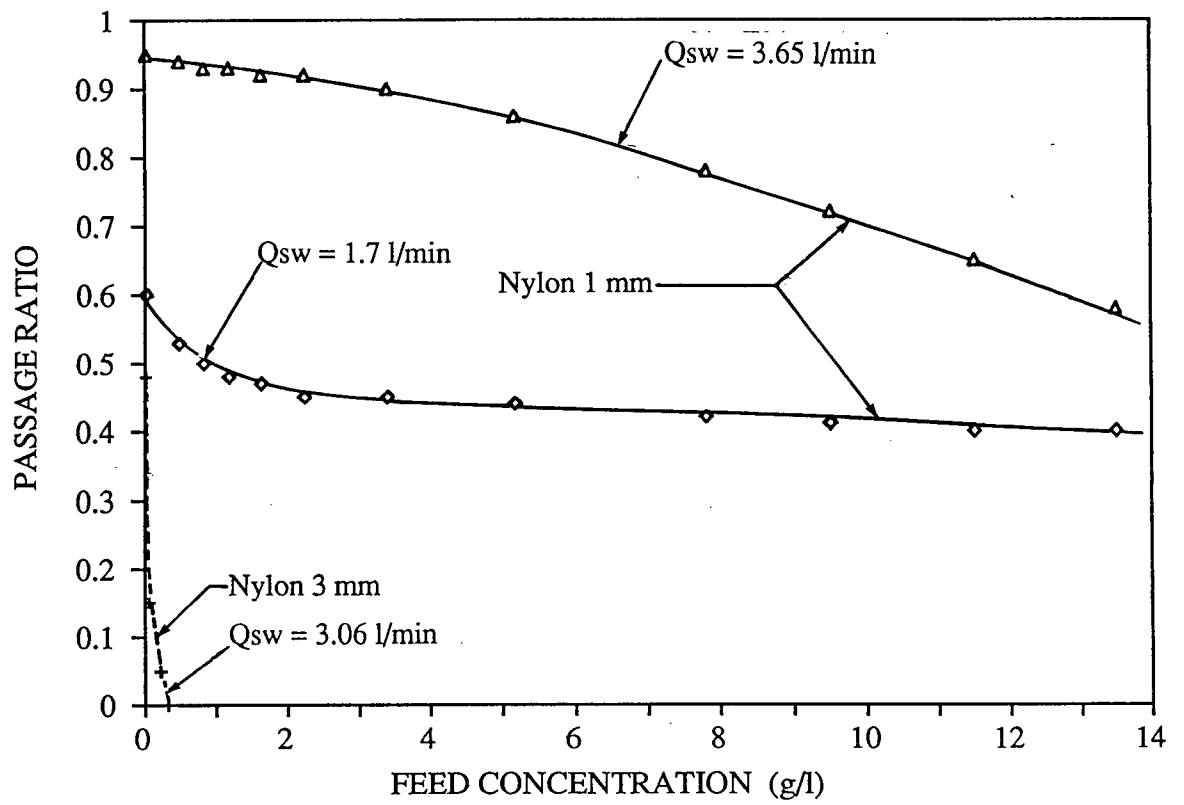
Figure 5.13: Effect of feed concentration on the passage ratios of 1 and 3 mm nylon fibres.

of the modes of stapling depends on consistency. The mode of stapling and the consistency then determine the passage ratio. 1 mm nylon fibres at $L/W = 2$ were found not to contact the upstream edge of the slot. This was shown earlier in Figure 5.2(a). At dilute concentrations ($N << 1$), only a few fibres were observed because, due to rotation, fibres at the downstream edge of the slot either go into the main flow or pass into the slot, and other fibres take their place. With an increase in feed concentration, enough fibres were present to crowd the downstream edge of the slot. With a further increase in feed concentration, those newly arriving fibres which contact the slot, can not find a fulcrum because the downstream edge is already occupied by the fibres. Thus, these fibres tend to stay with those fibres which are already present in the slot, and may also contact the upstream wall of the slot as shown in Figure 5.14 (a). However, this situation is unstable. As soon as the staples grow to a certain level, they quickly go either into the main flow or pass into the slot. The accumulation of fibres on the downstream edge of the slot results in a smaller effective slot size ($We < W$) and thus yields the passage ratio which does not change with the increase in feed concentration. At low accept flow rates, 1 mm nylon fibres resulted in a constant passage ratio above a feed concentration of about 3 g/l ($N = 1$). At higher accept flow rates, the passage ratio decreased moderately in the whole range of feed concentration (0–13.5 g/l).

As predicted, 3 mm nylon fibres at $L/W = 6$ contact the upstream wall of the slot. At dilute concentrations, the downstream edge of the slot was not fully covered as shown earlier in Figure 5.2(b). Therefore, fibres could pass through the slot. Also, the immobilized fibres rotated to enter into the slot above a certain slot velocity. The force exerted on the fibre by the upstream wall of the slot was overcome. With an increase in feed concentration, more fibres contacted the slot and at some concentration, the downstream edge of the slot was fully covered as
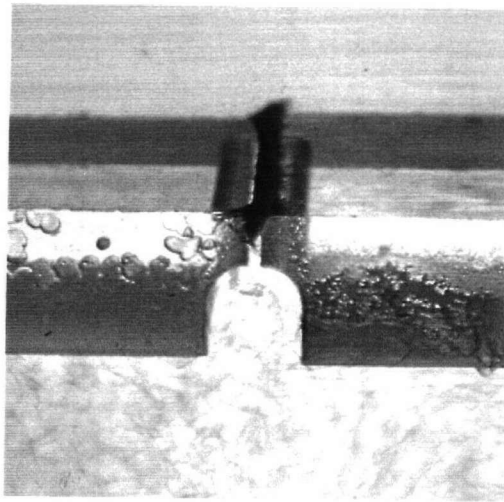
(a) Nylon 1 mm
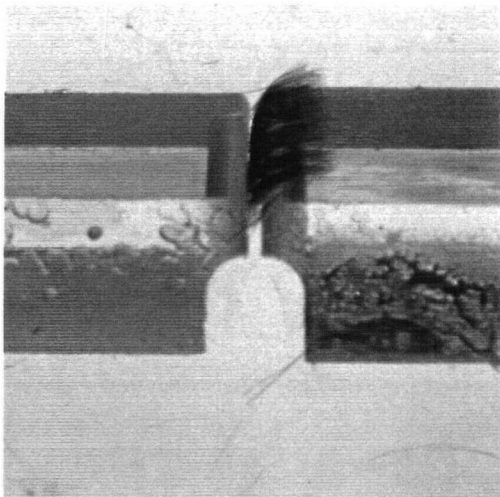
(b) Nylon 3 mm fibres, downstream edge of the slot is fully covered.
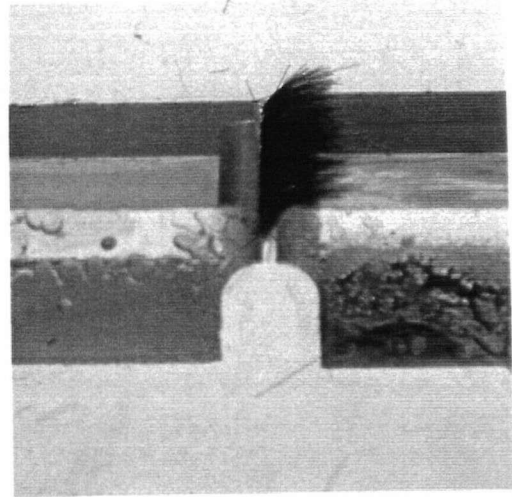
(c) Nylon 3 mm fibres, slot is completely plugged.

Figure 5.14: Fibre accumulation of 1 and 3 mm nylon fibres at the slot entry. $W = 0.5$ mm.

shown in Figure 5.14(b). Further increase in feed concentration plugged the slot completely ($P = 0$) as the staples became strong and the force exerted by the wall was not overcome by the slot velocity when the upstream velocity was kept constant at 6.5 m/s.

5.2.2 Effect of Feed Concentration on the shape of Passage Ratio Curves

At higher feed concentrations, staples form and build-up over the slot entry. A hydrodynamic force strong enough to remove them is needed to rupture the staples and prevent them from building up. For 1 mm nylon fibres, this was achieved by increasing the feed pressure P_1 while maintaining the upstream velocity at 6.5 m/s. In Figure 5.15, the passage ratios of 1 mm long nylon fibres obtained at this higher feed pressure are plotted against the velocity ratio with feed concentration as a parameter. It can be seen that for $L/W = 2$, the shape of the passage ratio curves at higher feed concentrations is similar to that of curve A obtained at dilute concentration and the passage ratio values are very similar. At feed concentrations that exceed the critical concentration up to 9.5 g/l ($N = 3.1$), passage ratios were maintained by merely increasing the pressure on the feed side of the slot so that an accept flow rate approximately equal to the flow rate at zero feed concentration was obtained.

The photographs of Figure 5.16 show the difference between a partially plugged and a fully purged slot. In Figure 5.16(a), there is a significant fibre build-up over the slot at a feed concentration of 2.24 g/l ($N = 0.74$) and the the slot looks completely plugged. However, this is not the case as a passage ratio of 0.22 was obtained. A few fibres keep breaking away from the accumulated mass and they either pass through the slot or go into the mainstream flow. Fibre build-up reduces
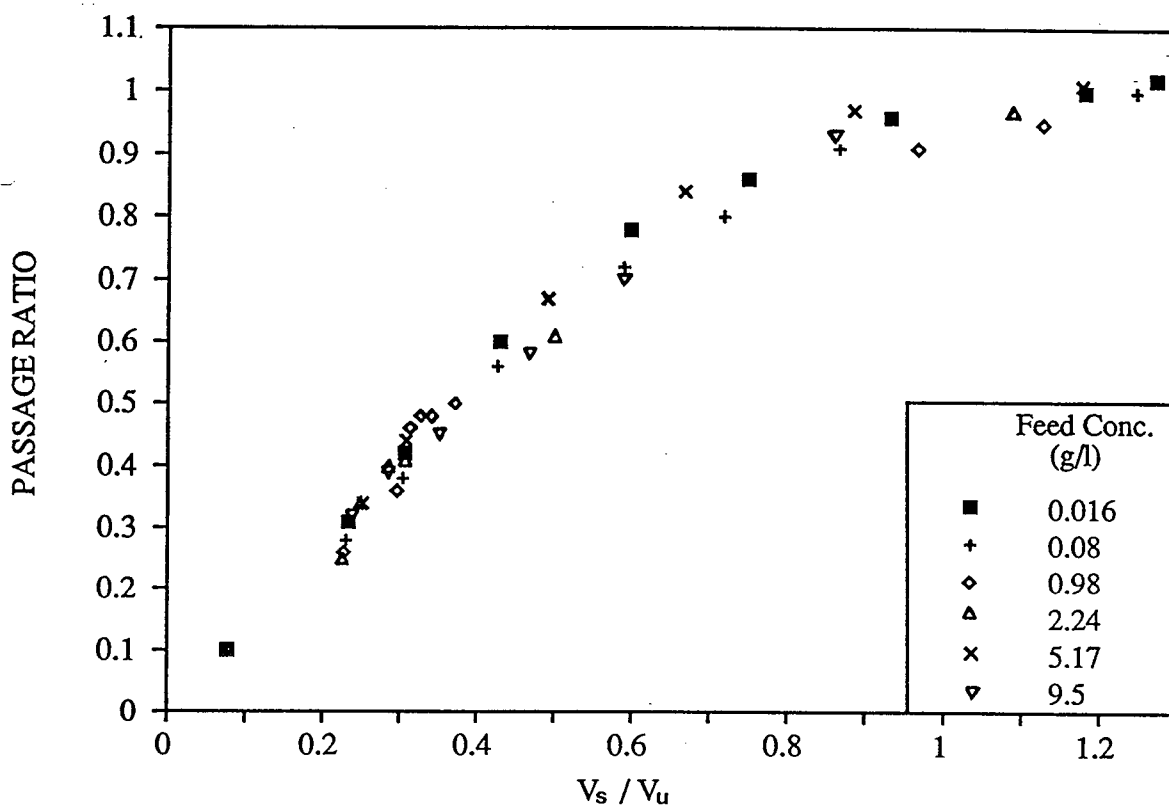
Figure 5.15: Passage ratios of 1 mm nylon fibres against V_s/V_u with feed concentration as a parameter.
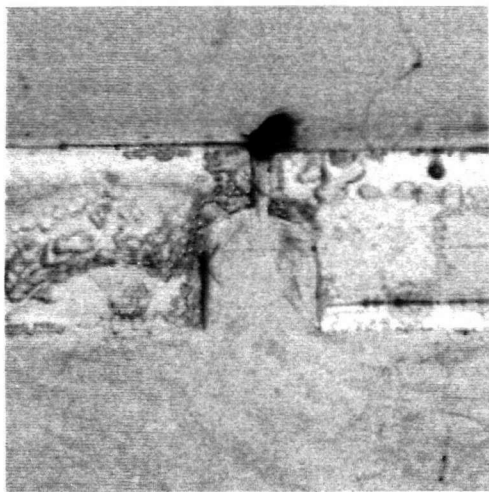
Figure 5.16: Differences in slot plugging due to differences in the pressure drop across the slot. Nylon 1 mm fibres. $W = 0.5$ mm.

the slot size $(We < W)$ and flow through the slot. When P_1 was increased to obtain an equal flow rate, the fibres which were stapling on the downstream edge of the slot at a lower slot velocity, were now forced to rotate and pass through the slot at the higher slot velocity. The staples were observed to shed continuously and to pass through the slot as shown in Figure 5.16(b). This dynamic situation was detected by visual observation and by filming the movement of staples at the slot using a high speed video camera.

For 3 mm long nylon fibres with $L/W = 6$, curve B was not obtained above a feed concentration of 0.33 g/l ($N = 1.2$) as the slot was completely plugged. Efforts to remove the staples from the slot by applying a higher pressure drop across the

slot while maintaining a V_u of 6.5 m/s failed to purge the slot. In short, it appears that for stiff fibres that follow curve "B" behaviour, stapling at conditions just above the very dilute range ($N = 1.2$) can not be overcome by only increasing the pressure on the feed side. The increase in P_1 is insufficient to overcome stapling if a V_u of 6.5 m/s is to be maintained. Other means must be employed.

5.2.3   Effect of Fibre Flexibility on Plugging Concentration

The effect of fibre flexibility is shown in Figures 5.17 and 5.18 where the passage ratios for 1 mm nylon and 1 mm rayon fibres are plotted against feed concentration. It is apparent that 1 mm nylon fibres which follow the A type behaviour resulted in an equilibrium passage ratio up to a feed concentration of 13.5 g/l ($N = 4.4$) used here. On the other hand, 1 mm flexible rayon fibres which also follow the A type curve, plugged the slot completely at a feed concentration of about 6–8 g/l.

The difference in the behaviour of short nylon and rayon fibres is due to the extent of bending these fibres undergo when subjected to the hydrodynamic force. Rayon fibres being more flexible than nylon fibres bend more as shown earlier in Figure 5.2 and have a greater tendency to staple on the downstream edge of the slot. As described earlier in Section 5.1.1, stapling at dilute concentrations was not significant enough to affect the passage of fibres through the slot. However, with increase in feed concentration, staples grow and become strong enough to resist the rotation in either way. Moreover, flexible rayon fibres form string like flocs (longer than their fibre length) and were draping into the slot as shown in Figure 5.19 while nylon fibres were present mainly at the slot entry and were very susceptible to rotation over the slot.
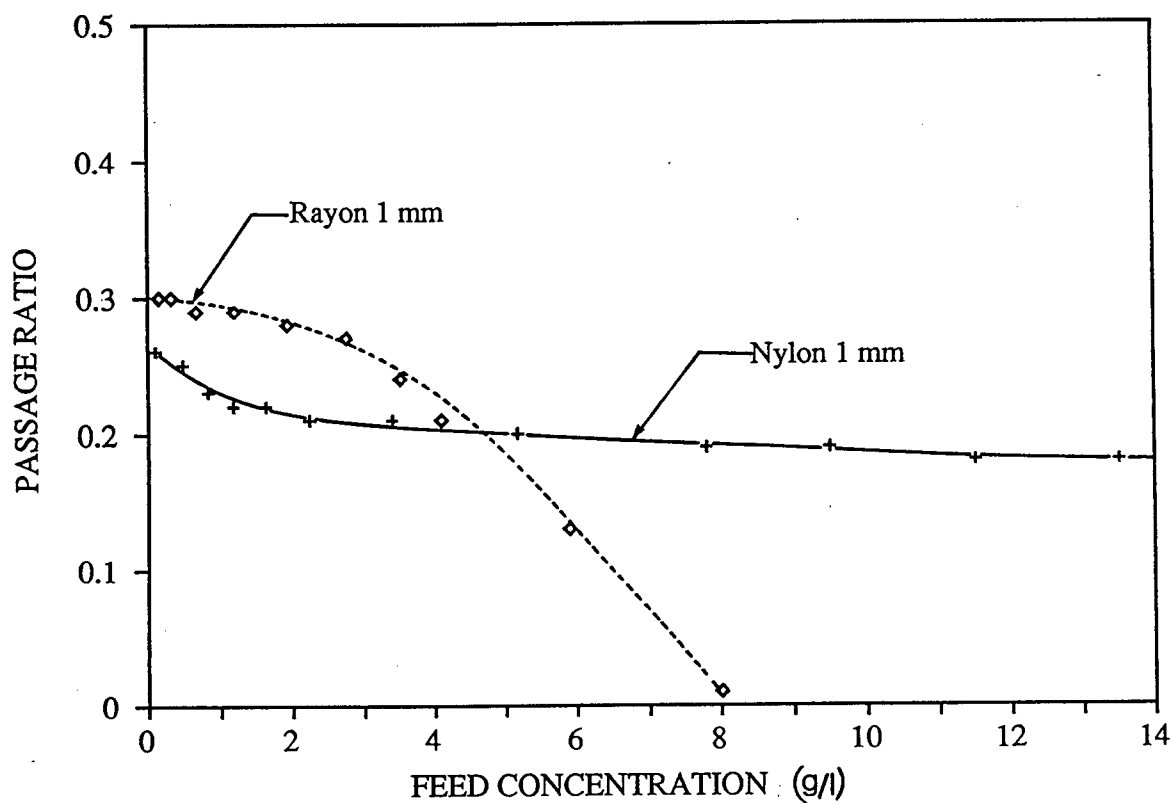
Figure 5.17: Passage ratios of 1 mm nylon and rayon fibres versus feed concentration showing the effect of fibre flexibility. Q_{SW}, the flow through an unobstructed slot (no stapling condition) = 0.9 l/min.
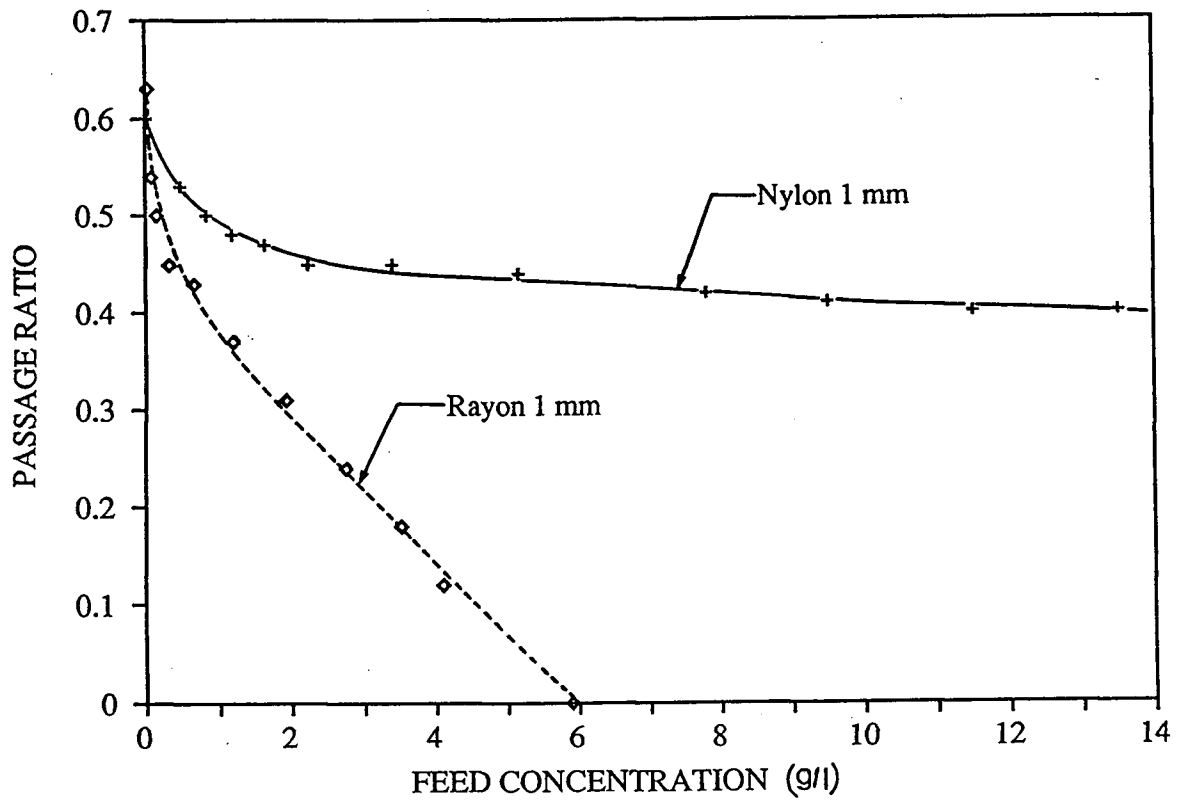
Figure 5.18: Passage ratios of 1 mm nylon and rayon fibres versus feed concentration showing the effect of fibre flexibility. $Q_{SW} = 1.7$ l/min.
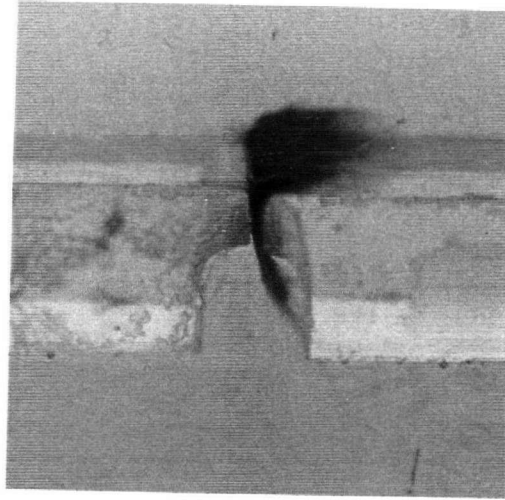
Figure 5.19: 1 mm rayon fibres stapling over a 0.5 mm wide slot. The long string-like flocs are evident.

5.2.4 Summary

1. In general, the passage ratio decreased with increased feed concentration. 1 mm nylon fibres ($L/W = 2$) which follow the "A" curve at dilute concentrations, yielded an equilibrium passage ratio with increase in feed concentration up to 13.5 g/l ($N = 4.4$). On the other hand, 3 mm nylon fibres ($L/W = 6$) which follow the "B" curve at dilute concentrations, plugged the slot completely at a feed concentration of 0.33 g/l ($N = 1.2$) when an upstream velocity of 6.5 m/s was maintained. Extra purging will be needed to purge the slot beyond this concentration.

2. For 1 mm nylon fibres at $L/W = 2$, curve "A" was reproducible up to a feed concentration of about 9.5 g/l ($N = 3.1$) by simply maintaining the flow rate through the slot at the level when no stapling takes place and thus the passage ratios were maintained. For 3 mm nylon fibres, the curve "B" could

not be obtained beyond a feed concentration of 0.33 g/l ($N = 1.2$).

3. As expected, the short and flexible rayon fibres bend and staple more. At dilute concentrations, these fibres at $L/W = 2$ also follow the A type curve like 1 mm nylon fibres, but plug the slot completely ($P = 0$) at a feed concentration of 6–8 g/l.

5.3 Effect of Entry Geometry

In industrial pulp screening, many different contoured screen plate configurations are in use. Our aim here was to test the robustness of the previous findings of Section 5.1 in relation to a general contoured configuration shown in Figure 4.4 (Smooth vs. Contoured slots C1 and C2).

5.3.1 Passage Ratio Comparison at Dilute Concentrations ($N << 1$)

Passage ratios of 1 mm nylon fibres for $L/W = 2$ are plotted against V_s/V_u for smooth and contoured slots C1 and C2 in Figure 5.20. It is evident that the passage ratio curves shifted in magnitude but their shape remained essentially of type A. The similar trend was observed with 1 mm flexible rayon fibres for $L/W = 2$ as shown in Figure 5.21.

The passage ratios of 3 mm nylon fibres for $L/W = 6$ are plotted in Figure 5.22. For contoured slot C1, the passage ratio curve shifted in magnitude and the shape of the curve was less pronounced than the S shape of curve B. In the case of the C2 slot, the passage ratio curve shifted in magnitude and the shape of the passage ratio curve, though still detectable, was less distinct than for the smooth or C1 slot.
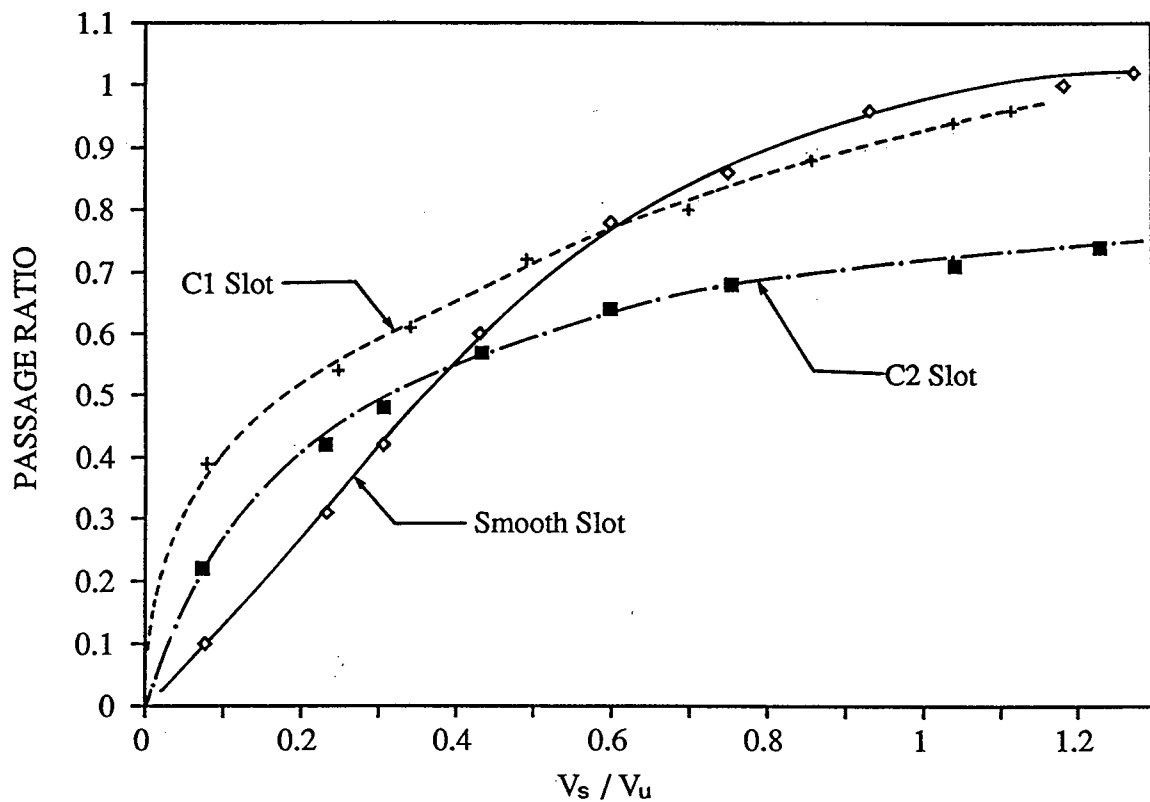
Figure 5.20: Effect of slot geometry on the passage ratio of 1 mm nylon fibres. $W = 0.5$ mm.
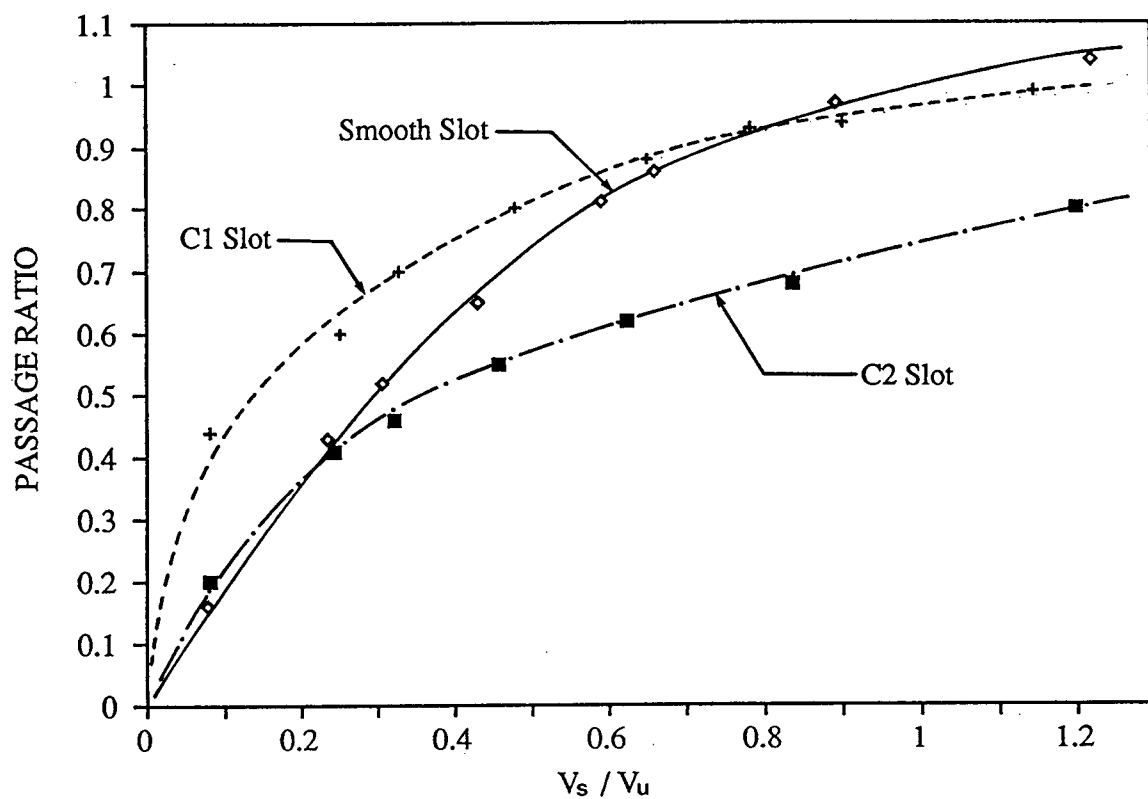
Figure 5.21: Effect of slot geometry on the passage ratio of 1 mm rayon fibres. $W = 0.5$ mm.
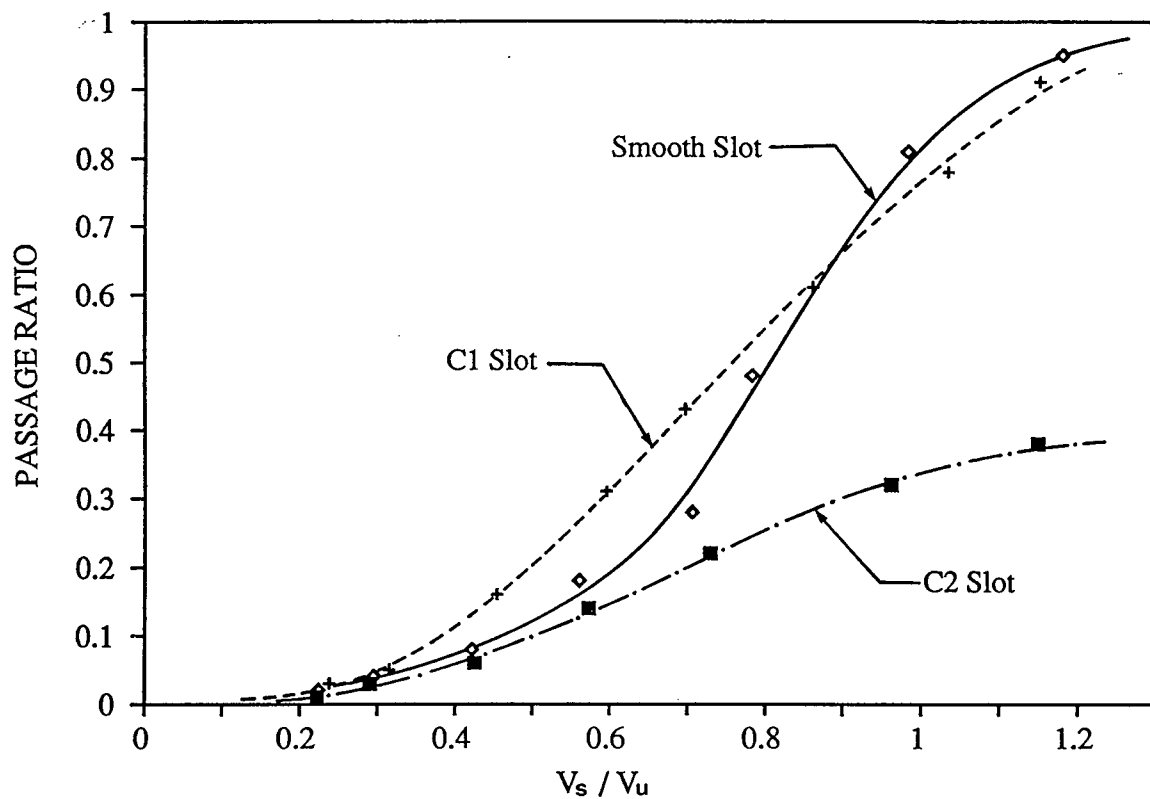
Figure 5.22: Effect of slot geometry on the passage ratio of 3 mm nylon fibres. $W = 0.5$ mm.

A comparison of the passage ratios for a smooth slot with contoured slots in Figures 5.20, 5.21 and 5.22 shows that the C1 slot yielded passage ratios which were either higher or lower than the smooth slot. The difference was greater at lower V_s/V_u values (< 0.3) and decreased at higher V_s/V_u (> 0.4). Passage ratios for the C2 slot were mainly lower than those of the C1 slot. Though the difference in passage ratios between C1 and C2 slots increased with increasing V_s/V_u for both nylon and rayon fibres, the difference was large for 3 mm nylon fibres, particularly at higher V_s/V_u. The C1 slot was shallow with a groove depth of 0.5 mm compared to the C2 slot with groove depth of 1.2 mm. It is interesting to note that increasing the contour depth from 0.5 mm to 1.2 mm lowered the passage ratios significantly. This finding is significant for industry as a deep contoured slot like C2 will give higher removal efficiency when the aim is to remove long and stiff fibres (shives in screening or long fibres in fractionation). This suggests the dimensions of contour as an important design parameter to achieve the desired screening performance. However, it is beyond the scope of the present work to extend the analysis to include the effect of contour dimensions.

5.3.2   Explanation for the differences in passage ratios between smooth and contoured slots

The difference in the passage ratios of smooth and contoured slots shown in Figures 5.20 to 5.22 can be explained on the basis of fibre interaction with the slot. The photographs of Figure 5.23 show the difference in the ways 1 mm nylon fibres were observed contacting the slots. The presence of fibres as vertical staples on the downstream edge of a smooth slot has been discussed in earlier sections. In the case of the contoured slots used here, the entry to the aperture is not in the same plane as the wall but is at a plane recessed by a distance Z below the feed flow. In case of shallow C1 slot ($Z = 0.5$ mm), 1 mm nylon fibres were observed as both

vertical and horizontal staples as shown in Figure 5.23(b). At dilute concentrations ($N \ll 1$), fibres did not stay in the slot and thus the whole area of the slot was utilized for fibre passage. Also, the vertical staples on the downstream edge of the C1 slot have a greater tendency to rotate to enter into the slot as V_u within the recessed contour of the C1 slot will be lower than V_u in the case of the smooth slot. Thus a greater effective V_s/V_u promotes a higher passage ratio which is evident in Figure 5.20.

On the other hand, a fibre has to travel a greater distance to penetrate in order to pass through the deeper C2 slot ($Z = 1.2$ mm). During experimentation, 1 mm nylon fibres were not observed to staple in the C2 slot. They were occasionally seen in the corner of the downstream edge of the contour as shown in Figure 5.23(c) but this did not affect the passage of other fibres through the slot. In this case, the passage ratio is governed by the penetration parameter only. Since the fibres were not immobilized on the downstream edge of the slot, the rotation parameter which increases the passage ratio at higher V_s/V_u in the case of the smooth and C1 slots did not play any role in the case of the C2 slot. Indeed, this is the case as can be seen in Figure 5.20 in which the passage ratio for the C2 slot did not increase with increase in V_s/V_u at the same rate as for the smooth and the C1 slot.

The interaction of 3 mm nylon fibres with the slot is illustrated in Figure 5.24. In the case of smooth and C1 slots, fibres contact the upstream wall of the slot which exerts a force, F_w, on the fibre as is evident in Figures 5.24(a) and (b). Increasing V_s/V_u reduces F_w and after a threshold V_s/V_u is reached, the passage ratio starts increasing. This threshold V_s/V_u was somewhat lower for the C1 slot than the smooth slot (Figure 5.22) but the passage ratio behaviour was similar. At the same fibre concentration, 3 mm nylon fibres were not observed in the C2 slot. Occasionally, a few fibres were seen in the corner of the downstream edge of the
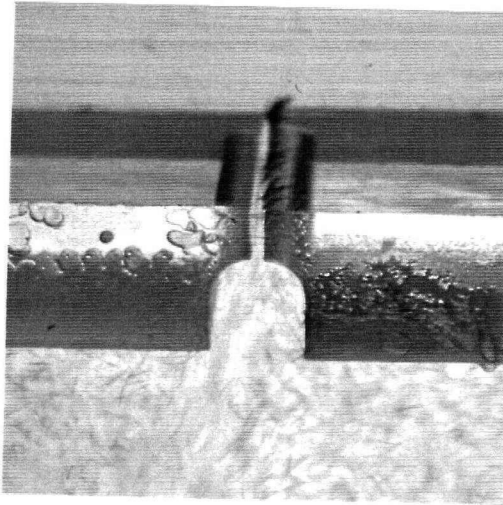
(a) Smooth slot.
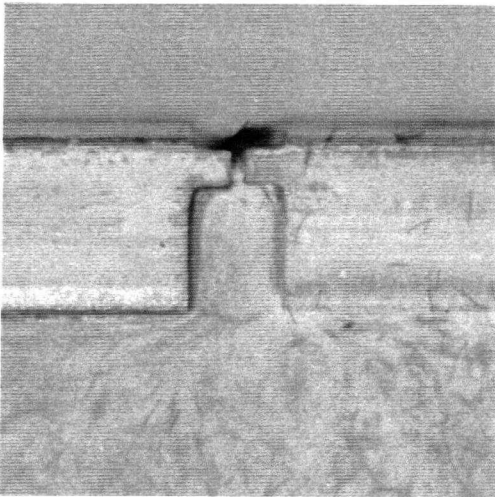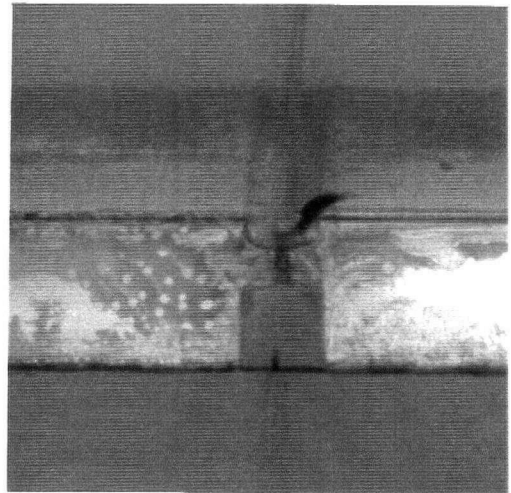
(b) C1 slot.

(c) C2 slot.

Figure 5.23: Stapling of 1 mm nylon fibres at the slot entry of smooth and contoured slots.
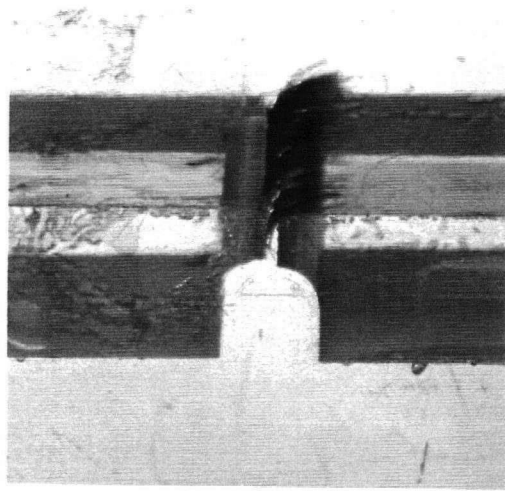
(a) Smooth slot.
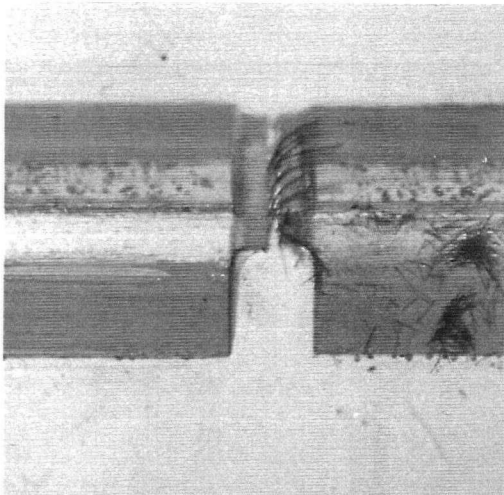
(b) C1 slot.
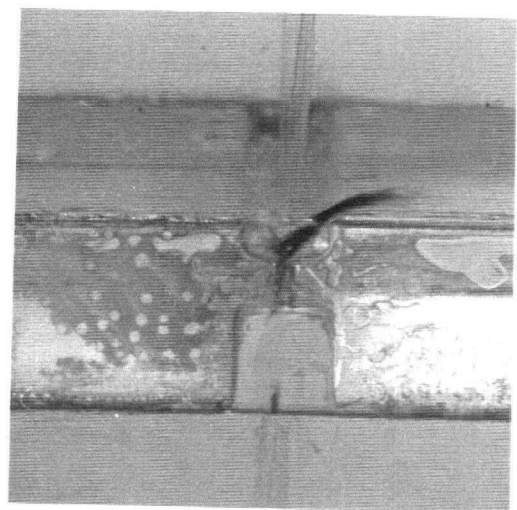
(c) C2 slot.

Figure 5.24: Stapling of 3 mm nylon fibres at the slot entry of smooth and contoured slots.

contour as is evident in Figure 5.24(c) but the 3 mm nylon fibres did not contact the upstream wall of the slot in the same manner as they did in smooth and C1 slots, and thus $F_w = 0$. The passage ratio then depends on the fibres which pass through the slot mainly governed by penetration; the rotation parameter does not play any role in increasing the passage ratio. Since penetration into the deeper C2 slot is more difficult than into a smooth or C1 slot, lower passage ratios result. Also, passage ratio does not increase at the same rate as for the smooth or C1 slots with increase in V_s/V_u (see Figure 5.22).

5.3.3 Passage Ratio Comparison at Higher Concentrations

In Figure 5.25, the passage ratios of 1 mm nylon fibres are plotted against feed concentration for $V_s/V_u = 0.43$–0.49 (no stapling condition). It can be seen that for the smooth and C2 slots, the passage ratios decreased moderately in the beginning and then levelled off up to a feed concentration of 13.5 g/l ($N = 4.4$). The passage ratios for the C1 slot were higher than for both smooth and C2 slots up to a feed concentration of about 2.5 g/l ($N = 0.8$) but, beyond this concentration, they decreased sharply. The slot was plugged ($P = 0$) at a feed concentration of about 3.4 g/l ($N = 1.1$). The reason appears to be the presence of horizontal staples which are evident in Figure 5.26(a). In a smooth slot, the presence of vertical staples resulting in an equilibrium slot size led to an equilibrium passage ratio. In the C2 slot, fibres were not present in the slot up to a feed concentration of 13.5 g/l ($N = 4.4$).

Figure 5.27 shows the variation of the passage ratios with feed concentration at $V_s/V_u = 1$ (no stapling condition). As is evident, the passage ratios decreased only moderately for all the three slots. The horizontal staples which plugged the
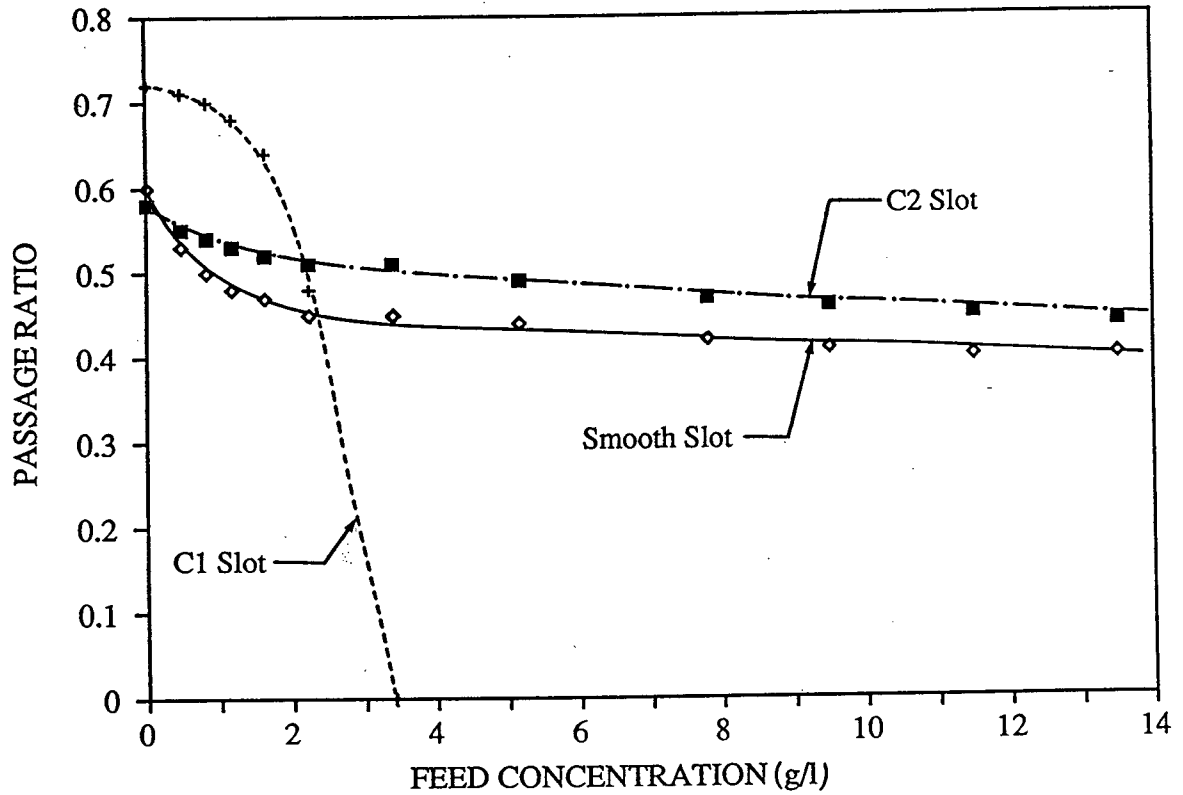
Figure 5.25: Passage ratio of 1 mm nylon fibres with increasing feed concentration showing the difference in passage ratio of smooth and contoured slots. V_s/V_u (at $C_{bF} = 0$) = 0.43– 0.49.
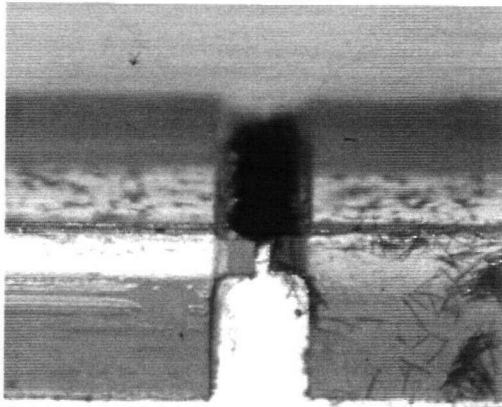
(a) Completely plugged C1 slot. Feed concentration = 3.4 g/l.
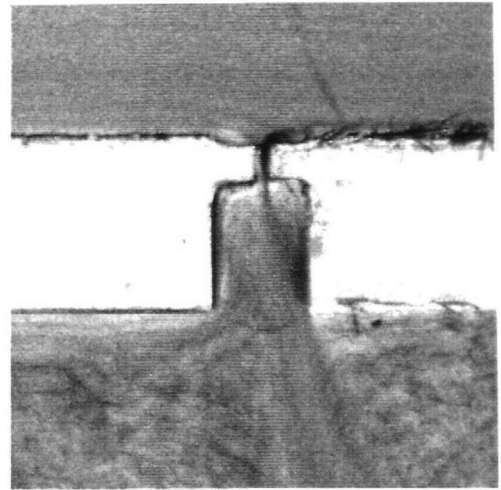
(b) C1 slot is purged by increasing the pressure on the feed side of the slot (P_1). Feed concentration = 9.5 g/l.

Figure 5.26: 1 mm nylon fibres as vertical and horizontal staples in contoured slot C1 at higher feed concentration.
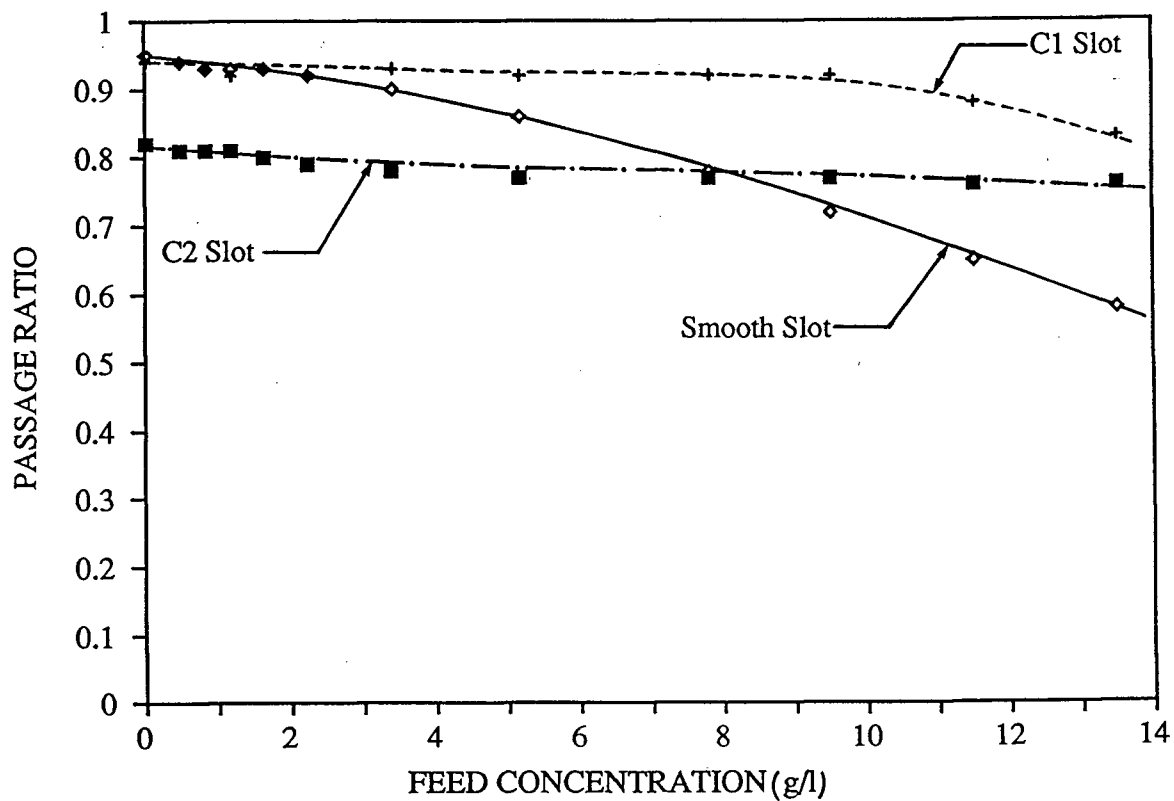
Figure 5.27: Passage ratio of 1 mm nylon fibres with increasing feed concentration showing the difference in passage ratio of smooth and contoured slots. V_s/V_u (at $C_{bF} = 0) = 1$.
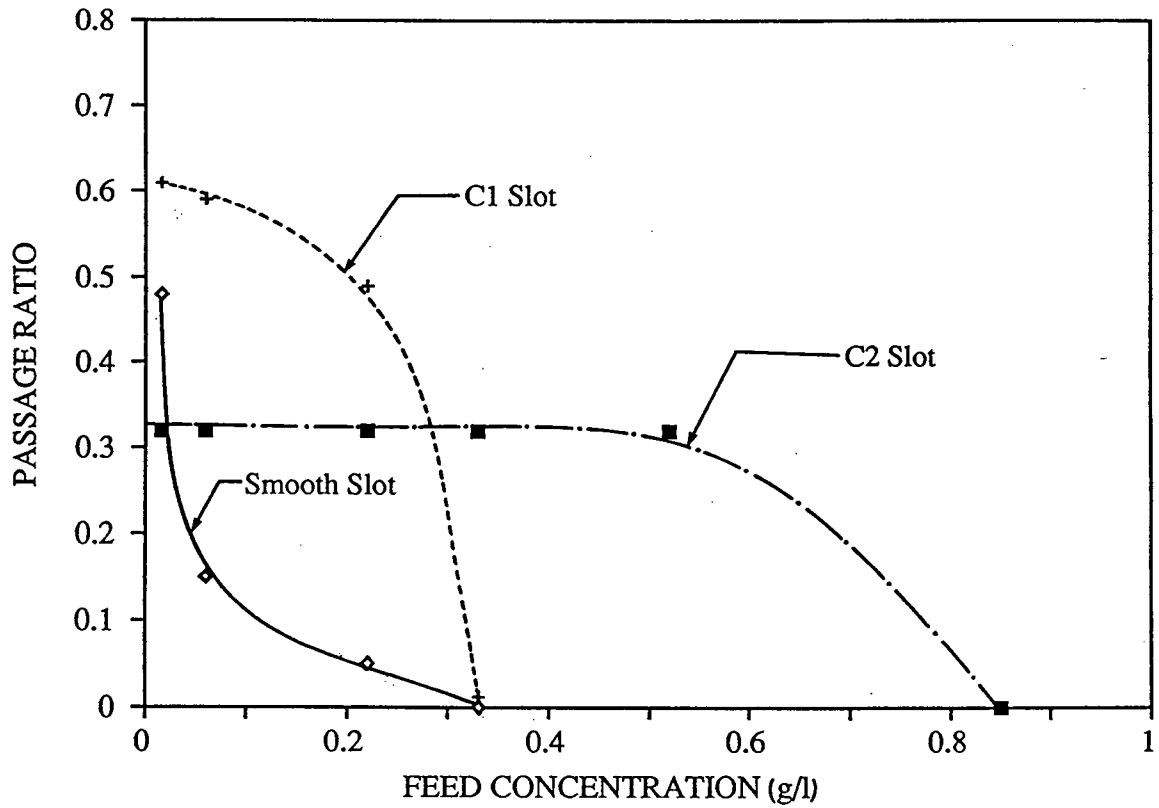
Figure 5.28: Passage ratios of 3 mm nylon fibres against feed concentration showing the difference in the passage ratio and plugging concentration of smooth and contoured slots. V_s/V_u (no stapling condition) $\simeq 1$.

mainly on the downstream edge of the contour. However, at a feed concentration of 0.85 g/l ($N = 3$), the C2 slot was also plugged (see Figure 5.28) because the number of fibres trying to pass through the slot increased substantially thereby reducing the effective slot size initially and eventually plugging the slot completely.

5.3.4 Effect of feed concentration on the shape of passage ratio curves

Passage ratios of 1 mm nylon fibres at a feed concentration of 9.5 g/l ($N = 3.1$) are plotted against V_s/V_u in Figure 5.30 for smooth, C1 and C2 slots. The shape of the
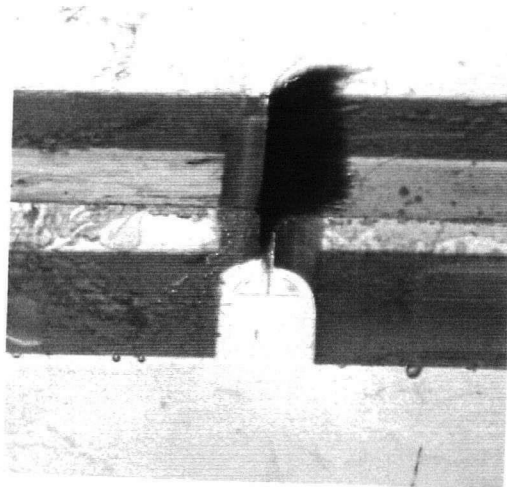
(a) Smooth slot.
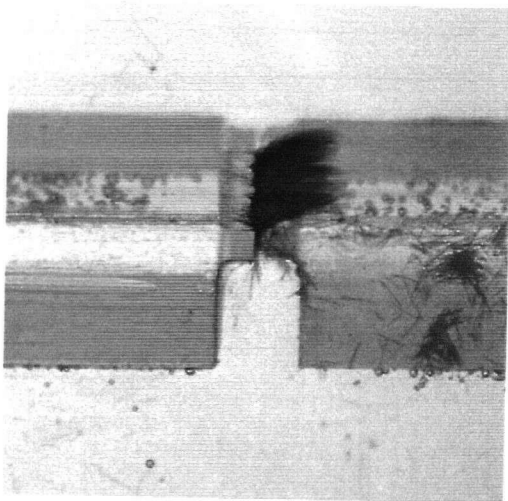
(b) C1 slot.
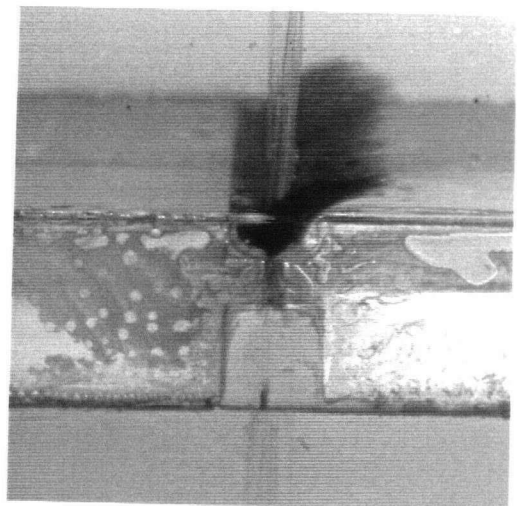
(c) C2 slot.

Figure 5.29: Photographs showing the completely plugged smooth and contoured slots.
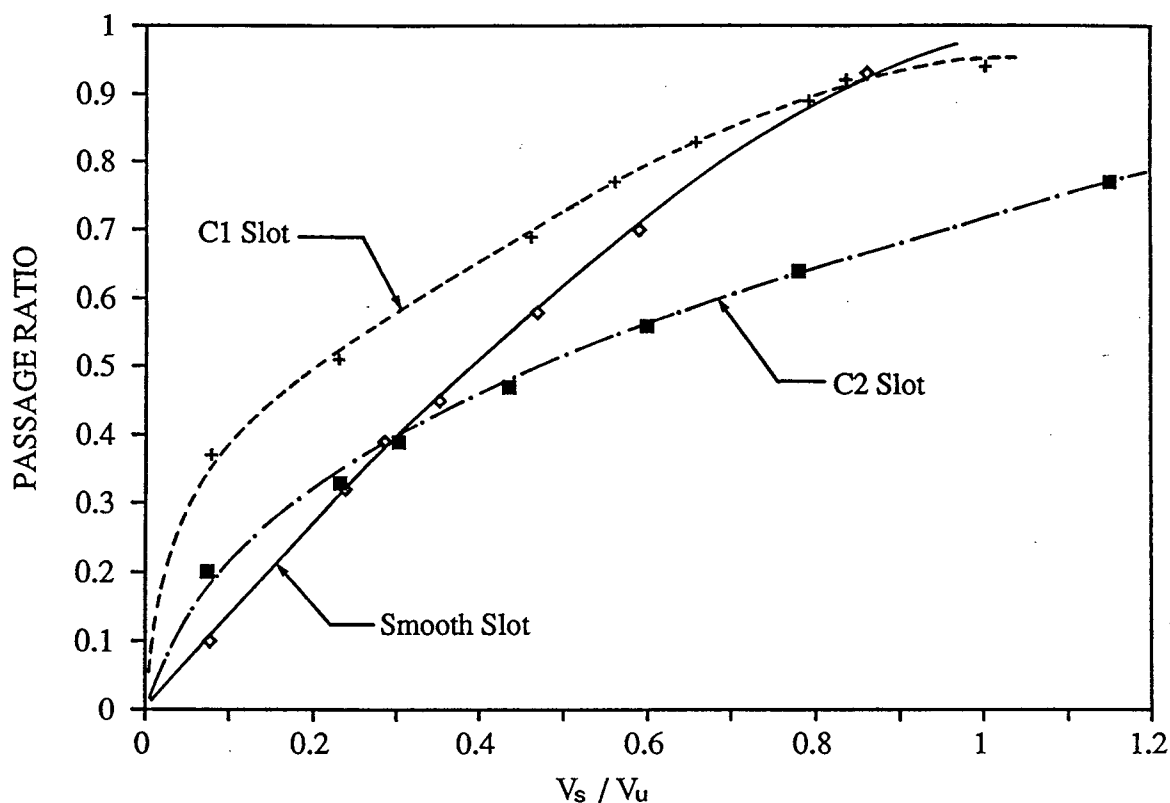
Figure 5.30: Passage ratio of 1 mm nylon fibres against V_s/V_u at a feed concentration of 9.5 g/l ($N = 3.1$) for smooth and contoured slots.

passage ratio curves is similar to that of curve A. As in case of the smooth slot with 1 mm nylon fibres ($L/W = 2$), contoured slots C1 and C2 were purged at higher feed concentrations by simply maintaining the flow rate through the slots equal to that of the no stapling conditions. A purged C1 slot at a feed concentration of 9.5 g/l is shown in Figure 5.26(b). The trend and differences in the passage ratios between smooth and contoured slots at 9.5 g/l are similar to those observed at dilute feed concentrations (compare Figure 5.30 with Figure 5.20). For the longer 3 mm fibres ($L/W = 6$), Curve B behaviour could not be obtained beyond a feed concentration of 0.33 g/l for smooth and C1 slots, and above 0.85 g/l for the C2 slot.

5.3.5 Summary

1. At dilute feed concentrations ($N \ll 1$) and with short fibres ($L/W = 2$), the shape of the passage ratio curves for contoured slots C1 and C2 remained of type "A". For 3 mm nylon fibres ($L/W = 6$), the shape of the passage ratio curve for the shallow C1 slot was less pronounced than the S-shaped nature of curve "B". For deep contoured slot C2, the shape of the passage ratio curve, though still detectable, was less distinct than for smooth and C1 slots.

2. At higher feed concentrations, curve "A" for short nylon fibres ($L/W = 2$) was reproducible up to a feed concentration of about 9.5 g/l ($N = 3.1$) for both C1 and C2 slots by simply maintaining the flow through the slot equal to that of the no stapling condition. For 3 mm nylon fibres ($L/W = 6$), curve B could not be obtained beyond a feed concentration of 0.33 g/l ($N = 1.2$) for the C1 slot and 0.85 g/l ($N = 3$) for the C2 slot.

5.4 Studies in the Sectional Screen

This last portion of the study examined the robustness of the earlier findings under conditions approaching those of a pulp screen — at elevated concentrations with rotor induced pulsations and turbulence. The tests were carried out in the sectional screen (SS) described earlier in Section 4.3.

5.4.1 Dilute Concentrations ($N \ll 1$)

Passage Ratio vs Slot Velocity

To compare the results of the sectional screen with those from the single slot channel, studies were carried out in the SS using a 0.5 mm wide single slot. A

	L (mm)	L/W	Feed Conc. (fibres/l)
◇	1	2	32,400
▲	3.17	6.3	3,450
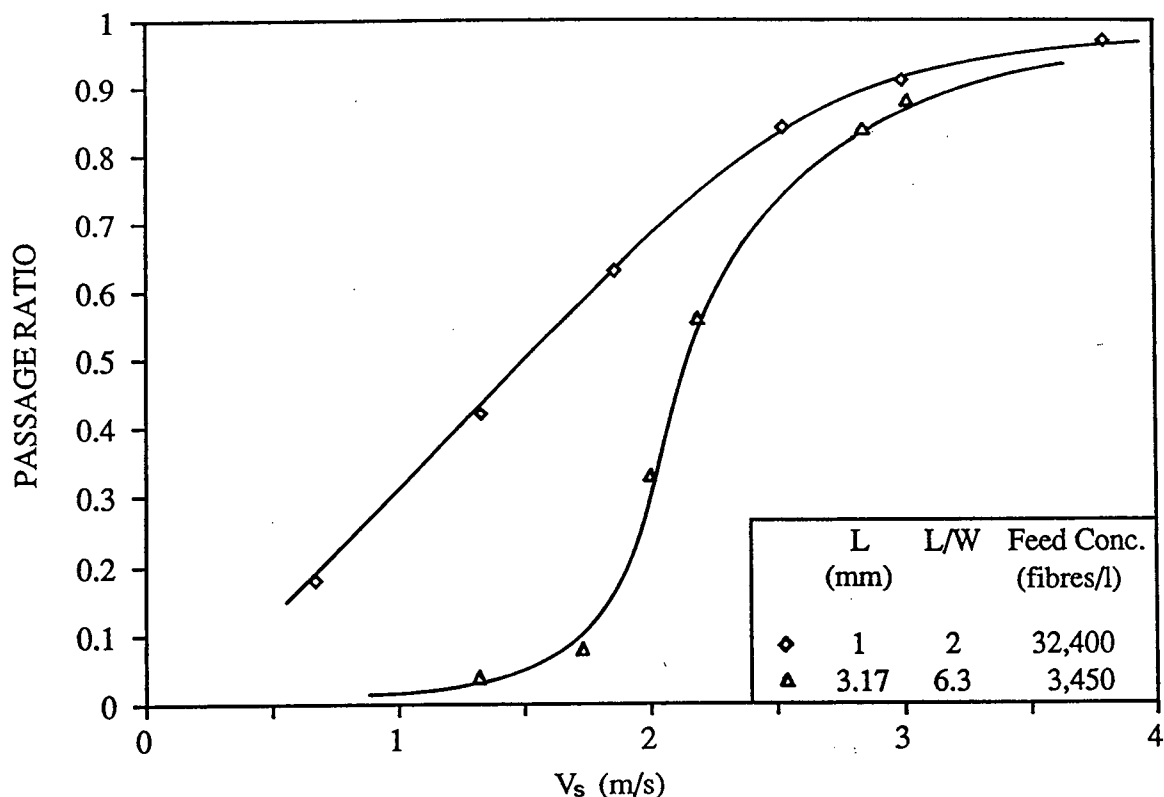
Figure 5.31: Passage ratio of nylon fibres against slot velocity for a 0.5 mm wide single slot in SS at $V_t = 6.5$ m/s.

rotor speed of 430 rpm giving a tip speed of 6.5 m/s (equal to V_u in single slot channel) was used. The bulk slot velocity was varied in the range of 0–3.8 m/s. The passage ratios for 1 and 3 mm nylon fibres are plotted against slot velocity in Figure 5.31. As is evident, the shape of the passage ratio curves for 1 and 3 mm nylon fibres remained same as those of curves "A" and "B" (see Figure 5.1) for a single slot channel.

The screen plate in an industrial pressure screen has multiple apertures. To study the effect of multiple apertures, passage ratio measurements were made in the SS with a screen plate having ten slots in series. The width of the slots was 0.5 mm and the distance between the centres of two adjacent slots (slot spacing)

106
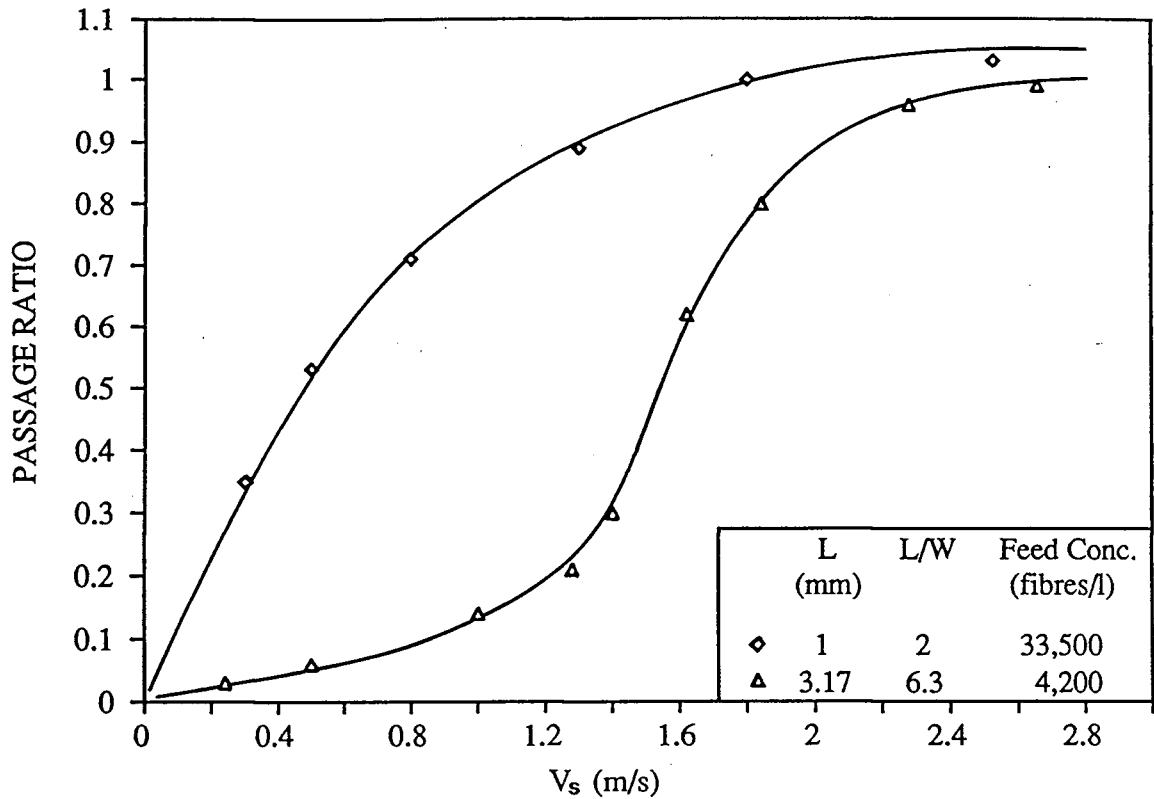
Figure 5.32: Passage ratio of nylon fibres against slot velocity for multiple slots in SS at $V_t = 6.5$ m/s.

was 3 mm. A rotor tip speed of 6.5 m/s was maintained and the slot velocity was varied from 0–2.7 m/s. The passage ratios for 1 and 3 mm nylon fibres are plotted against slot velocity in Figure 5.32. Here too, it is evident that the shape of the passage ratio curves for short and long stiff fibres were similar to those of curves "A" and "B" for a single slot channel. For a given slot velocity, the passage ratios in the SS for multiple slots were larger than the passage ratios for a single slot in the SS.

Although the shape of passage ratio curves was the same for both single slot channel and sectional screen with single and multiple slots, the magnitude of passage ratio values differed. This is probably due to the fact that the passage ratio

Table 5.2: Slot Velocity at which $P = 1$ for 1 mm Nylon Fibres and $P = 0.9$ for 3 mm Nylon Fibres. Values Obtained from Figures 5.1, 5.31 and 5.32.

System	Nylon 1 mm V_s at $P = 1$ (m/s)	Nylon 3 mm V_s at $P = 0.9$ (m/s)
Channel	6.95	7.05
SS (Single Slot)	4	3.23
SS (Multiple Slot	1.8	2.03

comparisons can not be made at exactly comparable conditions because the aperture velocities in the sectional screen vary greatly because of pulsations. Also, the velocity parallel to the screen plate surface in the SS is not known with the certainty of the channel tests.

As an alternative comparison, the passage ratio curves for the single slot channel and the SS were compared on the basis of the slot velocity that gave passage ratio of 1.0 for 1 mm nylon fibres and about 0.9 for 3 mm nylon fibres. This slot velocity is referred to as $V_{s(max)}$ (see Table 5.2). This is a somewhat arbitrary basis for comparison, but one which facilitates direct comparison of the curves as shown in Figure 5.33. It can be seen that compared on this basis, the shapes of the passage ratio curves for all the three cases are similar. This comparison shows that the behaviour of fibre passage in SS through multiple slots is qualitatively similar to the fibre passage through a single slot. The following study involving the sectional screen was then carried out with the screen plate having ten slots which were 0.5 mm wide.
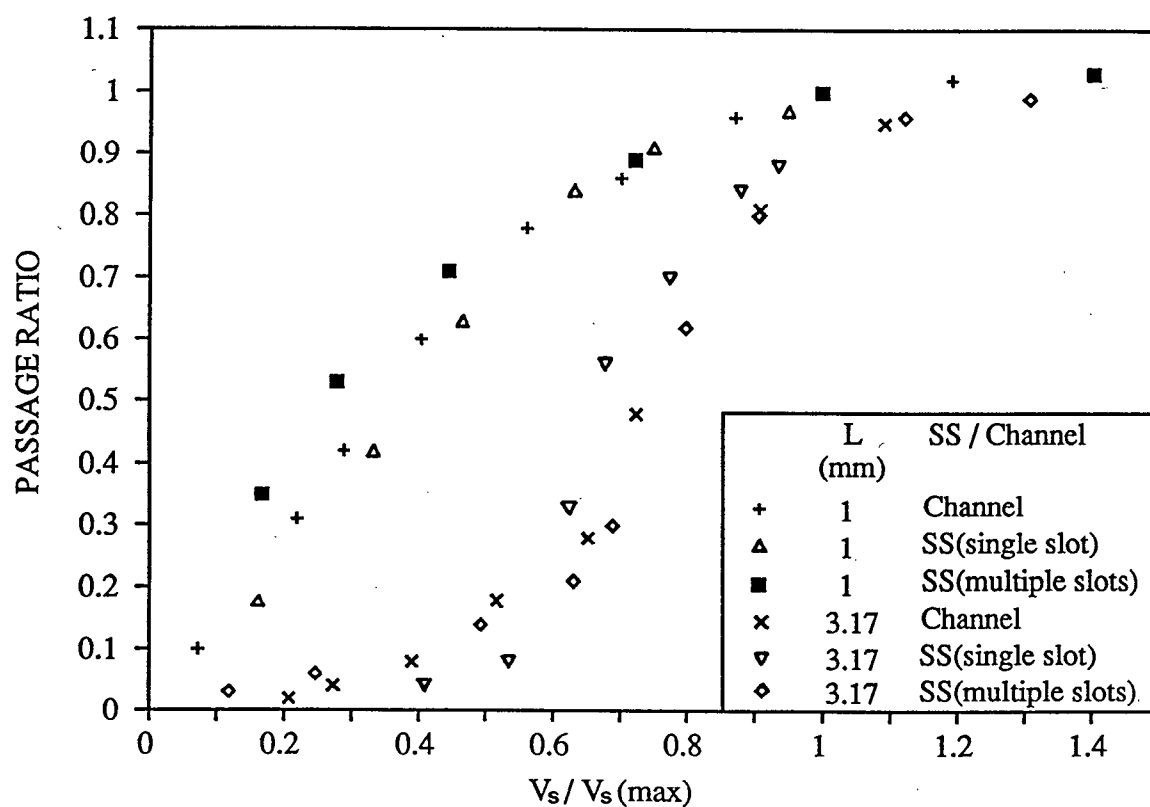
Figure 5.33: Passage ratio of nylon fibres against adjusted normalized slot velocity comparing the single slot channel results with those of the sectional screen (single as well as multiple slots). The purpose is to show directly the similarity of the shapes of the curves.

Effect of the Tip Speed of the Rotor (V_t)

Passage ratios of 1 mm nylon fibres were determined when varying the rotor tip speed from 3.5 m/s to 10.8 m/s. Passage ratios are plotted against slot velocity as a function of V_t in Figure 5.34. It is apparent that the curves shifted in magnitude but remained type "A" in shape. In general, the passage ratios at a given slot velocity decreased with increased rotor tip speed in slot velocity range of 0.4–2 m/s. The slot velocity at which the passage ratio equals 1 is lower for the lower V_t and at slot velocities greater than 2.5 m/s, passage ratios approach 1.0 irrespective of the rotor tip speed. Also, there is no significant difference in the change in passage ratios with the change in slot velocity in the range of V_t considered here. This effect of increasing rotor tip speed is similar to the effect of increasing V_u in case of single slot channel (see Figure 5.5).

5.4.2 Higher Concentrations

Observations from the study of stapling regimes in a single slot channel (Appendix F) suggest V_s/V_u as a key variable which affect the modes of stapling. The modes of stapling and the consistency then determine the passage ratio and the plugging concentration. In the case of the sectional screen, the rotor induces pulsations which may influence the modes of stapling. However, slot velocity and rotor tip speed in the case of the SS are expected to influence the passage ratio at higher concentrations as well. Thus, passage ratio measurements were made in the SS with increasing feed concentration by varying the accept flow rate and the rotor tip speed. The effect of fibre flexibility on passage ratio and plugging concentration was also studied by using rayon fibres. In view of the differences in the velocities and factors such as pulse frequency and strength, only qualitative comparisons are made.
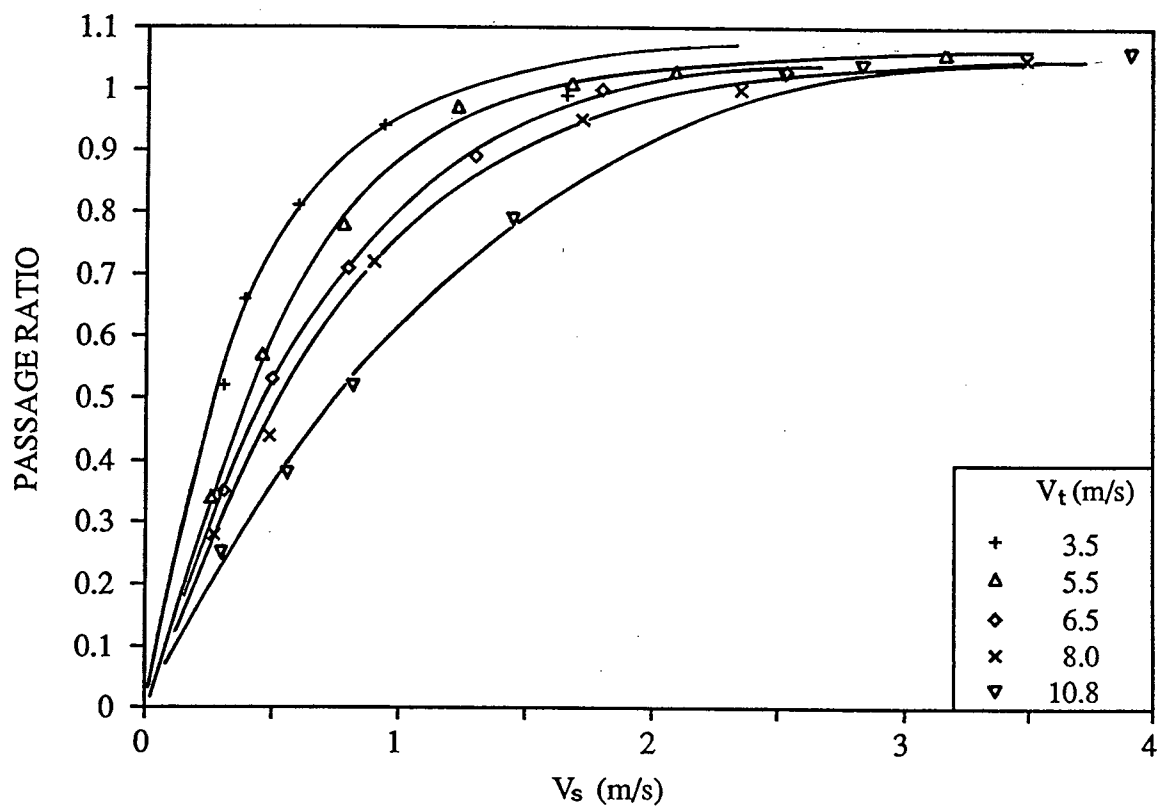
Figure 5.34: Effect of rotor tip speed on the passage ratio of 1 mm nylon fibres. $C_{nF} = 35,000$ fibres/l. ($N = 0.002$).
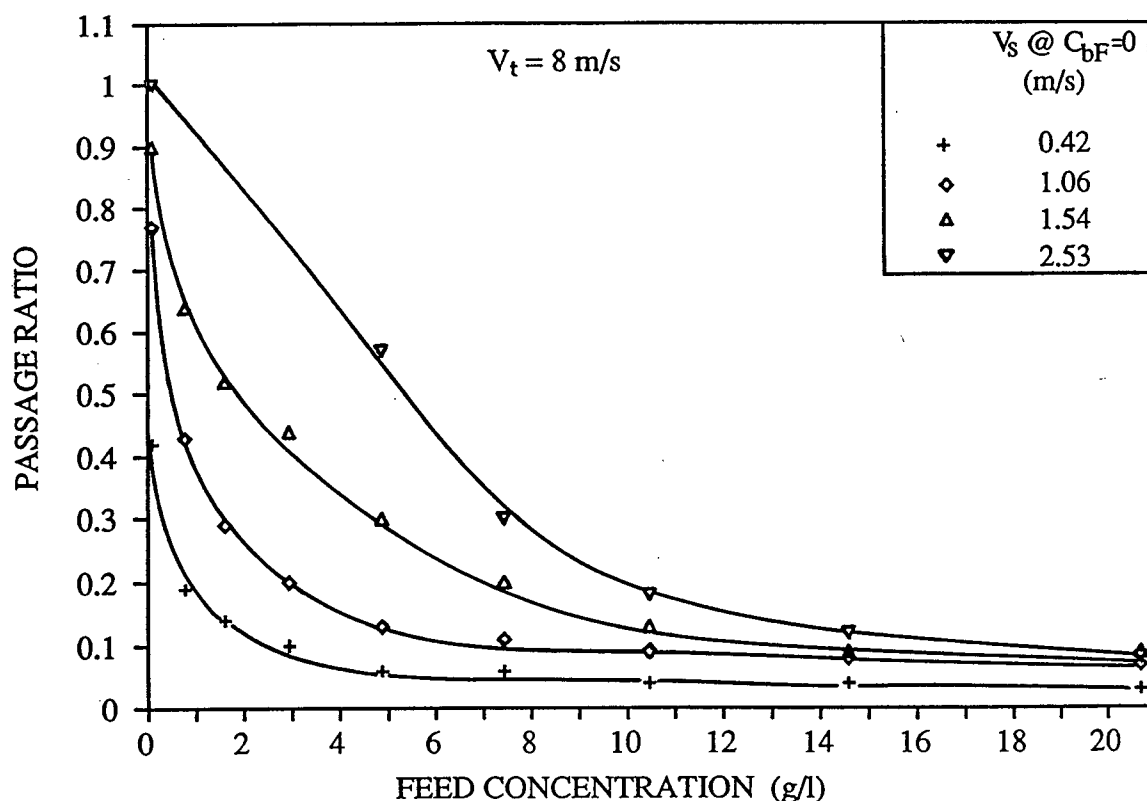
Figure 5.35: Effect of feed concentration on passage ratio of 1 mm nylon fibres as a function of V_s at $C_{bF} = 0$. $V_t = 8$ m/s.

Effect of Accept Flow Rate

The effect of increasing feed concentration on the passage ratio of 1 mm nylon fibres is shown in Figure 5.35. In these tests, the rotor tip speed was set at 8 m/s and the slot velocity at zero feed concentration (V_s at $C_{bF} = 0$) was set at 4 levels, $i.e.$ 0.42, 1.06, 1.54 and 2.53 m/s. Initially, the passage ratios decreased with increasing feed concentration and then levelled off. The concentration at which the passage ratios levelled off was higher for a higher slot velocity. At feed concentrations greater than 14 g/l ($N = 4.6$), the passage ratios were independent of the accept flow rate.

This effect of increasing feed concentration in the SS is similar to the effect of feed concentration on the passage ratio in a single slot channel (see Figure 5.13).

In both cases, an equilibrium passage ratio for 1 mm nylon fibres resulted from increased feed concentration.

Effect of the Rotor Tip Speed

The combined effect of feed concentration and the rotor tip speed is shown in Figure 5.36. At dilute concentrations, passage ratio always decreased with increased rotor tip speed as shown earlier in Figure 5.34. However, with increased feed concentration, the passage ratios at a low rotor tip speed of 3.5 m/s were lower than those for higher tip speeds. The rotor tip speed in the SS is similar to the upstream velocity in the channel with an added effect of pulsation (pulse strength and frequency). At low feed concentrations, lower rotor tip speeds are sufficient to keep the slots purged and thus maintain a given passage ratio. However, at higher feed concentrations, higher rotor tip speeds are needed to accomplish this. This suggests that at higher feed concentrations, a stronger pressure pulse of higher frequency is needed to keep the slots clear for fibre passage. Though the strength of the pulse was not measured, it is obvious that the magnitude and frequency of the pulse generated by the rotor will increase with increased rotor tip speed.

Effect of Fibre Flexibility

The effect of fibre flexibility on the passage ratio and plugging concentration was also studied. The passage ratios of 1 mm rayon fibres were measured with increasing feed concentration at different rotor tip speeds and accept flow rates. The passage ratios of 1 mm rayon fibres are compared with those of 1 mm nylon fibres in Figure 5.37 at a rotor tip speed of 8 m/s and for V_s at $C_{bF} = 0$ of 1.06 m/s and 2.53 m/s. At the lower slot velocity, the passage ratios of rayon fibres were higher than those of nylon fibres up to a feed concentration of about 7 g/l. At feed
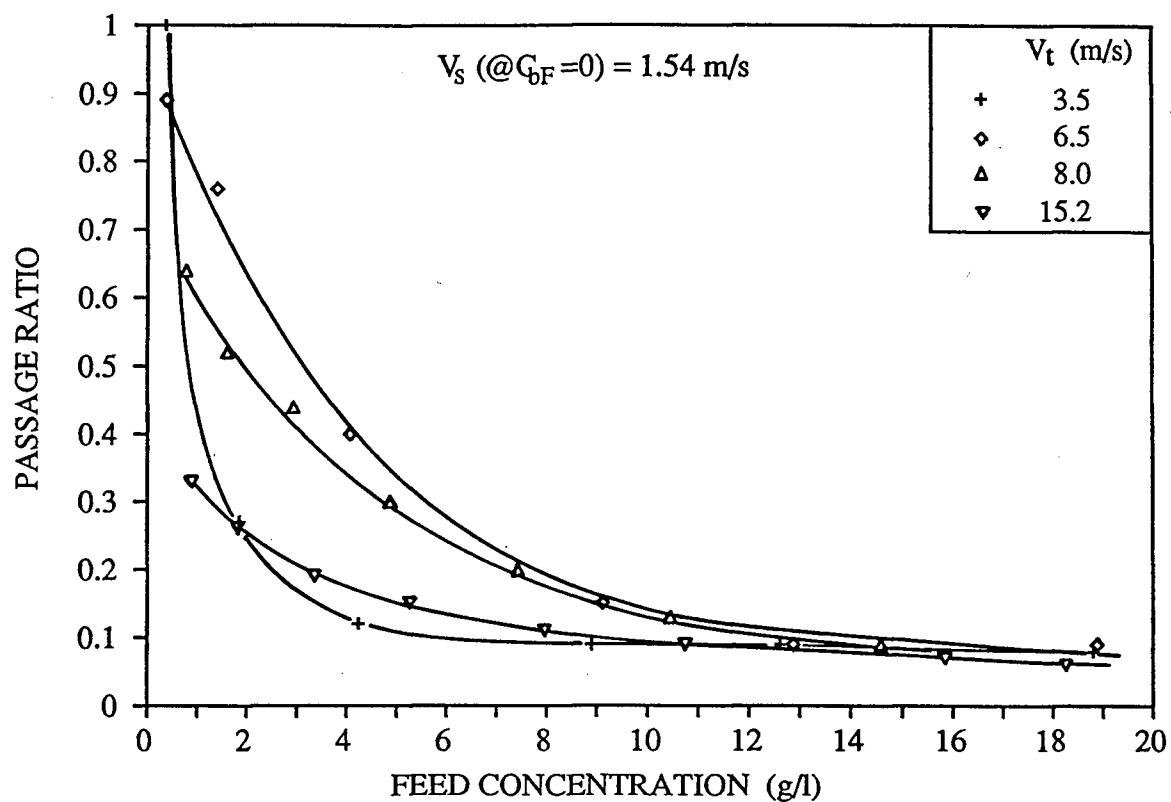
Figure 5.36: Effect of feed concentration on the passage ratios of 1 mm nylon fibres as a function of rotor tip speed. V_s (at $C_{bF} = 0$) = 1.54 m/s.

114
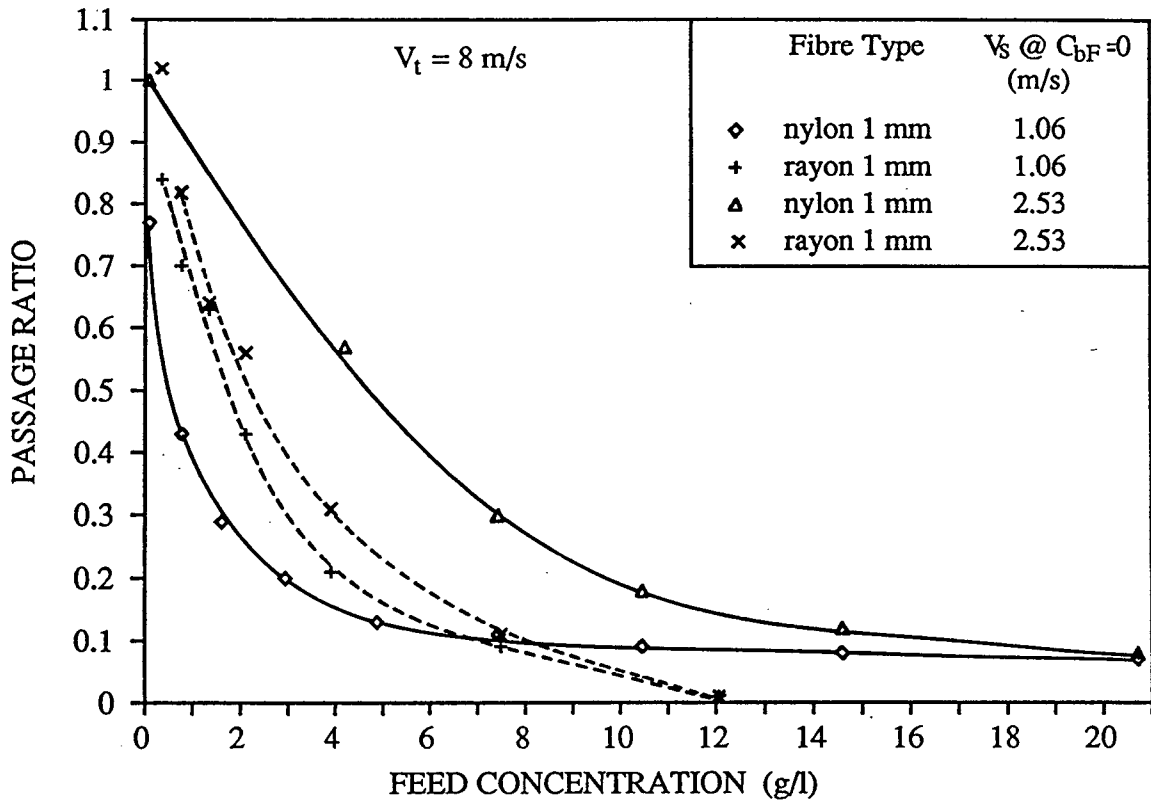
Figure 5.37: Passage ratio against feed concentration showing the effect of fibre flexibility at two levels of slot velocity. $V_t = 8$ m/s.

concentrations greater than 7 g/l, the passage ratios of rayon fibres became lower and the slots were completely plugged ($P = 0$) at a feed concentration of about 12 g/l. At the higher slot velocity, the passage ratios of rayon fibres were always lower than those of nylon fibres and the slots were plugged at 12 g/l. On the other hand, 1 mm nylon fibres resulted in an equilibrium passage ratio of about 0.1 and the slots were not plugged completely up to a feed concentration of 40 g/l ($N = 13$). It can be concluded that flexible rayon fibres yield higher passage ratios at dilute feed concentrations but plug the slot completely at lower feed concentrations than do stiff fibres. The same behaviour was observed in a single slot channel as shown earlier in Figures 5.17 and 5.18.

Passage ratios for 1 mm nylon and rayon fibres at a higher rotor tip speed of 15.2 m/s are plotted in Figure 5.38. By increasing the rotor tip speed from 8 m/s to 15.2 m/s, the plugging concentration for rayon fibres increased from 12 g/l to about 20 g/l. Also, the passage ratios of 1 mm nylon fibres at the higher slot velocity increased substantially. This is due to the effect of increased pulse frequency and perhaps the increased pulse strength. It means that the passage ratio and the plugging concentration are dependent on fibre flexibility and the pulse strength. At higher concentrations, the slot can be purged by increasing the rotor tip speed. Thus, a given passage ratio can be maintained or a given throughput can be achieved. For flexible fibres and higher concentrations, a stronger pulse is required to keep the slots purged in order to obtain a given passage ratio and capacity.

5.4.3 Summary

1. In the case of the sectional screen with a single or multiple slots, the shape of the passage ratio curves at dilute concentrations remained similar to those of curve "A" and curve "B" obtained for a single slot channel. In the SS, at a given slot velocity and the rotor tip speed, the passage ratios for multiple slots in the SS were higher than those of a single slot. The effect of varying rotor tip speed in the case of the SS was also similar to that found with increasing upstream velocity in the channel tests. For example, the passage ratios decreased with increasing rotor tip speed at dilute concentrations.

2. In general, the effect of increasing feed concentration in the SS was also similar to that found for the channel. Passage ratios at a given rotor tip speed decreased with increasing feed concentration. The short and stiff 1 mm nylon fibres eventually reached an equilibrium passage ratio, while short and

116
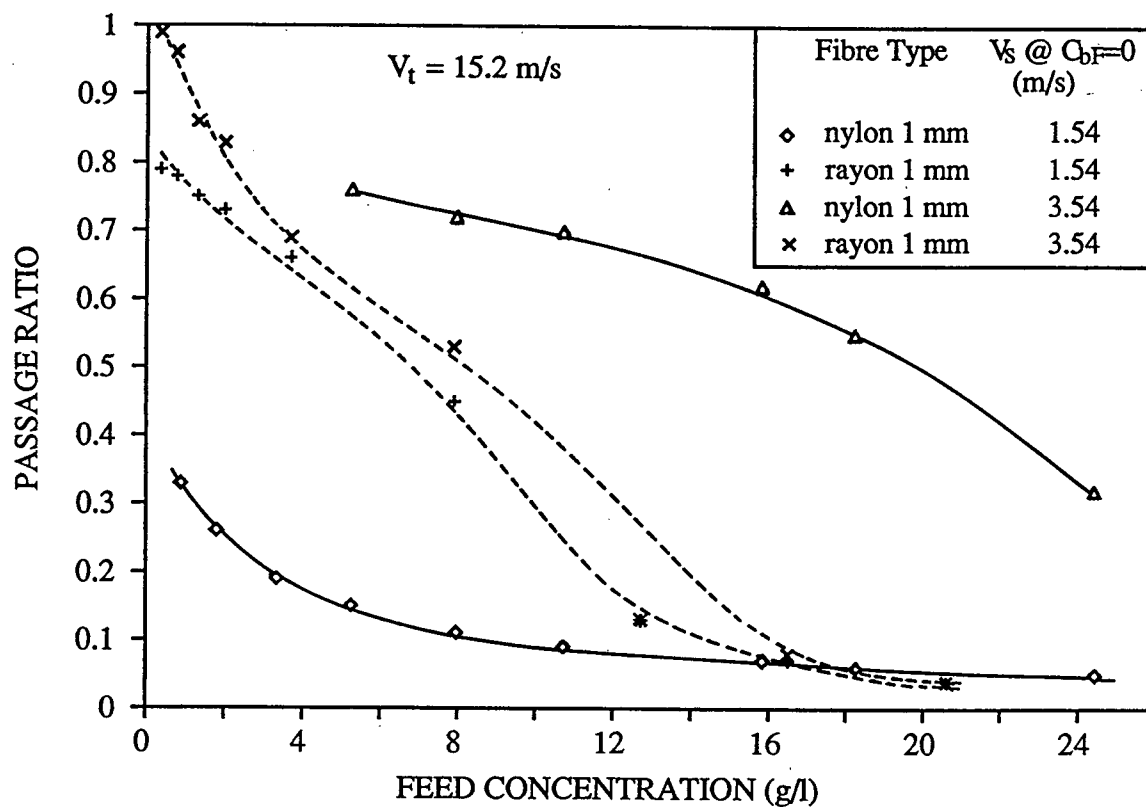
Figure 5.38: Passage ratio against feed concentration showing the effect of fibre flexibility at two levels of slot velocity. $V_t = 15.2$ m/s.

flexible 1 mm rayon fibres plugged the slot completely ($P = 0$).

3. In addition to producing a fluid speed V_u, the rotor also provides pulsations which can be controlled by varying the rotor design. This factor is of utmost importance in the SS and was absent in the single slot channel. Though the size and duration of pressure pulse was not measured, the observations at higher rotor tip speeds suggest that a stronger pulse of higher magnitude and frequency is required for flexible fibres. The same holds true at higher feed concentrations. In other words, a specific type of rotor compatible with the screen plate should be designed for a given type of fibre and operating consistency in order to achieve the desired passage ratio and capacity.

Chapter 6

Summary

The findings of this study are summarized below.

1. The dependence of passage ratio of stiff fibres on the ratio of slot velocity to upstream velocity followed an exponential curve ("A" behaviour) when the fibre length to slot width ratio (L/W) was ≤ 2, and a cumulative distribution curve ("B" behaviour) when L/W was > 2. Increasing flexibility of fibres tended to shift the behaviour from "B" type to "A" type when $L/W > 2$.

2. "A" curve behaviour was postulated to occur from flow splitting from the main flow, and hence was dependent on upstream conditions. The data for this behaviour correlated very well to a dimensionless penetration parameter that reflected the fractional amount of feed flow drawn into the slot.

3. "B" curve behaviour was postulated to occur from fibre contact with the upstream wall during rotation and bending of the fibre over the downstream edge of the slot. The data for this type of curve could not be correlated to the penetration parameter. A bending parameter reflecting the stiffness and bending forces acting on the fibres and the penetration parameter correlated the data well.

119

4. Increased concentration of the feed flow beyond the dilute range up to $N = 4$, caused stapling. The latter lowered the passage ratio values for "A" curve behaviour to a finite equilibrium value. The original value could be restored if the slot flow was increased to its original value for an unobstructed slot. On the other hand, fibres which followed "B" curve behaviour at dilute concentrations plugged the slot completely at $N = 1$.

5. The above findings for a single slot at dilute concentrations were found to hold qualitatively for slots having contoured entries, elevated fibre concentrations, multiple slots, and pulses induced by a rotor of the type used in commercial pulp screens.

Chapter 7

Conclusions

1. Fibre passage through narrow apertures can be usefully described in terms of three conceptual components — penetration, rotation and bending.

2. Dimensionless numbers can be derived for each of these components from simple material and moment balances.

3. The penetration parameter is a key factor in determining the passage of stiff fibres having a fibre length to slot width ratio less than 2 *i.e.* $L/W < 2$.

4. When $L/W > 2$, the experimental findings of this study strongly support, but do not prove, that fibre contact with the upstream wall of the slot significantly changes the relationship between passage ratio and slot velocity from the shape of an exponential curve to that of a cumulative probability distribution curve.

5. The finding of two differing characteristic curves appears to hold at higher concentrations, contoured entry geometries, multiple slots, and in the presence of pulses induced by a rotor. The findings are therefore likely to apply to commercial pulp screens.

6. Since large differences in passage ratio lead to good separation, long stiff fibres appear to be best fractionated from short stiff fibres by a slot having

a width which yields $L/W < 2$ for the desired short fibres and $L/W > 2$ for the longer fibre fraction.

7. When $L/W < 2$, flexible fibres behave like stiff fibres. When $L/W \simeq 6$, flexible fibres tend to exhibit behaviour between that of stiff short $(L/W = 2)$ and long $(L/W = 6)$ fibres.

Chapter 8

Recommendations for Future Work

1. The role of fibre stapling in screening has been shown to be important even
   at low concentrations. Accordingly, this aspect of screening should be the
   subject for further detailed study. Two studies are recommended here:

   (a) The relative importance of turbulence at the aperture entry and pul-
       satile flow within the aperture on removing stapled fibres should be ex-
       amined. This may be accomplished by exploring experimental methods
       of inducing these effects separately.

   (b) The dynamic nature of fibre stapling should be examined, that is, the
       degree to which fibres continually form and shed with time. Measure-
       ment of time-dependent pressure drop across the slots could yield this
       information from the time-dependent flow resistance.

2. This study did not examine the trajectories of individual fibres. However,
   some of the postulates put forward, for example, fibre penetration, could
   benefit from such a study. Given the difficulties found in earlier work of
   filming fibres as small as pulp fibres, the possibility of carrying out future
   experiments on scaled-up apertures and scaled-up fibres should be explored.
   By establishing geometric and dynamic similitude, it may be possible to

conduct meaningful tests to elucidate the fibre behaviour in passage and stapling of apertures.

3. Lastly, the existence of "A" and "B" curves and the usefulness of the dimensionless numbers relating passage ratio to slot velocity should be tested on commercial pulp screens at conditions of industrial interest in order to determine their usefulness in pulp and paper applications.

Nomenclature

Symbol	Definition	Units
A_s	area of the slot	m^2
B_e	bending parameter in Equation (3.12)	dimensionless
C_D	drag coefficient	dimensionless
C_m	mass concentration	fraction
C_v	volumetric concentration	fraction
$C_{v,cr}$	critical volumetric concentration	fraction
C_{nF}	feed concentration	fibres/l
C_{bF}	feed concentration	g/l
d	fibre diameter	m
E	modulus of elasticity	N/m^2
E_R	reject efficiency	fraction
F	fibre flexibility	$N^{-1} \cdot m^{-2}$
g	acceleration due to gravity	m/s^2
I	area moment of inertia	m^4
k_1	constant in Equation (3.1)	as appropriate
k_2	constant in Equation (3.2)	as appropriate
k_3	constant	as appropriate
L	fibre length (general)	m
L_n	number average fibre length	m
L_w	weighted average fibre length	m
m	mass	kg
N	crowding factor	

Symbol	Definition	Units
P	passage ratio in general	
P_c	passage ratio of contaminants in Equations (2.3) and (2.4)	
P_p	passage ratio of pulp fibres in Equations (2.3) and (2.4)	
P_e	penetration parameter	dimensionless
Q_S	volumetric flow rate through the slots	l/min
Q_{SW}	volumetric flow rate through the slot at $C_{bF} = 0$	l/min
R	reject rate in Equation (2.1) and (2.2)	fraction
R^2	coefficient of multiple determination	dimensionless
R_0	rotation parameter	dimensionless
R_{ep}	particle Reynolds number	dimensionless
S	fibre stiffness in bending	N·m^2
v	volume	m^3
V_s	bulk slot velocity	m/s
V_u	bulk upstream velocity	m/s
V_t	rotor tip speed	m/s
W	slot width	m
W_e	effective slot width	m
$WRRk$	water retention ratio at knee (see sections A.3 and B.1)	kg water/ kg o.d. fibre
y	exit layer thickness	m
Y	penetration distance	m
Z	depth of contour (Figure 4.4)	m

Symbol	Definition	Units

Greek Letters

α	a screening constant also known as screening quotient in Equation (2.1)	
β	a screening constant in Equation (2.2)	
θ_1 and θ_2	angles that fibre makes with the plate surfaces on the downstream edge of the slot	degrees
ρ	density	kg/m^3
δ	fibre deflection in bending	m

Subscripts

f	fibre	
s	slot	
u	upstream	
w	water	
wf	free water	

References

A1 Axegard, P. and A. Teder, "Model Experiments in Bleaching of Shives and Bark Particles", Proc. of Intern. Bleaching Conf., Chicago, pp. 35–43 (1976).

A2 Annergren, G.E. and P.O. Lindblad, "Shives/Brightness: A Problem of Bleaching Optimization", Tappi J., **59**(11):95–98 (1976).

A3 Axegard, P., "Particles Difficult to Bleach in Softwood Kraft Pulp", Svensk Papperstid., **81**(14):449–456 (1978).

A4 Ali, S.F., "Fibre Fractionation in Pulp Processing", Preprints of 73rd Annual Meeting, CPPA Technical Section, Montreal, A1–A6 (1987).

A5 Andersson, O. and W. Bartok, "Application of Feedback to Fibre Classifiers", Svensk Papperstid., **58**(10):367–373 (1955).

A6 Abrams, R.W., "Retention of Fibres in Filtration of Dilute Suspensions", Tappi J., **47**(12):773–778 (1964).

B1 Badger, W.L. and J.T. Banchro, "Introduction to Chemical Engineering", McGraw-Hill, New York, 618–636 (1955).

B2 Brereton, T., "Probability Screening and the Effects of Major Operating Variables", Filtration and Separation, **12**:692–696 (1975).

B3 Browning, B.H. and J.R. Parker, "The Characterization of Offset Lint and the Testing of Offset Papers", Proc. of the Symp. on Mechanical Pulps, Eucepa, 67–81 (1970).

B4 Bulger, W.H., "Some Basic Principles of High Capacity Screening", Proc. of 49th Annual Meeting, CPPA Technical Section, Montreal, D111–115 (1963).

B5 Breck, D.H., D.L. Young and W.D. May, "An Aspect of Screening Thermomechanical Pulp", Proc. of Intern. Mechanical Pulping Conf., Helsinki, paper no. 10 (1977).

B6 Brecht, W. and A. Weidhaas, "Relations of Groundwood Screening Procedure", Tappi J., **45**(5):383–390 (1962).

B7 Brewer, J.L. and J.A. Bolton, "Fibre Fractionation of High Yield Kraft Pulp", Tappi J., **57**(6):121–122 (1974).

B8 Bugliarello, C. and C. Hsiao, "Phase Separation in Suspensions Flowing Through Bifurcations — A Simplified Hemodynamic Model", Science, **143**:469–471 (1964).

B9 Boettcher, P.C., "Results from a New Design of Contoured Screen Plate", Proc. of TAPPI Pulping Conf., Toronto, 279–283 (1986).

B10 Bennington, C.P.J., "Mixing Pulp Suspensions", PhD Thesis, Dept. of Chemical Engineering, University of British Columbia, Vancouver (1988).

C1 Clark, J. d'A, "Pulp Technology and Treatment for Paper", Miller Freeman Publications Inc., San Francisco, 734–736 (1985).

C2 Cowan, W.F., "The Screening of Groundwood Pulp — A Reappraisal", Pulp & Paper Mag. Can., **70**(1):T11–15 (1969).

C3 Chollet, J., Duffy, M. and O. Sepall, "Studies of Dirt in Sulfite Pulp", Pulp & Paper Mag. Can., **60**(4):T123–128 (1959).

C4 Claudio-da-Silva, Jr., E., "The Flexibility of Pulp Fibres — A Structural Approach", Intern. Paper Physics Conf., Harwich Port, MA, 13–25, September 18–22 (1983).

C5 CRC Handbook of Chemistry and Physics, 65th ed., F–10.

C6 Clarke-Pounder, I.J., "Pipe Line Screening", Preprints of 56th Annual Meeting, CPPA Technical Section, Montreal, 79–85 (1970).

C7 Constantino, J., M.D.A. Frith and D.M. Mackie, "CTMP Expansion at Powell River", Preprints of CPPA Pacific and Western Branches Technical Conference, Whistler, BC (1988).

C8 Carvill, R.E., "High Consistency Pressurized Pulp Screening", Tappi J., **51**(9): 104A–107A (1968).

C9 Cox, M.T., "Application of Hot Stock Pulp Fractionation at Mead Coated Board", Tappi J., **72**(2):97–100 (1989).

C10 Cockett, S.R., "An Introduction to Man-Made Fibres", Pitman & Sons, London, 38–43 (1966).

D1 Drolet, R. and C. Grenier, "Optimization of the Reject Rates", Pulp & Paper Can., **83**:C:T96–99 (1982).

D2 Doshi, M.R. and M.G. Prein, "Effective Screening and Cleaning of Secondary Fibres", Proc. of TAPPI Pulping Conference, Toronto, 67–73 (1986).

E1 Estridge, R., "The Initial Retention of Fibres by Wire Grids", Tappi J., **45**(4):285–291 (1962).

E2 Ehrnrooth, E.M.L. and P. Kolseth, "The Tensile Testing of Single Wood Pulp Fibres in Air and in Water", Wood and Fiber Science, **16**(4):549–566 (1984).

F1 Forbes, D.R., "Pulp Mill Screening is Key to Pulp Quality, Maximum Fibre Utilization", Pulp and Paper, **61**(11):107–112 (1987).

F2 Fulton, C., "TMP Screening — Another Approach", Tappi J., **67**(1):60–62 (1984).

F3 Frejborg, F., "Improved Operation of TMP Plant Through Optimization of screening", Pulp & Paper Can., **89**(1):T20–24 (1988).

F4 Frith, M.D. and D.J. Fisher, "The Effect of Consistency on Screening of TMP at Powell River", MacMillan Bloedel Research Ltd. Internal Report, October (1978).

G1 Gooding, R.W., "The Passage of Fibres Through Slots in Pulp Screening", MASc Thesis, Dept. of Chemical Engineering, University of British Columbia, Vancouver (1986).

G2 Gooding, R.W. and R.J. Kerekes, "Derivation of Performance Equations for Solid-Solid Screens", Can. J. Chem. Eng., **67**(5):801–805 (1989).

G3 Gustafsson, H. and P. Vihmari, "Viewpoints on Screening and Cleaning of Mechanical Pulps", Proc. of Intern. Mechanical Pulping Conference, Helsinki, Paper no. 41 (1977).

G4 Gooding, R.W. and R.J. Kerekes, "The Motion of Fibres Near a Screen Slot", J. Pulp & Paper Sci., **15**(2):J59–62 (1989).

G5 Greenwood, B., J. Gullichsen, E. Harkonen, O. Ferristius and G. Tistad, "Implications of Medium Consistency Screening", Preprints of 56th Annual Meeting,CPPA Technical Section, Montreal, A7–A16 (1986).

H1 Hill, J., H. Hoglund and E. Johnsson, "Evaluations of Screens by Optical Measurements", Tappi J., **58**(10):120–124 (1975).

H2 Hopkins, R.M., R. McPherson and L.J. Morin, "Analysis of The Effects of Centrifugal Pulp Cleaners on Newsprint Runnability", Pulp & Paper Mag. Can., **63**(12):T563–570 (1962).

H3 Hooper, A.W., "The Screening of Chemical Pulp" in "Pulp and Paper Manufacture — Volume 5", Joint Textbook Committee of the Pulp Industry, CPPA, 318–366 (1989).

H4 Hooper, A.W., "Mechanical Pulp Screening Advances Improve Quality of Printing Grades", Pulp and Paper, **53**(1):174–178 (1979).

H5 Høydahl, H.E. and S. Hauan, "Mini Shives in Mechanical Pulp", Norsk Skogindustri, **26**(3):62–65 (1972).

H6 Høydahl, H.E., "Practical and Theoretical Aspects of Groundwood Screening", Norsk Skogindustri, **27**(9):252–258 (1973).

H7 Hooper, A.W., "Speck Dirt Removal with Slotted Screens", Pulp & Paper Can., **90**(5):T164–168 (1989).

H8 Horie, M., "Time Dependent Shear Flow of Artificial Slurries", PhD Thesis, Dept. of Chemical Engineering, University of British Columbia, Vancouver (1978).

H9 Halonen, L., R. Ljokkoi and K. Peltonen, "Improved Screening Concepts", TAPPI Proc. of Annual Meeting, Atlanta, GA, 207–212 (1990).

I1 Isenberg, I.H., "Pulpwoods of the United States and Canada", Vol. I & II, The Institute of Paper Chemistry, Appleton, WI (1980).

J1 Jepsen, A., "New Wave Screen Baskets Upgrade Existing Systems", Proc. of TAPPI Pulping Conf., San Francisco, 515–520 (1984).

K1 Kubat, J. and B. Steenberg, "Screening at Low Particle Concentrations", Svensk Papperstid., **58**(9):319–324 (1955).

K2 Klemn, K.H., "New Principles for Groundwood Screening", Paper trade J., **140**(1):20–29 (1956).

K3 Kerekes, R.J., R.M. Soszynski and P.A. Tam Doo, "The Flocculation of Pulp Fibres", Trans. of the Eighth Fundamental Research Symp., Oxford, 1:265–310 (1985).

K4 Kerekes, R.J. and C. Schell, "Characterization of Fibre Flocculation Regimes by a Crowding Factor", CPPA Technical Section Annual Meeting, Montreal, January 1991.

K5 Kubat, J., "Screening Process Involving Particle Interaction", Svensk Papperstid., **59**(5):175–178 (1956).

K6 Koffinke, R.A., "Secondary Fibre Trend Give Impetus to Pressure Screening", Pulp & Paper, **49**(7):116–118 (1975).

L1 Laurila, P., G. Smook, K. Cutshall and J. Mardon, "Shives — How They Affect Paper Machine Runnability", Pulp & Paper Can., **79**(9):T285–289 (1978).

L2 Lehman, D.F., "Pulp Screening" in "Handbook of Pulp Paper Technology", K.W. Britt, ed., Van Nostrand Reinhold, New York, 209–220 (1970).

L3 Leblanc, P.E., "Screening Technology and Methods", Tappi J., **60**(10):61–62 (1977).

L4 Lambert, J.E., "The Comparative Evaluation of Screens and Screening Efficiencies", Pulp & Paper Mag. Can., 64(9):T406–424 (1963).

L5 Leblanc, P.E., "A Breakthrough in Pressure Screening", Proc. of TAPPI Pulping Conf., Toronto, 75–77 (1986).

L6 Lissenburg, R.C.D., J.O. Hinze and H. Leijdens, "An Experimental Investigation of a Constriction on Turbulent Pipe Flow", App. Sci. Res., 31:343–362 (1975).

M1 Mathews, C.W., "Screening", Chemical Engineering, 79:76–83 (1977).

M2 MacDonald, R.G., "Pulp and Paper Manufacture", Vol. I, McGraw Hill, New York, 726–739 (1969).

M3 MacMillan, F.A., W.R. Farrell and F.G. Booth, "Shives in Newsprint: Their Detection, Measurement and Effects on Paper Quality", Pulp & Paper Mag. Can., 66(7):T361–369 (1965).

M4 McNowen, J.S., "Mechanics of Manifold Flow", Trans. of the American Society of Civil Engineers, 119:1103–1142 (1954).

M5 Moujaes, S.F., "Measurements of Slurry Concentration and Flow Rate in Shell and Tube Heat Exchangers", Can. J. Chem. Eng., 62:62–67 (1984).

M6 Mason, S.G., "The Motion of Fibres in Flowing Liquids", Pulp & Paper Mag. Can., 51(4):93–100 (1950).

M7 Macey, G.D., "Evaluation of Waved Screen Baskets in Kraft Brown Stock Screening", Screening and Cleaning Seminar, CPPA Pacific Coast Branch, Technical Section, Vancouver, June 17–19 (1987).

M8 Mackie, D.M., M.D. Frith, J. Constantino and S.M. Parker, "Low Medium Consistency Screening", Preprints of 76th Annual Meeting, CPPA Technical Section, Montreal, A305–311 (1990).

N1 Nelson, G.L., "The Screening Quotient: A Better Index for Screening Performance", Tappi J., 64(5):133–134 (1981).

N2 Nuttall, G.H., "Screens and Cleaners", Theory and Operation of the Fourdrinier Paper Machine, Chapter 2, S.C. Phillips, London, 101–115 (1967).

N3 Nevalainen, K., "Optimization of Groundwood screening", Paperi ja Puu, 51(9):
667–678 (1969).

N4 Nasr-El-Din, H., C.A. Shook and M.N. Esmail, "Wall Sampling in Slurry Systems", Can. J. Chem. Eng., 63:746–753 (1985).

N5 Nasr-El-Din, H. and C.A. Shook, "Particle Segregation in Slurry Flow Through Vertical Tees", Int. J. Multiphase Flow, **12**(3):427–443 (1986).

N6 Nasr-El-Din, H., A. Afacan and J.H. Masliyah, "Solids Segregation in Slurry Flow Through a T-Junction With a Horizontal Approach", Int. J. Mutliphase Flow, **15**(4):659–671 (1989).

N7 Norman, B.G., R. Moller, R. Ek and G.G. Duffy, "Hydrodynamics of Papermaking Fibres in Water Suspension", Fibre-Water Interactions in Paper-Making, Vol. I, Trans. Fundamental Research Symp., Oxford, **1**:195–249 (1978).

P1 Perry's Chemical Engineer's Handbook, Sixth ed., McGraw-Hill, **21**:13–18 (1984).

P2 Panshin, A.J. and C. de Zeenw, "Textbook of Wood Technology", 4th ed., McGraw Hill, New York, 131–135 & 166–172 (1980).

P3 Pekkarinen, T., P. Haikkala and K. Ebeling, "Function of Pressure Screen in Groundwood Screening", An unpublished report of Tampell Ltd., Paper Machinery Division (1980).

P4 Pemble, G.G., "Brown Stock Screening — A New Approach", Proc. of TAPPI Pulping Conference, Washington, DC, 7–11 (1987).

P5 Piirainen, R., "Optical Method Provides quick and Accurate Analysis of Fibre Length", Pulp and Paper, **59**(11):69–71 (1985).

R1 Roberts, E.J., P. Stavenger, J.P. Bowersox, A.K. Walton and M. Mehta, "Solid/Solid Separations", Chemical Engineering, Deskbook Issue, 89–98 (1971).

R2 Rydholm, S.A., "Pulping Processes", Interscience Publishers, New York, 47–52 (1965).

R3 Riese, J.W., P. Spiegelberg and S.R. Kellnberger, "Mechanism of Screening: Dilute Suspensions of Stiff Fibres at Normal Incidence", Tappi J., **52**(5):895–903 (1969).

S1 Sjostrom, E., "Wood Chemistry — Fundamentals and Applications", 6–11, Academic Press, New York (1981).

S2 Shallhorn, P.M. and A. Karnis, "A Rapid Method for Measuring Wet Fibre Flexibility", Preprints of 67th Annual Meeting, CPPA Technical Section, Montreal, A167–174 (1981).

S3 Sears, G.R., R.F. Tyler and C.W. Denzer, "The Role of Shives in Paper Web Breaks", Pulp & Paper Mag. Can., **66**(7):T351–360 (1965).

S4 Schniewind, H.P., G. Ifju and D.L. Brink, "Effect of Drying on the Flexural Rigidity of Single Fibres", in "Consolidation of the Paper Web", Vol. I, F. Bolam, ed., B.P. & B.M.A., London, 538–543 (1966).

S5 Samuelson, L.G., "Stiffness of Pulp Fibres", Svensk Papperstid., **67**:905–910 (1964).

S6 Soszynski, R.M., "The Formation and Properties of Coherent Flocs in Fibre Suspensions", PhD Thesis, Dept. of Chemical Engineering, University of British Columbia, Vancouver, BC (1987).

S7 Stone, J.E., A.M. Scallan and G.M.A. Aberson, "The Wall Density of Native Cellulose Fibres", Pulp & Paper Mag. Can., **67**(5):T263–267 (1966).

S8 Seifert, P., "Screening of Pulp", TAPPI Stock Preparation Course, April 16–17, Atlanta, GA, 19–27 (1980).

S9 Steenberg, B., "Principles of Screening System Design", Svensk Papperstid., **56**(20):771–778 (1953).

S10 Scallan, A.M. and H.V. Green, "A Technique for Determining the Transverse Dimensions of the Fibres in Wood", Wood and Fiber, 5(4):323–333 (1974).

T1 Tam Doo, P.A. and R.J. Kerkes, "A Method to Measure Wet Fibre Flexibility", Tappi J., **64**(3):113–116 (1981).

T2 Tappi "Screening Symbols, Terminology and Equations", Technical Information Sheets, TIS 0604-04 (1989).

T3 Travers, C.S., "Mill Operating Experience with a Beloit S-Screen", Preprints of 74th Annual Meeting, CPPA Technical Section, Montreal, B255–B267 (1988).

T4 Tappi Test Methods, "Dirt in Pulp", T213 OM-85.

T5 Tappi Useful Methods, 240–242, "Shive Content of Mechanical Pulp".

T6 Thomas, A.S.W. and K.C. Cornelius, "Investigation of Laminar Boundary-Layer Section Slot", AIAA J., **20**(6):790–796 (1982).

T7 Torrest, R.S. and R.W. Savage, "Particle Collection from Vertical Suspension Flows Through Small Side Ports — A Correlation", Can. J. Chem. Eng., **37**:224–236 (1975).

Y1 Young, D.L., "Fractionation of TMP by Screening", Preprints of 64th Annual Meeting, CPPA Technical Section, Montreal, A149 (1978).

Appendix A

Fibre and Suspension Properties

A.1 Fibre Dimensions

Fibre length is the most important fibre property that influences the screening process. The average length of wood fibres is given in a number of publications (I1,M2,P2,R2,S1). Wood fibres are about 1–3 mm long, 20–45 μm in diameter and have a high aspect ratio (*i.e.* length/diameter) of about 50–100. Nylon and rayon fibres of 1–3 mm average fibre length were used to represent the typical length range of wood pulp fibres. The average fibre length and its distribution for the fibres used in this study was determined by Kajaani FS-100 Fibre Length Analyzer (P5) which counts fibres as well as measure their lengths. This instrument provides the population distribution which is described as the number of fibres in a certain fibre length range as a percentage of the total number of fibres analyzed. It also gives the length-weighted distribution which is defined as the percentage of fibres by length in each range as a percentage of the total length of fibres. The two average fibre lengths are defined as follows:

$$L_n = \frac{\sum_{i=1}^n n_i l_i}{\sum_{i=1}^n n_i} \tag{A.1}$$

and

$$L_w = \frac{\sum_{i=1}^{n} n_i l_i^2}{\sum_{i=1}^{n} n_i l_i} \tag{A.2}$$

where

L_n	=	Number average fibre length
L_w	=	Length-weighted average fibre length
n_i	=	number of fibres in each length range
l_i	=	average length in each range
i	=	number of ranges = 1, 2, 3, ... 24

The length distributions of the fibres used in this study are given in Tables A.1 to A.6. The standard printout from the Kajaani FS-100 gives the upper limit of each length range. This is reported in terms of range boundaries. The population as well as the length-weighted distribution are reported in these tables.

A.2 Fibre Stiffness

Fibre flexibility is an important property affecting the screening process. Flexibility is defined as the reciprocal of fibre stiffness in bending, S, which is the product of elastic modulus, E, and the area moment of inertia, I, of the fibre. Thus

$$F = \frac{1}{S} = \frac{1}{EI} \tag{A.3}$$

where $I = (\pi d^4/64)$ for a rod with uniform circular cross-section. Various testing methods, as briefly mentioned in Section 2.2, have been developed to measure fibre stiffness. The stiffness values for pulp and model fibres taken from the literature are given in Table A.6.

136

Table A.1: Length Distribution of 1 mm Nylon Fibres.

Fibre Length (mm)	Population Distribution	Weighted Distribution	Fibre Length (mm)	Population Distribution	Weighted Distribution
0.00–0.07	0.49	0.01	1.20–1.27	6.05	7.40
0.07–0.14	0.17	0.02	1.27–1.34	1.65	2.14
0.14–0.21	0.11	0.02	1.34–1.41	1.11	1.51
0.21–0.28	0.21	0.05	1.41–1.48	0.46	0.66
0.28–0.35	0.25	0.08	1.48–1.55	0.36	0.53
0.35–0.42	0.27	0.10	1.55–1.62	0.22	0.35
0.42–0.49	0.18	0.08	1.62–1.69	0.19	0.31
0.49–0.56	0.27	0.14	1.69–1.76	0.14	0.24
0.56–0.63	0.50	0.30	1.76–1.83	0.12	0.21
0.63–0.70	1.59	1.06	1.83–1.90	0.12	0.22
0.70–0.77	3.96	2.91	1.90–1.97	0.14	0.26
0.77–0.84	6.22	5.00	1.97–2.04	0.14	0.28
0.84–0.91	12.33	10.78	2.04–2.11	0.12	0.25
0.91–0.98	17.03	16.07	2.11–2.18	0.09	0.20
0.98–1.05	19.07	19.33	2.18–2.25	0.08	0.17
1.05–1.12	16.41	17.78	2.25–2.32	0.06	0.14
1.12–1.20	9.90	11.41	> 2.32	0.27	0.64

Number of fibres counted = 4742		
CHAR %	Arithmetic (mm)	Weighted (mm)
10	0.80	0.85
25	0.91	0.94
50	1.01	1.04
75	1.11	1.14
90	1.21	1.25
Avg.	1.01	1.05

Table A.2: Length Distribution of 1.5 mm Nylon Fibres

Fibre Length (mm)	Population Distribution	Weighted Distribution	Fibre Length (mm)	Population Distribution	Weighted Distribution
0.00–0.07	0.41	0.01	1.20–1.27	0.83	0.70
0.07–0.14	0.20	0.01	1.27–1.34	3.06	2.72
0.14–0.21	1.12	0.13	1.34–1.41	5.07	4.75
0.21–0.28	2.60	0.44	1.41–1.48	13.55	13.35
0.28–0.35	2.24	0.48	1.48–1.55	20.02	20.68
0.35–0.42	0.05	0.01	1.55–1.62	20.73	22.40
0.42–0.49	0.12	0.04	1.62–1.69	14.96	16.89
0.49–0.56	0.20	0.07	1.69–1.76	6.60	7.77
0.56–0.63	0.19	0.08	1.76–1.83	4.00	4.90
0.63–0.70	0.14	0.06	1.83–1.90	1.03	1.31
0.70–0.77	0.04	0.02	1.90–1.97	0.65	0.86
0.77–0.84	0.05	0.03	1.97–2.04	0.23	0.31
0.84–0.91	0.04	0.03	2.04–2.11	0.18	0.25
0.91–0.98	0.06	0.04	2.11–2.18	0.15	0.22
0.98–1.05	0.19	0.13	2.18–2.25	0.18	0.27
1.05–1.12	0.30	0.22	2.25–2.32	0.20	0.32
1.12–1.20	0.62	0.49	> 2.32	0.87	1.39

Number of fibres counted = 2016		
CHAR %	Arithmetic (mm)	Weighted (mm)
10	1.28	1.40
25	1.45	1.49
50	1.55	1.57
75	1.64	1.66
90	1.73	1.75
Avg.	1.47	1.56

138

Table A.3: Length Distribution of 3 mm Nylon Fibres.

Fibre Length (mm)	Population Distribution	Weighted Distribution	Fibre Length (mm)	Population Distribution	Weighted Distribution
0.00–0.20	4.65	0.09	3.50–3.70	16.98	19.72
0.20–0.41	1.30	0.13	3.70–3.91	6.96	8.55
0.41–0.61	1.10	0.18	3.91–4.11	3.54	4.59
0.61–0.82	0.65	0.18	4.11–4.32	0.12	0.16
0.82–1.02	0.53	0.16	4.32–4.52	0.11	0.15
1.02–1.23	0.75	0.27	4.52–4.73	0.08	0.12
1.23–1.44	0.93	0.40	4.73–4.94	0.07	0.10
1.44–1.64	0.77	0.38	4.94–5.14	0.04	0.07
1.64–1.85	0.42	0.23	5.14–5.35	0.03	0.06
1.85–2.05	0.13	0.08	5.35–5.55	0.07	0.13
2.05–2.26	0.27	0.19	5.55–5.76	0.12	0.23
2.26–2.47	0.47	0.36	5.76–5.97	0.18	0.35
2.47–2.67	1.11	0.92	5.97–6.17	0.19	0.37
2.67–2.88	1.58	1.42	6.17–6.38	0.27	0.56
2.88–3.08	11.42	10.99	6.38–6.58	0.35	0.73
3.08–3.29	20.80	21.40	6.58–6.79	0.42	0.92
3.29–3.50	23.58	25.82	> 6.79	0.45	1.00

Number of fibres counted = 2008		
CHAR %	Arithmetic (mm)	Weighted (mm)
10	1.47	2.98
25	3.07	3.18
50	3.32	3.39
75	3.56	3.62
90	3.78	3.88
Avg.	3.17	3.45

Table A.4: Length Distribution of 1 mm Rayon Fibres

Fibre Length (mm)	Population Distribution	Weighted Distribution	Fibre Length (mm)	Population Distribution	Weighted Distribution
0.00–0.07	0.58	0.01	1.20–1.27	9.75	11.89
0.07–0.14	0.65	0.07	1.27–1.34	2.13	2.75
0.14–0.21	1.93	0.34	1.34–1.41	1.43	1.94
0.21–0.28	2.88	0.70	1.41–1.48	0.67	0.95
0.28–0.35	2.43	0.76	1.48–1.55	0.60	0.90
0.35–0.42	0.91	0.35	1.55–1.62	0.47	0.73
0.42–0.49	0.38	0.17	1.62–1.69	0.40	0.65
0.49–0.56	0.53	0.28	1.69–1.76	0.27	0.46
0.56–0.63	0.60	0.39	1.76–1.83	0.22	0.38
0.63–0.70	1.01	0.67	1.83–1.90	0.17	0.32
0.70–0.77	1.34	0.98	1.90–1.97	0.18	0.35
0.77–0.84	1.80	1.44	1.97–2.04	0.17	0.33
0.84–0.91	5.61	4.88	2.04–2.11	0.14	0.28
0.91–0.98	9.20	8.66	2.11–2.18	0.13	0.28
0.98–1.05	16.40	16.57	2.18–2.25	0.15	0.33
1.05–1.12	19.99	21.60	2.25–2.32	0.17	0.39
1.12–1.20	16.67	19.17	> 2.32	0.71	1.60

Number of fibres counted = 5015		
CHAR %	Arithmetic (mm)	Weighted (mm)
10	0.53	0.90
25	0.95	1.01
50	1.07	1.10
75	1.17	1.19
90	1.25	1.30
Avg.	1.02	1.11

Table A.5: Length Distribution of Kraft Pulp (WR Cedar, R12 fraction).

Fibre Length (mm)	Population Distribution	Weighted Distribution	Fibre Length (mm)	Population Distribution	Weighted Distribution
0.00–0.20	3.08	0.07	3.50–3.70	8.24	9.47
0.20–0.41	1.51	0.15	3.70–3.91	8.53	10.36
0.41–0.61	0.86	0.14	3.91–4.11	7.61	9.75
0.61–0.82	0.86	0.20	4.11–4.32	6.03	8.12
0.82–1.02	0.91	0.27	4.32–4.52	5.35	7.56
1.02–1.23	1.13	0.41	4.52–4.73	3.87	5.71
1.23–1.44	1.52	0.65	4.73–4.94	3.05	4.71
1.44–1.64	2.20	1.08	4.94–5.14	1.62	2.61
1.64–1.85	2.89	1.61	5.14–5.35	1.01	1.69
1.85–2.05	3.54	2.21	5.35–5.55	0.28	0.49
2.05–2.26	4.41	3.04	5.55–5.76	0.16	0.29
2.26–2.47	5.15	3.89	5.76–5.97	0.04	0.08
2.47–2.67	5.01	4.12	5.97–6.17	0.04	0.08
2.67–2.88	4.36	3.87	6.17–6.38	0.05	0.09
2.88–3.08	4.42	4.21	6.38–6.58	0.05	0.10
3.08–3.29	5.12	5.21	6.58–6.79	0.05	0.12
3.29–3.50	7.03	7.62	> 6.79	0.19	0.43

Number of fibres counted = 4641		
CHAR %	Arithmetic (mm)	Weighted (mm)
10	1.45	2.27
25	2.35	3.04
50	3.38	3.74
75	4.03	4.29
90	4.54	4.75
Avg.	3.17	3.62

141

A.3 Apparent Density of Fibres

Wood pulp fibres are hydrophillic and retain the imbibed water in the fibre wall, lumen and microfibrills. Therefore, pulp fibres must be dealt with as entities having an apparent mass and volume. The quantity of imbibed water is a function of fibre morphology and chemical or physical treatment to which fibre is exposed. Soszynski (S6) has adequately addressed the apparent density (ρ_a) of wood pulp fibres in aqueous suspension. ρ_a can be calculated by using the following equation:

$$\rho_a = \frac{\rho_{\text{water}}\left(1 + WRRk\right)}{\frac{\rho_{\text{water}}}{\rho_{\text{wall}}} + WRRk} \tag{A.4}$$

$WRRk$ is the water retention ratio at knee which is the best possible estimate of the ratio of the mass of imbibed water to the mass of dry, solid, fibre material. The knee in the water retention curve refers to the point of inflection when one mechanism of water removal changes to another within a range of centrifugal acceleration.

The apparent density of the fibres used in this study is given in Table A.7. The typical values for water retention ratio or the water absorbed by the fibres was taken from the published information. The density of water was taken as 998 kg/m^3 at 20°C.

Table A.6: Stiffness of Wood Pulp Fibres and Model Fibres.

Fibre Type		Fibre Stiffness (N·m² × 10¹²)	Reference
TMP (Primary discharge)		157	
TMP (Secondary discharge)		83	
Stone groundwood		71	T1
Semibleached kraft		2.7	
Sulfite early wood		1.6–2.2	
Sulfite late wood	spruce	1.6–2.6	S5
Sulfate early wood	pulps	3.9–4.9	
Sulfate late wood		3.3–4.9	
Bleached kraft pulp (E. grandis)		5.4	C4
Nylon 15 denier		329	S6
Rayon 70% stretched	(dry)	3.2	
	(wet)	0.13	E2
Shives, mechanical pulp	(estimated)	10^4–10^7	G1

Table A.7: Apparent Density of Pulp and Model Fibres.

Fibre Type	Density (kg/m^3)	WRRk (kg/kg)	ρ_a (kg/m^3)
Wood pulp fibres	1500 (S7)	2* (S6)	1123
Nylon 15 denier	1140 (B10, H8, S6)	0.074 (S6)	1130
Rayon 4.5 denier	1510 (C10)	1** (C10)	1202
Kraft (R12 fraction) Western Red Cedar	1500	2	1123*

*   –   typical value for softwoods
** –   water imbibition given as 100%

144

Appendix B

B.1 Relationship Between Various Fibre Concentrations

In this thesis, the concentrations of dilute fibre suspensions are expressed, for low concentrations, as number of fibres/volume, and at higher concentration as mass/volume (g/l). It is sometimes necessary to convert the concentration from one system of units to the other and vice versa for comparing results. The following equations can be used for this purpose:

The volumetric concentration is defined as

$$C_v = \frac{v_f}{v_f + v_{wf} + v_w} \tag{B.1}$$

where:

$$
\begin{array}{lll}
C_v & - & \text{fractional volumetric concentration in fraction} \\
v_f & - & \text{volume of solid particle (fibre, moisture free)} \\
v_w & - & \text{volume of the suspending liquid (water)} \\
v_{wf} & - & \text{volume of the water retained by the fibre} \\
& & \text{at saturation}
\end{array}
$$

v_{wf} can be expressed by using the Water Retention Ratio at knee ($WRRk$) which is defined as

$$WRRk = \frac{\rho_w v_{wf}}{\rho_f v_f} \qquad \text{(S6)} \tag{B.2}$$

145

where:

ρ_w –   water density

ρ_f –   fibre density (moisture free)

Substituting Equation (B.2) into Equation (B.1), yields the following expression

$$C_v = \frac{1}{1 + \frac{\rho_f}{\rho_w}(WRRk) + \frac{v_w}{v_f}} \tag{B.3}$$

Considering the fibre as a cylinder of length, L, and diameter, d, the volume of n fibres is

$$v_f = \frac{\pi}{4} d^2 L n \tag{B.4}$$

All factors in Equation (B.3) are known. Thus, C_v can be calculated and related to the number of fibres/volume.

The mass concentration C_m is defined as

$$C_m = \frac{m_f}{m_f + m_{wf} + m_w} \tag{B.5}$$

where:

m_f –   mass of fibre (moisture free)

m_{wf} –   mass of the water absorbed by fibre at saturation

m_w –   mass of suspending liquid (water)

Thus,

$$C_m = \frac{v_f \rho_f}{v_f \rho_f + v_{wf} \rho_w + v_w \rho_w} \tag{B.6}$$

or, upon substituting Equation (B.2) into Equation (B.6),

$$C_m = \frac{1}{1 + WRRk + \frac{v_w \rho_w}{v_f \rho_f}} \tag{B.7}$$

As all factors in Equation (B.7) are known, C_m can be calculated and related to the mass of fibres/volume.

146

B.2   Crowding Factor and Critical Concentration

It was suggested by Mason (M6) that fibre-fibre interaction becomes important when a "Critical Concentration" is exceeded. He defined this condition as one in which there is less than one fibre in a volume of diameter equal to the length of a single fibre. The critical volumetric concentration, as a fraction, for cylindrical particles is given as:

$$C_{v,cr} = 1.5 \left(\frac{d}{L}\right)^2 \tag{B.8}$$

This concept was extended by Kerekes et al. (K3) to the more general case of N fibres in the swept volume of a given fibre. N is called the "Crowding Factor" which represents the number of fibres in the volume swept out by the length of a single fibre. This indicates the level of interfibre contact and restraint of rotational motion. N can be calculated from the volumetric concentration of fibres, C_v, fibre length, L, and fibre diameter, d using the following equation:

$$N = \frac{2}{3}C_v \left(\frac{L}{d}\right)^2 \tag{B.9}$$

For pulp fibre suspension, it is more conventient to express N as:

$$N = \frac{0.5\rho\, C_m\, L^2}{w}$$

where C_m is the mass concentration expressed as a fraction, ρ is the density of water, and w is the fibre coarseness. A fibre suspension can be termed dilute, semiconcentrated or concentrated depending on the level of interfibre contact and thus on the value of N (K4). Table B.1 gives, for comparison, the concentrations

in different units as well as the corresponding Critical Concentrations and the
Crowding Factors for all of the fibres used in this study.

Table B.1: Comparison of Various Fibre Concentrations for the Fibres used in this Study.

Fibre Indentification	Suspension concentration expressed as				$C_{v,cr}$ (%)	N
	fibres/l	C_v (%)	g/l	C_m (%)		
Nylon 1 mm	10^3	0.00014	0.001639	0.00016		–
	10^4	0.0014	0.01639	0.00164		–
	10^5	0.014	0.1639	0.0164	0.283	0.05
	10^6	0.144	1.639	0.164		0.54
	10^7	1.417	16.39	1.611		5.3
Nylon 3 mm	10^3	0.00047	0.00532	0.00053		0.02
	10^4	0.0047	0.0532	0.0053		0.2
	10^5	0.0465	0.532	0.053	0.027	1.9
	10^6	0.465	5.32	0.529		19
Rayon 1 mm	10^3	0.000032	0.00048	0.000048		–
	10^5	0.0032	0.0484	0.0048		0.06
	10^7	0.032	4.841	0.478	0.058	5.9
	10^8	2.966	48.41	4.405		54
Kraft (R12) Western Red Cedar	10^3	0.0002	0.0035	0.00035		0.14
	10^4	0.002	0.035	0.0035	0.014	1.4
	10^5	0.02	0.35	0.035		14.3

Appendix C

Fibre Concentration Measurements and Data Reproducibility

C.1 Measurement of Fibre Concentration

Passage ratio was defined as the concentration of fibres in the aperture flow divided by the corresponding concentration upstream of the aperture. To determine passage ratio, accept and reject samples were collected and their concentrations were measured by one of the following techniques depending on the level of concentration used.

C.1.1 Manual Counting

In this method, fibres were directly filtered from a known volume of the sample and then counted manually on the filter paper. The range of concentration over which this method can be used effectively was found to be about 500 to 4000 fibres per litre. Lower concentrations gave highly variable results while higher concentrations made counting difficult. To make counting easy and reliable, the volume of the samples was varied to be in the above range. For concentrations higher than 4000 fibres per litre, the sample was suitably diluted before counting the fibres. The manual counting method is tedious, and can only be used efficiently when all fibres

in the suspension are alike *e.g.* for synthetic fibres which were precisely cut to give a very narrow fibre length distribution. The disadvantage of this method is that it is not possible to differentiate between a short and a long fibre and therefore is not suitable for fibres having a wide length distribution.

C.1.2 Kajaani FS-100 Fibre Length Analyzer (P5)

This is an optical method based on the ability of fibres to change the direction of light polarization. The FS–100 operates by drawing a 50–75 ml of a dilute sample (0.001% mass concentration for pulp fibres) through a glass capillary of 0.2 mm in diameter. There is a light source on one side of the capillary tube and a light detecting element on the other. The light is focussed and polarized. When this polarized light meets a fibre passing through the capillary, the direction of polarization changes. After exiting from the capillary, the light beam meets another polarization filter. The polarization direction of this filter reacts to the light that has not encountered fibres and that portion of the original light beam is absorbed. The unabsorbed light (whose polarization was affected by fibres in the capillary) pass through a second filter to an array of photodiodes. When the fibre reaches a certain point in the capillary, its light image covers a portion of the diodes. The length of a fibre can then be determined from the number of the diodes covered. It takes about 10 minutes to carry out the analysis and over 3000 fibres are measured. The analyzer assigns the fibres to 24 different length ranges and provides population and length-weighted distributions.

The advantage of this analyzer is that it counts fibres as well as measures their lengths. This means that fibres of varying length can be used in a test and changes in fibre concentration can be measured for a range of fibre lengths. The Kajaani analyzer is well suited to pulp fibres but care has to be exercised for stiff synthetic

fibres. Nylon fibres are much stiffer than pulp fibres and tend to plug the capillary tube at the concentration levels recommended for pulp fibres. For 1 mm long nylon fibres, a feed concentration of 10,000 to 30,000 fibres/l was found suitable. At higher concentrations, the sample was diluted to be in the above range. 3 mm Nylon fibres could not be used due to the frequent problem of capillary blockage. Rayon fibres are flexible like pulp fibres and there was no problem in using them at the concentrations recommended for pulp fibres.

C.1.3 Fibre Weighing Method

At higher concentrations, counting the fibres is not feasible. There is a possibility of introducing error when samples are diluted several times and sub samples are taken for counting by the FS–100. In the weighing method, a known volume of fibre suspension was filtered on a filter paper and then dried in an oven which was maintained at a temperature of $105\pm 2°C$. The oven dried fibres were weighed on an analytical balance, and thus the fibre concentration as o.d. weight of fibres in g/l was obtained. This method was found to be less tedious and more accurate than counting the fibres, particularly at higher concentrations. Like manual counting, the disadvantage is that it is not possible to differentiate between a short fibre and a long one. Thus, it is not possible to determine the passage ratio for a desired fibre length range when a fibre sample having a wide fibre length distribution is used. This method was found suitable for concentrations higher than about 0.4 g/l. At lower concentrations, large accept samples have to be collected in order to achieve reliable results. For concentrations lower than 0.4 g/l, the sample was suitably diluted and the concentration measured by using the Kajaani FS–100.

C.2 Data Reproducibility

The accuracy of a measurement increases with the number of samples taken. For a small number of samples (less than 30), the t-test is used to estimate the data accuracy. If $\bar{x}$ is the mean value of x based on n number of samples and s_x is the standard deviation, the error of $\bar{x}$ is given by

$$E = t_{\alpha/2,n-1} \cdot s_x/\sqrt{n} \qquad (C.1)$$

where $(1 - \alpha)$ is the probability and $(n - 1)$ is the degree of freedom to determine the t-values. The percentage error (PE) is then given by

$$PE = \frac{E}{\bar{x}} \cdot 100 \qquad (C.2)$$

Passage ratio was defined as the accept concentration divided by the feed concentration. Thus, PE for passage ratio is given as

$$PE \text{ in passage ratio} = \sqrt{(PE \text{ in accept})^2 + (PE \text{ in feed})^2} \qquad (C.3)$$

A 10% PE in passage ratio means a 7% PE for the accept sample and a 7% PE for the feed sample. Preliminary results of fibre counting in the range of 500–4000 fibres/l gave a coefficient of variation (CV) in the range of about 4–8%. By fixing the above values of PE and CV, it is estimated that 3 to 5 samples of accept and feed flows should be taken for concentration measurement to achieve a 90% confidence limit. Accordingly, 3 to 5 samples were taken in most of the tests when passage ratio was determined using concentrations measured by manual or Kajaani counting. Passage ratios based on the weighing method gave more reliable results, and therefore, 3 samples were taken in the case of the fibre weighing method.
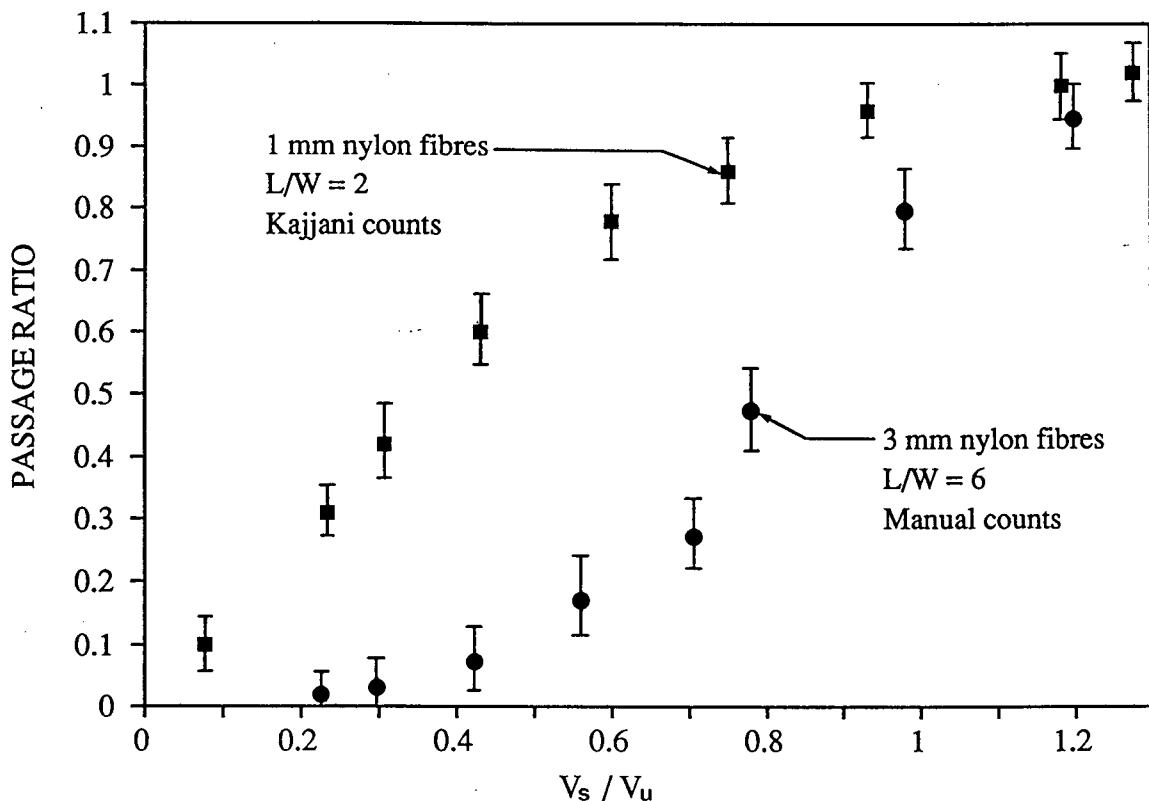
Figure C.1: Passage ratio data of 1 and 3 mm nylon fibres showing 95% confidence interval.

Figure C.1 shows the 95% confidence interval for the passage ratio data of Figure 5.1. Passage ratio data for 1 mm nylon fibres are based on 4 samples using the Kajaani FS-100 for fibre counting, and the data for 3 mm nylon fibres are based on 4 samples using manual counting. Figure C.2 shows the 95% confidence interval for the passage ratio data of Figure 5.18 based on 3 samples using the fibre weighing method.
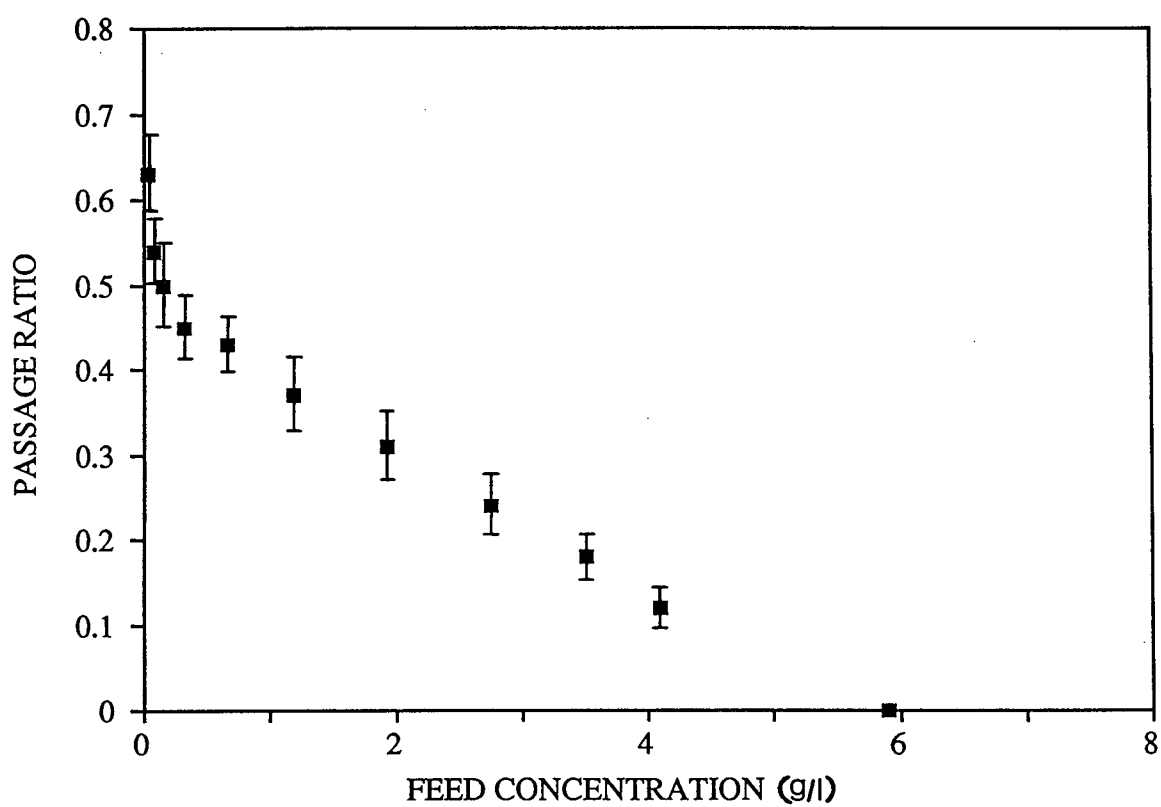
Figure C.2: Passage ratio data of 1 mm rayon fibres showing 95% confidence interval.

Appendix D

Single Slot Channel Data

Table D.1: Passage Ratios of 1 mm Nylon Fibres for a Single Slot of Varying Width. $V_u = 6.5$ m/s.

$C_{nF} = 12,500$ fibres/l		$C_{nF} = 10,000$ fibres/l		$C_{nF} = 9,800$ fibres/l	
$N = 0.006$		$N = 0.005$		$N = 0.005$	
$W = 1$ mm		$W = 0.5$ mm		$W = 0.25$ mm	
V_s (m/s)	P	V_s (m/s)	P	V_s (m/s)	P
0.25	0.09	0.50	0.10	1.05	0.02
0.83	0.32	1.52	0.31	2.84	0.22
1.09	0.43	2.0	0.42	3.36	0.28
1.55	0.59	2.8	0.60	4.05	0.39
2.25	0.76	3.9	0.78	4.55	0.45
2.94	0.84	4.88	0.85	4.89	0.48
4.16	0.93	6.06	0.96	6.22	0.73
5.17	0.98	7.7	1.0	7.1	0.82
		8.3	1.02		

Note: C_{nF} is the feed concentration in number of fibres/l. Passage ratios are based on Kajaani counts.

Table D.2: Passage Ratios of 3 mm Nylon Fibres for a Single Slot of Varying Width. $V_u = 6.5$ m/s; $C_{nF} = 3000$ fibres/l ($N = 0.06$).

$W = 0.5$ mm		$W = 1$ mm		$W = 1.5$ mm	
V_s (m/s)	P	V_s (m/s)	P	V_s (m/s)	P
1.46	0.02	1.07	0.04	0.53	0.02
1.92	0.04	2.24	0.27	0.72	0.05
2.75	0.08	2.93	0.48	1.06	0.13
3.65	0.18	4.19	0.69	1.59	0.3
4.6	0.28	5.83	0.89	2.15	0.42
5.1	0.48			3.32	0.69
6.4	0.80			4.33	0.78
7.7	0.95			4.83	0.83

Passage ratios are based on manual counts.

Table D.3: Passage Ratios of 1 mm Nylon Fibres for a 0.5 mm Wide Slot With Varying Upstream Velocity (V_u). $C_{nF} = 12,500$ fibres/l; ($N = 0.06$).

$V_u = 8.5$ m/s		$V_u = 6.5$ mm	
V_s (m/s)	P	V_s (m/s)	P
		0.5	0.1
1.92	0.21	1.52	0.31
2.51	0.33	2	0.42
3.53	0.51	2.8	0.6
4.82	0.71	3.9	0.78
5.92	0.81	4.88	0.86
7.26	0.85	6.06	0.96
		7.7	1
		8.3	1.02
$V_u = 5$ mm		$V_u = 3.5$ m/s	
V_s (m/s)	P	V_s (m/s)	P
1.20	0.29	0.98	0.28
2.36	0.58	1.31	0.40
3.21	0.77	1.87	0.60
3.89	0.83	2.58	0.78
4.76	0.89	3.12	0.82
5.9	0.95	3.68	0.87
		5.31	0.95

Passage ratios are based on Kajaani counts.

Table D.4: Passage Ratios of 3 mm Nylon Fibres for a 0.5 mm Wide Slot With Varying Upstream Velocity (V_u). $C_{nF} = 3000$ fibres/l; ($N = 0.06$).

$V_u = 8.5$ m/s		$V_u = 6.5$ mm		$V_u = 4.5$ mm	
V_s (m/s)	P	V_s (m/s)	P	V_s (m/s)	P
2.5	0.03	1.46	0.02	0.4	0.01
3.5	0.07	1.92	0.04	1.2	0.02
4.75	0.21	2.75	0.08	1.6	0.03
5.38	0.43	3.65	0.18	2.24	0.10
6.2	0.71	4.80	0.28	2.95	0.2
7.9	0.91	5.1	0.48	3.47	0.33
		6.4	0.80	4.18	0.54
		7.7	0.95	5.3	0.8

$V_u = 3.2$ m/s		$V_u = 1.8$ mm	
V_s (m/s)	P	V_s (m/s)	P
0.96	0.02	1	0.06
1.4	0.04	1.9	0.26
1.8	0.09	2.3	0.59
2.18	0.17	2.8	0.77
2.93	0.48	4	0.87
4.66	0.79		
5.2	0.87		

Passage ratios are based on manual counts.

Table D.5: Passage Ratios of 1 mm Rayon Fibres and 3.6 mm Western Red Cedar Kraft Pulp (R12 fraction). $V_u = 6.5$ m/s; $W = 0.5$ mm.

Rayon Fibres		Kraft (R12 fraction)	
$C_{nF} = 25,000$ fibres/l		$C_{nF} = 3,500$ fibres/l	
$N = 0.015$		$N = 0.49$	
V_s (m/s)	P^*	V_s (m/s)	P^{**}
0.51	0.16	0.50	0.04
1.53	0.43	1.45	0.12
2	0.52	1.92	0.17
2.8	0.65	2.56	0.28
3.85	0.81	3.44	0.44
4.3	0.86	4.25	0.57
5.81	0.97	5.45	0.74
7.95	1.04	6.52	0.89

*   Passage ratios based on Kajaani counts.
**   Passage ratios based on manual counts.

Table D.6: Passage Ratios of 1 mm Nylon Fibres at Different Levels of Feed Concentration (C_{bF}). $V_u = 6.5$ m/s; $W = 0.5$ mm.

| $C_{bF} = 0.016$ g/l | | $C_{bF} = 0.08$ g/l | | $C_{bF} = 0.98$ g/l | |
| $N = 0.005$ | | $N = 0.03$ | | $N = 0.32$ | |
V_s (m/s)	P^*	V_s (m/s)	P^*	V_s (m/s)	P^{**}
0.5	0.1	0.5	0.1	0.5	0.1
1.52	0.31	1.5	0.28	1.48	0.26
2	0.42	1.98	0.38	1.93	0.36
2.8	0.60	2.78	0.56	2.04	0.46
3.9	0.78	3.84	0.72	2.13	0.48
4.88	0.86	4.68	0.80	2.22	0.48
6.06	0.96	5.64	0.91	2.42	0.50
7.7	1.0	8.13	1.0	6.29	0.91
8.3	1.02			7.34	0.95

| $C_{bF} = 2.24$ g/l | | $C_{bF} = 5.17$ g/l | | $C_{bF} = 9.5$ g/l | |
| $N = 0.74$ | | $N = 1.70$ | | $N = 3.1$ | |
V_s (m/s)	P^{**}	V_s (m/s)	P^{**}	V_s (m/s)	P^{**}
0.50	0.1	1.64	0.34	1.55	0.32
1.47	0.25	2.01	0.44	1.86	0.39
1.62	0.34	3.2	0.67	2.29	0.45
1.86	0.40	4.35	0.84	3.05	0.58
2	0.41	5.76	0.97	3.84	0.70
3.26	0.61				
7.08	0.97	7.67	1.01	5.60	0.93

*   Passage ratios based on Kajaani counts.

**   Passage ratios based on weighing method.

Table D.7: Passage Ratios of 1 mm Nylon Fibres with Increased Feed Concentration (C_{bF}). $V_u = 6.5$ m/s; $W = 0.5$ mm.

C_{bF} (g/l)	N	$Q_{SW} = 0.912$ l/min		$Q_{SW} = 1.7$ l/min		$Q_{SW} = 3.65$ l/min	
		Q_s (l/min)	P	Q_s (l/min)	P	Q_s (l/min)	P
0.016	0.005	0.912	0.31	1.68	0.60	3.64	0.95
0.10	0.03	0.906	0.26	—	—	—	—
0.48	0.16	0.888	0.25	1.56	0.53	3.44	0.94
0.83	0.27	0.888	0.23	1.41	0.50	3.41	0.93
1.18	0.39	0.882	0.22	1.36	0.48	3.34	0.93
1.63	0.54	0.882	0.22	1.27	0.47	3.25	0.93
2.24	0.74	0.882	0.21	1.22	0.45	3.13	0.92
3.40	1.10	0.816	0.21	1.22	0.45	2.93	0.90
5.17	1.7	0.792	0.20	1.21	0.44	2.61	0.86
7.80	2.5	0.762	0.19	1.14	0.42	2.31	0.78
9.50	3.1	0.75	0.19	1.13	0.41	2.18	0.72
11.50	3.7	0.72	0.18	1.11	0.40	2.0	0.65
13.5	4.4	0.708	0.18	1.08	0.40	1.83	0.58

Q_{SW} is the volumetric flow rate through an unobstructed slot *i.e.* at $C_{bF} = 0$.

162

Table D.8: Passage Ratios of 1 mm Rayon Fibres with Increasing Feed Concentration (C_{bF}). $V_u = 6.5$ m/s; $W = 0.5$ mm.

C_{bF} (g/l)	N	$Q_{SW} = 0.912$ l/min		$Q_{SW} = 1.7$ l/min	
		Q_s (l/min)	P	Q_s (l/min)	P
0.03	0.037	0.906	0.33	1.61	0.63
0.08	0.10	0.90	0.29	1.48	0.54
0.15	0.18	0.888	0.30	1.37	0.50
0.32	0.40	0.87	0.30	1.18	0.45
0.66	0.81	0.858	0.29	1.02	0.43
1.19	1.46	0.798	0.29	0.810	0.37
1.93	2.37	0.768	0.28	0.456	0.31
2.75	3.38	0.534	0.27	0.354	0.24
3.51	4.3	0.294	0.24	0.186	0.18
4.1	5.0	0.24	0.21	0.126	0.12
5.9	7.2	0.234	0.13	0	0
8.0	9.8	0.06	0.01		

Q_{SW} is the volumetric flow rate through an unobstructed slot *i.e.* at $C_{bF} = 0$.

Table D.9: Passage Ratios of Nylon and Rayon Fibres for Contoured Slot C1. $V_u = 6.5$ m/s; $W = 0.5$ mm.

Nylon 1 mm		Nylon 3 mm		Rayon 1 mm	
$C_{nF} = 10,500$ fibres/l		$C_{nF} = 3,200$ fibres/l		$C_{nF} = 25,500$ fibres/l	
$N = 0.006$		$N = 0.06$		$N = 0.015$	
V_s (m/s)	P^*	V_s (m/s)	P^{**}	V_s (m/s)	P^*
0.52	0.39	—	—	0.53	0.44
1.62	0.54	1.55	0.03	1.64	0.60
2.22	0.61	2.05	0.05	2.14	0.70
3.20	0.72	2.96	0.16	3.12	0.80
4.55	0.80	3.88	0.31	4.24	0.88
5.58	0.88	4.54	0.43	5.10	0.93
6.76	0.94	5.61	0.61	5.87	0.94
7.25	0.96	6.74	0.78	7.47	0.99

*   Passage ratios based on Kajaani counts.
**   Passage ratios based on manual counts.

164

Table D.10: Passage Ratios of Nylon and Rayon Fibres for Contoured Slot C2. $V_u = 6.5$ m/s; $W = 0.5$ mm.

Nylon 1 mm		Nylon 3 mm		Rayon 1 mm	
$C_{nF} = 10,200$ fibres/l		$C_{nF} = 3,200$ fibres/l		$C_{nF} = 30,000$ fibres/l	
$N = 0.006$		$N = 0.06$		$N = 0.02$	
V_s (m/s)	P^*	V_s (m/s)	P^{**}	V_s (m/s)	P^*
0.48	0.22	—	—	0.53	0.20
1.51	0.42	1.45	0.01	1.59	0.41
2	0.48	1.89	0.03	2.1	0.46
2.82	0.57	2.77	0.06	2.98	0.55
3.9	0.64	3.73	0.14	4.07	0.62
4.91	0.66	4.75	0.22	5.45	0.68
6.77	0.71	6.26	0.32	7.82	0.80
8.0	0.74	7.48	0.38	9.1	0.84
10.25	0.79	8.7	0.47		

*   Passage ratios based on Kajaani counts.

**   Passage ratios based on manual counts.

Table D.11: Passage Ratios of 1 mm Nylon Fibres for Contoured Slots C1 and C2 with Increasing Feed Concentration (C_{bF}). $V_u = 6.5$ m/s; $W = 0.5$ mm.

C_{bF} g/l	N	Contoured Slot C1			
		$Q_{SW} = 1.92$ l/min		$Q_{SW} = 4.06$ l/min	
		Q_S (1/min)	P	Q_S (1/min)	P
0.016	0.005	1.90	0.72	3.52	0.94
0.48	0.16	1.88	0.71	3.51	0.94
0.83	0.27	1.79	0.7	3.40	0.93
1.18	0.39	1.68	0.68	3.40	0.92
1.63	0.54	1.61	0.64	3.40	0.93
2.24	0.74	1.52	0.45	3.40	0.92
3.40	1.12	0	0	3.40	0.93
5.17	1.7			3.33	0.92
7.80	2.56			3.30	0.92
9.5	3.12			3.26	0.92
11.5	3.77			3.0	0.88
13.5	4.43			2.79	0.83

C_{bF} g/l	N	Contoured Slot C2			
		$Q_{SW} = 1.72$ l/min		$Q_{SW} = 4.68$ l/min	
		Q_S (1/min)	P	Q_S (1/min)	P
0.016	0.005	1.72	0.58	4.68	0.82
0.48	0.16	1.72	0.55	4.68	0.81
0.83	0.27	1.72	0.54	4.68	0.81
1.18	0.39	1.72	0.53	4.65	0.81
1.63	0.54	1.72	0.52	4.60	0.80
2.24	0.74	1.72	0.51	4.58	0.79
3.40	1.12	1.70	0.51	4.56	0.78
5.17	1.7	1.70	0.49	4.54	0.77
7.80	2.56	1.70	0.47	4.50	0.77
9.5	3.12	1.70	0.46	4.48	0.77
11.5	3.77	1.70	0.45	4.42	0.76
13.5	4.43	1.70	0.44	4.35	0.76

Q_{SW} is the volumetric flow rate through an unobstructed slot, $i.e.$ at $C_{bF} = 0$.

Table D.12: Passage Ratios of 3 mm Nylon Fibres for Smooth and Contoured Slots with Increasing Feed Concentration (C_{bF}). $V_u = 6.5$ m/s; $W = 0.5$ mm.

Feed Concentration (g/l)	N	Passage Ratio					
		Smooth Slot		C1 Slot		C2 Slot	
		Q_S (1/min)	P	Q_S (1/min)	P	Q_S (1/min)	P
0.016	0.06	3.06	0.48	3.42	0.61	4.68	0.32
0.06	0.21	1.28	0.15	3.39	0.59	4.61	0.32
0.22	0.78	1.01	0.05	3.04	0.49	4.61	0.32
0.33	1.2	0.38	0	0.20	0	4.40	0.32
0.52	1.9					4.07	0.32
0.85	3.0					0.18	0
0.92	3.3						
1.66	5.9						

Table D.13: Passage Ratios of 1 mm Nylon Fibres for Smooth and Contoured Slots at a Feed Concentration of 9.5 g/l $(N = 3.1)$. $V_u = 6.5$ m/s and $W = 0.5$ mm.

Smooth Slot		C1 Slot		C2 Slot	
V_S m/s	P	V_S m/s	P	V_S m/s	P
0.5	0.1	0.51	0.37	0.48	0.2
1.55	0.32	1.5	0.51	1.51	0.33
1.86	0.39	3	0.69	1.97	0.39
2.29	0.45	3.65	0.77	2.83	0.47
3.05	0.58	4.28	0.83	3.9	0.56
3.84	0.7	5.15	0.89	5.07	0.64
5.6	0.93	5.44	0.92	7.48	0.77
		6.52	0.94		

Passage ratios are based on weighing method.

Appendix E

Sectional Screen Experimental Data

Table E.1: Passage Ratios of 1 and 3 mm Nylon Fibres in SS with a Screen Plate Having a Single 0.5 mm Wide Slot. Rotor Tip Speed $(V_t) = 6.5$ m/s.

Nylon 1 mm		Nylon 3 mm	
$C_{nF} = 32{,}400$ fibres/l		$C_{nF} = 3{,}450$ fibres/l	
$N = 0.02$		$N = 0.07$	
V_s (m/s)	P^*	V_s (m/s)	P^{**}
0.67	0.18	1.32	0.04
1.33	0.42	1.73	0.08
1.86	0.63	2.0	0.33
2.53	0.84	2.19	0.56
3.0	0.91	2.5	0.70
3.8	0.97	2.84	0.84
		3.02	0.88

*   Passage ratio based on Kajaani counts.

**   Passage ratio based on manual counts.

Table E.2: Passage Ratios of 1 and 3 mm Nylon Fibres in SS with a Screen Plate Having Multiple Slots. (10 slots, 0.5 mm wide). $V_t = 6.5$ m/s.

Nylon 1 mm		Nylon 3 mm	
$C_{nF} = 33,500$ fibres/l		$C_{nF} = 4,200$ fibres/l	
$N = 0.02$		$N = 0.08$	
V_s (m/s)	P^*	V_s (m/s)	P^{**}
0.3	0.35	0.24	0.03
0.5	0.53	0.5	0.06
0.8	0.71	1.0	0.14
1.3	0.89	1.28	0.21
1.8	1.0	1.4	0.30
2.53	1.03	1.62	0.62
		1.84	0.80
		2.28	0.96
		2.66	0.99

*   Passage ratio based on Kajaani counts.
**   Passage ratio based on manual counts.

Table E.3: Passage Ratios of 1 mm Nylon Fibres in the SS with Multiple Slots. $C_{nF} = 35,000$ fibres/l. ($N = 0.02$).

$V_t = 3.5$ m/s		$V_t = 5.5$ m/s		$V_t = 8$ m/s		$V_t = 10.8$ m/s	
V_s (m/s)	P	V_s (m/s)	P	V_s (m/s)	P	V_s (m/s)	P
0.31	0.52	0.26	0.34	0.27	0.28	0.3	0.25
0.39	0.66	0.46	0.57	0.49	0.44	0.56	0.38
0.60	0.81	0.78	0.78	0.90	0.72	0.82	0.52
0.94	0.94	1.23	0.97	1.72	0.95	1.45	0.79
		1.68	1.01	2.35	1.0	2.83	1.04
1.66	0.99	2.09	1.03	3.49	1.05	3.91	1.06
2.52	1.02	3.16	1.06				

Passage ratios are based on Kajaani counts.

Table E.4: Passage Ratios of 1 mm Nylon Fibres with Increasing Feed Concentration in SS with Multiple Slots. $V_t = 3.5$ m/s.

C_{bF}	N	Passage Ratio			
		$V_s{}^*$ $= 0.37$ m/s	$V_s{}^*$ $= 0.89$ m/s	$V_s{}^*$ $= 1.27$ m/s	$V_s{}^*$ $= 1.54$ m/s
0.09	0.03	0.56	0.93	1.02	
0.36	0.12				1
0.67	0.22	0.4	0.9	0.99	
1.62	0.54	0.23	0.7	0.32	
1.84	0.61				0.27
2.82	0.93	0.14	0.16	0.14	
4.24	1.4				0.12
4.88	1.61	0.11	0.12	0.11	
6.44	2.13	0.1	0.12	0.11	
8.9	2.94				0.09
9.66	3.19	0.08	0.11	0.1	
12.86	4.25				0.09
16.25	5.37	0.07	0.11	0.1	
18.79	6.2				0.08

* Slot velocity at $C_{bF} = 0$

Table E.5: Passage Ratios of 1 mm Nylon Fibres with Increasing Feed Concentration in the SS with Multiple Slots. $V_t = 6.5$ m/s and 8 m/s.

C_{bF} (g/l)	N	$V_t = 6.5$ m/s	$V_t = 8$ m/s			
			Passage Ratio			
		$V_s{}^* = 1.54$ m/s	$V_s{}^* = 0.42$ m/s	$V_s{}^* = 1.06$ m/s	$V_s{}^* = 1.54$ m/s	$V_s{}^* = 2.53$ m/s
0.09	0.03		0.42	0.77	0.9	1
0.37	0.12	0.89				
0.77	0.25		0.19	0.43	0.64	
1.4	0.53		0.14	0.29	0.52	
1.6	0.55	0.76				
2.93	0.97		0.1	0.2	0.44	
4.06	1.34	0.40				
4.87	1.61		0.06	0.13	0.3	0.57
7.42	2.45		0.06	0.11	0.2	0.3
9.11	3	0.15				
10.45	3.45		0.04	0.09	0.13	0.18
12.86	4.25	0.09				
14.59	4.82		0.04	0.08	0.09	0.12
18.87	6.2	0.09				
20.7	6.8		0.03	0.07	0.09	0.08
22.18	7.3		0.03	0.07	0.09	0.08
26.98	8.9		0.03	0.07	0.09	0.08
36.04	11.9		0.02	0.06	0.07	0.07

* Slot velocity at $C_{bF} = 0$

Table E.6: Passage Ratios of 1 mm Nylon Fibres with Increasing Feed Concentration in the Sectional Screen with a Screen Plate Having ten 0.5 mm Wide Slots. $V_t = 15.2$ m/s.

C_{bF}	N	Passage Ratio			
		V_s^* $= 0.6$ m/s	V_s^* $= 1.54$ m/s	V_s^* $= 2.22$ m/s	V_s^* $= 3.54$ m/s
0.89	0.29	0.15	0.33	0.53	
1.8	0.60	0.11	0.26	0.45	
3.35	1.11	0.09	0.19	0.40	
5.27	1.74	0.06	0.15	0.38	0.76
7.97	2.63	0.05	0.11	0.34	0.72
10.74	3.55	0.04	0.09	0.32	0.7
15.85	5.24	0.03	0.07	0.22	0.62
18.25	6.0	0.03	0.06	0.19	0.55
24.45	8.1	0.02	0.05	0.12	0.32
30.61	10.1	0.02	0.05	0.06	0.21
37.31	12.3	0.02	0.04	0.06	0.06

* Slot velocity at $C_{bF} = 0$

Table E.7: Passage Ratios of 1 mm Rayon Fibres with Increasing Feed Concentration in the SS with Multiple Slots. $V_t = 8$ m/s and 15.2 m/s.

$V_t = 8$ m/s			
C_{bF}	N	Passage Ratio	
(g/l)		$V_s{}^* = 1.06$ m/s	$V_s{}^* = 2.53$ m/s
0.35	0.65	0.84	1.02
0.76	1.42	0.7	0.82
1.34	2.50	0.63	0.64
2.10	3.91	0.43	0.56
3.90	7.27	0.21	0.31
7.47	13.9	0.09	0.11
12.05	22.5	0.01	0.01
$V_t = 15.2$ m/s			
C_{bF}	N	Passage Ratio	
(g/l)		$V_s{}^* = 1.54$ m/s	$V_s{}^* = 3.54$ m/s
0.37	0.69	0.79	0.99
0.78	1.45	0.78	0.96
1.32	2.46	0.75	0.86
2.01	3.75	0.73	0.83
3.7	6.9	0.66	0.69
7.92	14.8	0.45	0.53
12.74	23.7	0.13	0.13
16.51	30.8	0.07	0.08
20.61	38.4	0.04	0.04

* Slot velocity at $C_{bF} = 0$

Appendix F

Identification of Stapling Regimes

F.1 Introduction

It is well known that at fibre concentrations of interest in commercial pulp screening, stapling and plugging of apertures take place unless means are supplied to remove fibres from the apertures. Indeed, this may be a problem at low concentrations as well, as suggested by the studies carried out in a single slot channel with steady flows. To gain insight into the nature of fibre accumulation in the vicinity of a slot, a qualitative study was undertaken to visually observe stapling at the slot entry, and determine the important parameters that influence it. Aperture plugging may be caused by a number of design and operating parameters. In this work, slot velocity V_s and upstream velocity V_u were varied over a wide range to observe their effect on fibre stapling. A dilute suspension of nylon fibres was used in the flow loop having a single slot channel, which was described earlier in Section 4.2. The observed stapling conditions are described in Table F.1. These visually observed conditions are specific to the type of fibres, feed concentration, slot geometry and the flow velocities used in this study and may not exactly be observed for other type of fibres and slot geometry.

Table F.1: Explanation of Stapling Conditions.

A1.   There are less than 10 fibres present in the slot. One end of the fibres is in the slot and the other end is bent over the fulcrum on the downstream edge of the slot. These are termed here as vertical staples.

A2.   Same as A1 except that more than 10 fibres are present.

B.   More than 10 fibres are present and, though they are mainly vertical, some horizontal staples start appearing. At any given time, a horizontal staple may or may not be present in the slot.

C.   More than 10 fibres are present and there is a mix of vertical and horizontal staples. Some horizontal staples are always present in the slot and their number increases with increased slot velocity.

D.   The staples present are mainly horizontal. There may be some vertical staples. Unstable clumps start forming, grow up and may plug the slot completely.

E1.   Mainly horizontal staples are present. Clumps start forming, slowly build up and grow to plug the slot. The clumps grow over several seconds to be about 8 mm wide and 6 mm high. The stapled fibres are evenly distributed on the up and downstream side of the slot.

E2.   Same as E1 except that stapled fibres are mainly on the downstream side of the slot and are vertical.

X1.   Less than 10 staples are present but both horizontal and vertical staples are appearing. Equivalent to A1 in terms of how plugged the slot is.

X2.   Same as X1 except that staples are mainly horizontal.

Y1.   After 10 seconds, the downstream edge of the slot is covered by fibres. The extent of coverage increases with increased slot velocity. No horizontal staples are present.

Y2.   Same as Y1 but horizontal fibres are present as a minority.

Z1.   Same as Y1 but it takes less than 10 seconds for the downstream edge of the slot to be fully covered.

Z2.   Same as Z1 but horizontal fibres are present as a minority.

F.2 Stapling Conditions Observed With 1 mm Nylon Fibres

Figure F.1 shows the stapling conditions as a function of V_s and V_u for 1 mm nylon fibres at a feed concentration of 0.08 g/l ($N = 0.03$). The following trend was visually observed when moving from a large V_u and small V_s to a small V_u and a large V_s. Initially, few fibres contact the downstream edge of the slot, stay for a fraction of a second and then leave. At any given time, some fibres may or may not be present in the slot. All such fibres have one end in the slot and the other end pointing upwards out of the slot. The fibre is bent over the downstream edge of the slot which acts as a fulcrum. Fibres in this situation are termed here as vertical staples.

At a fixed V_u, the number of vertical staples slowly increases with increase in V_s, and also increases the angle which fibres make with the horizontal on the downstream edge of the slot (see Figure F.3). At some point, horizontal staples start appearing. In this situation, a fibre lies across the slot from upstream to downstream and is slightly bowed. At this stage, there is a mix of vertical and horizontal staples. More and more horizontal staples start appearing and fewer vertical staples are present until all staples are horizontal. With further increase in V_s and decrease in V_u, clumps start forming in the corners. To start with, clumps are unstable meaning fibres stick together, stay for some time and then leave the slot. Finally, a condition is reached when the clumps form and build-up very fast to cover the entire slot and eventually plug it completely. The fibre mass then grows to few millimetres wide and high. At a very high slot velocity, $i.e.$ $V_s > V_u$, which is achieved by increasing the pressure on the feed side of the slot and partially closing the reject valve to maintain V_u, the slot can be purged again. In this situation, only a few staples may be present as most of the horizontal staples pass through
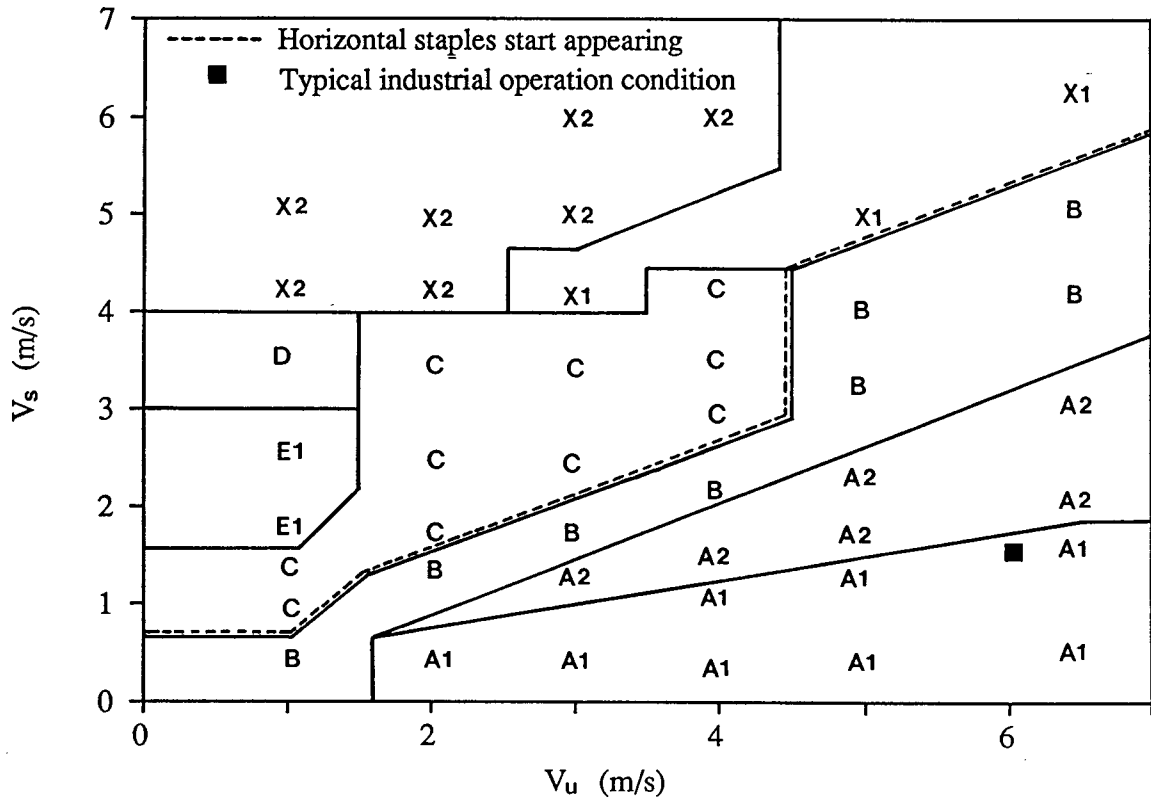
176

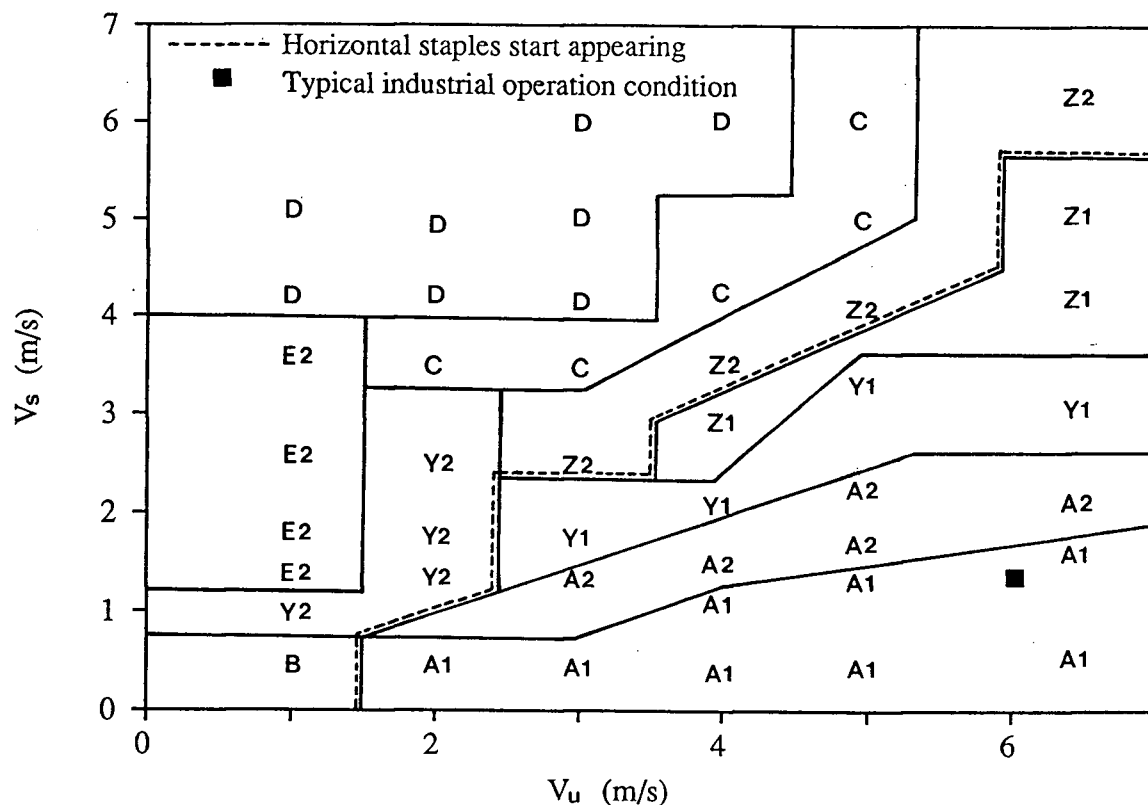Figure F.1: Stapling regimes for 1 mm nylon fibres. $W = 0.5$ mm; Feed concentration $= 0.08$ g/l.

Figure F.2: Stapling regimes for 3 mm nylon fibres. $W = 0.5$ mm; Feed concentration = 0.04 g/l.

the slot at such high V_s.

F.3 Stapling Conditions for 3 mm long Nylon Fibres

Figure F.2 shows the stapling conditions as a function of V_s and V_u for 3 mm nylon fibres at a feed concentration of 0.04 g/l ($N = 0.12$). These fibres did not show a clear trend as was observed with 1 mm long nylon fibres. In particular, 3 mm nylon fibres did not staple horizontally as easily as did 1 mm fibres for the reason given later when the formation of horizontal staples is discussed.

F.4   Types of Fibre Stapling

Based on the findings of Gooding and Kerekes (G1,G4) described in Section 2.6 and the visual observations in the present study, the following is postulated for the formation of horizontal and vertical staples.

F.4.1   Vertical stapling

As described in our analysis (Chapter 3), a fibre must enter one tip first in order to pass through the slot. Once over the slot, the fibre may turn if it is stiff or may turn and bend if it is flexible. A stiff fibre may not follow the flow streamlines to go through the slot. Vertical staples are formed when $V_u > V_s$. Due to the dominance of V_u, a stiff fibre may rotate over the slot and flip over. Depending upon its orientation when reaching the slot and V_s/V_u, a fibre may penetrate the slot or be swept away from the slot. If a fibre penetrates, it has one end in the slot and the other end points upwards out of the slot. The fibre is bent on the downstream edge of the slot which acts as a fulcrum. The angle that a fibre makes with the horizontal at the downstream slot wall, increases with increased V_s/V_u. The photographs of Figure F.3 show these vertical staples, and the difference in the angle fibres make with the downstream edge of the slot.

Based on the above description, we propose the mechanism of vertical staple formation illustrated in Figure F.4. Vertical stapling is likely to result when a fibre approaching the slot is either parallel to the wall or has a negative angle as shown in Figure F.4(a) and (b). If the leading edge of the fibre is much higher than the trailing edge as in Figure F.4(c), a fibre may not penetrate into the slot. As shown earlier, such factors as fibre flexibility and the ratio of fibre length to slot width (L/W) also influence the fibre passage through the slot, but the mode of stapling
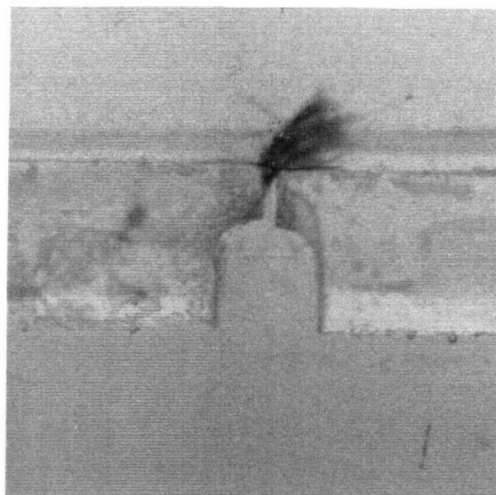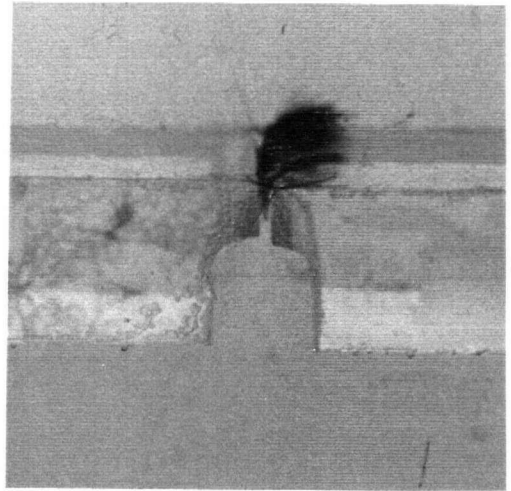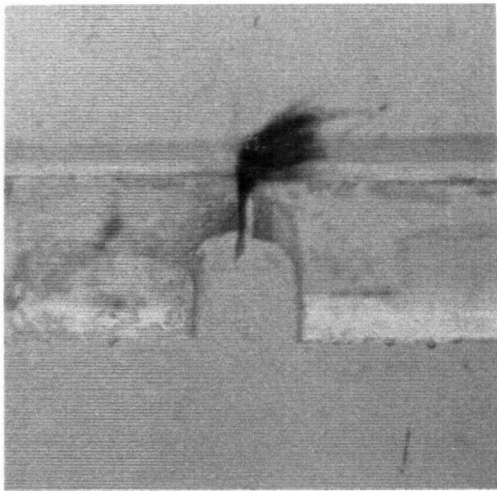
Figure F.3: 3 mm nylon fibres as vertical staples on the downstream edge of a 0.5 mm wide slot. The difference in the angle that fibres make with the downstream edge is evident.

is decided mainly by V_s/V_u.

F.4.2 Horizontal Stapling

The formation of horizontal staples is illustrated in Figure F.5. It is postulated that a fibre approaches the slot having its leading edge somewhat higher than the trailing edge. When the leading edge extends over the slot, the fibre tries to rotate. A stiff fibre can not rotate quickly enough to enter into the slot, and a high V_s pulls the fibre into a horizontal position over the slot. The horizontal staples are held in place by V_s while the reject velocity attempts to pull them away. As mentioned before, horizontal staples only appear when V_s/V_u is high. Indeed this was the case for 1 mm nylon fibres where V_s/V_u was greater than 1 for horizontal staples to form. Horizontal staples can clearly be seen in the photographs of Figure F.6.

The formation of horizontal staples is likely to be influenced by L/W and fibre flexibility. It was observed that 1 mm long nylon fibres stapled horizontally much more easily than 3 mm long nylon fibres. A longer 3 mm nylon fibre at the slot was observed as illustrated in Figure F.5(b). The force which holds the horizontal staple in place acts on that portion of the fibre which is over the slot (0.5 mm in the present case) and is independent of fibre length. A longer fibre protrudes out of the slot and may be pulled out of the slot by the reject stream. Also, the thin and flexible fibres like rayon were observed not to staple horizontally under such conditions. The reason is that a flexible fibre cannot support itself over the slot as a horizontal staple and thus passes through the slot.

F.5 Summary

In general, fibre accumulation at the slot entry can be described by 3 modes of stapling: vertical staples, horizontal staples and the mix of vertical and horizontal
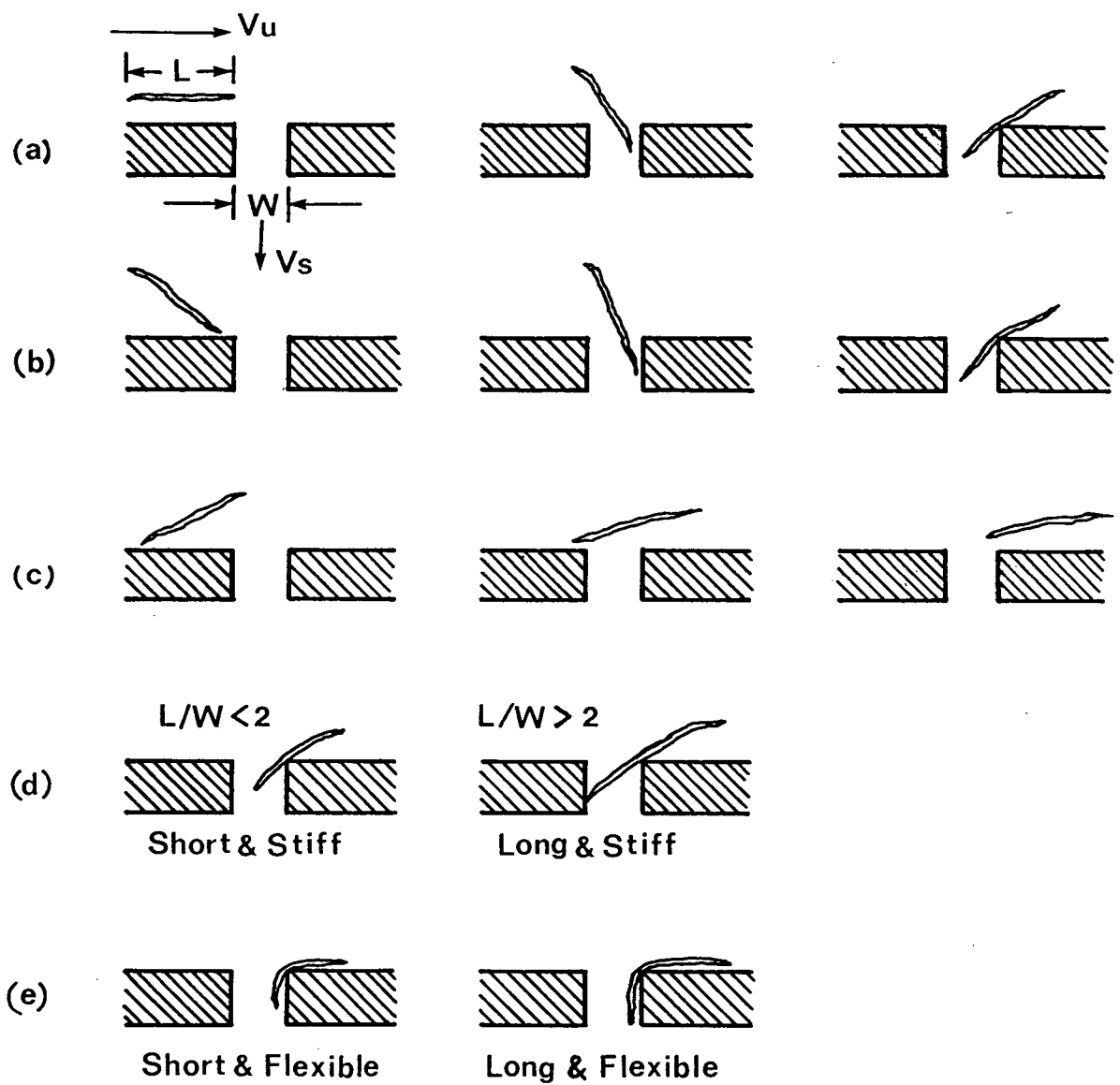
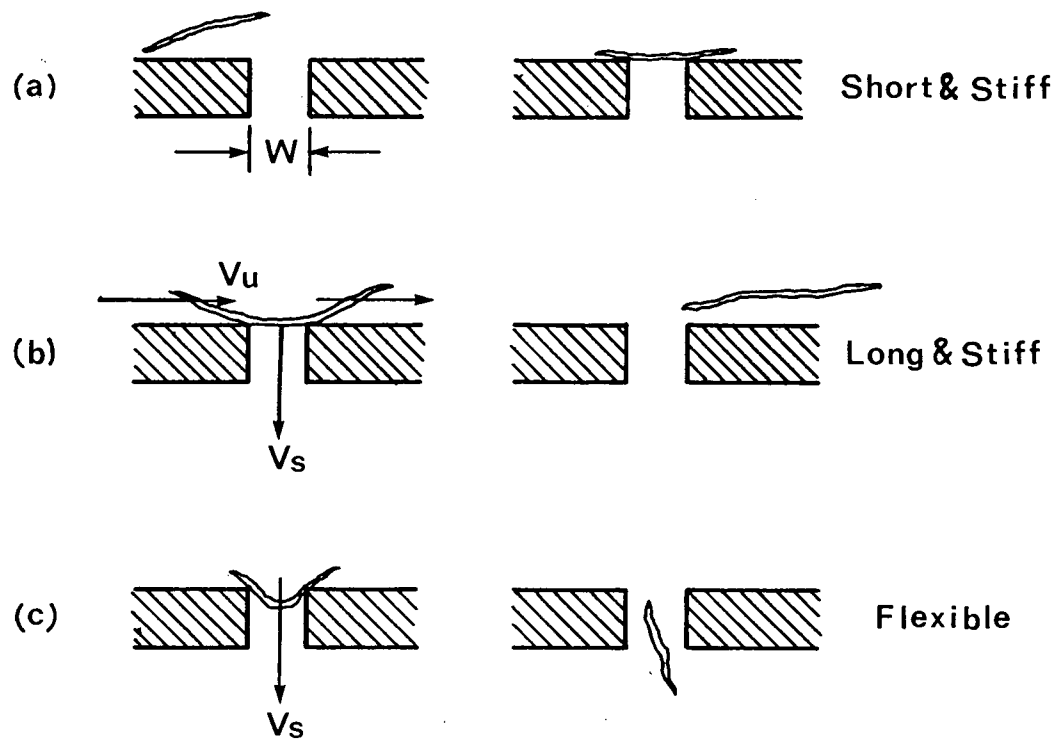Figure F.4: Illustration of the formation of vertical staples.

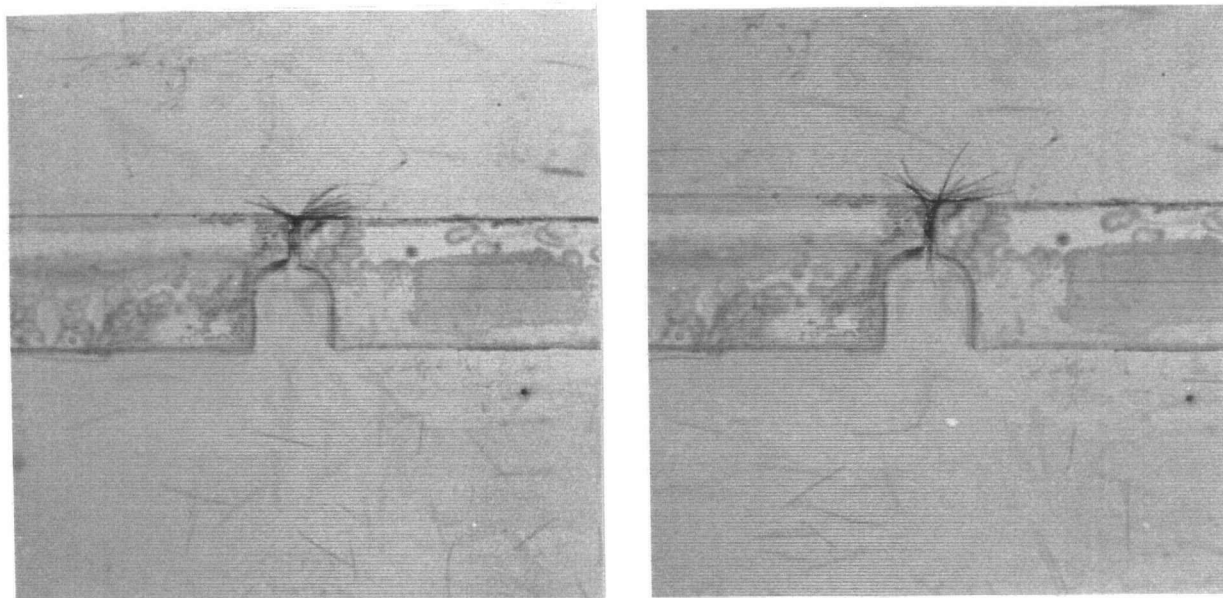Figure F.5: Illustration of the formation of horizontal staples.

Figure F.6: 3 mm nylon fibres as horizontal staples over a 0.5 mm wide slot. $V_s > V_u$.

staples. V_s/V_u is found to be a key variable in determining the way stapling takes place. The predominant mode of stapling seems to be one of fibres entering the slot, coming into contact with the downstream slot wall, and then bending over the fulcrum created by this wall and the channel wall. With increased V_s, the number of fibres in this position could increase to produce full blockage of the slot. When V_s is increased to a high level relative to V_u, fibres could block the slot by lying across its face. However, this mode of stapling is of little concern in pressure screens since the slot and upstream velocity required for such a condition lie outside the normal operating range of commercial pressure screens.